Electronic Supplementary Material (ESI) for RSC Advances.
This journal is © The Royal Society of Chemistry 2024

Supplementary Material

Photoswitchable hydrazones with pyridine-based rotors and halogen substituents

Lucie Kotásková, Pawel Jewula, Radovan Herchel, Ivan Nemec and Petr Neugebauer

NMR = Nuclear magnetic resonance
COSY = Correlation spectroscopy
HSQC = Heteronuclear single-quantum correlation spectroscopy
HMBC = Heteronuclear multiple-bond correlation spectroscopy
UV-VIS = Ultraviolet-visible spectroscopy
MS = Mass spectrometry

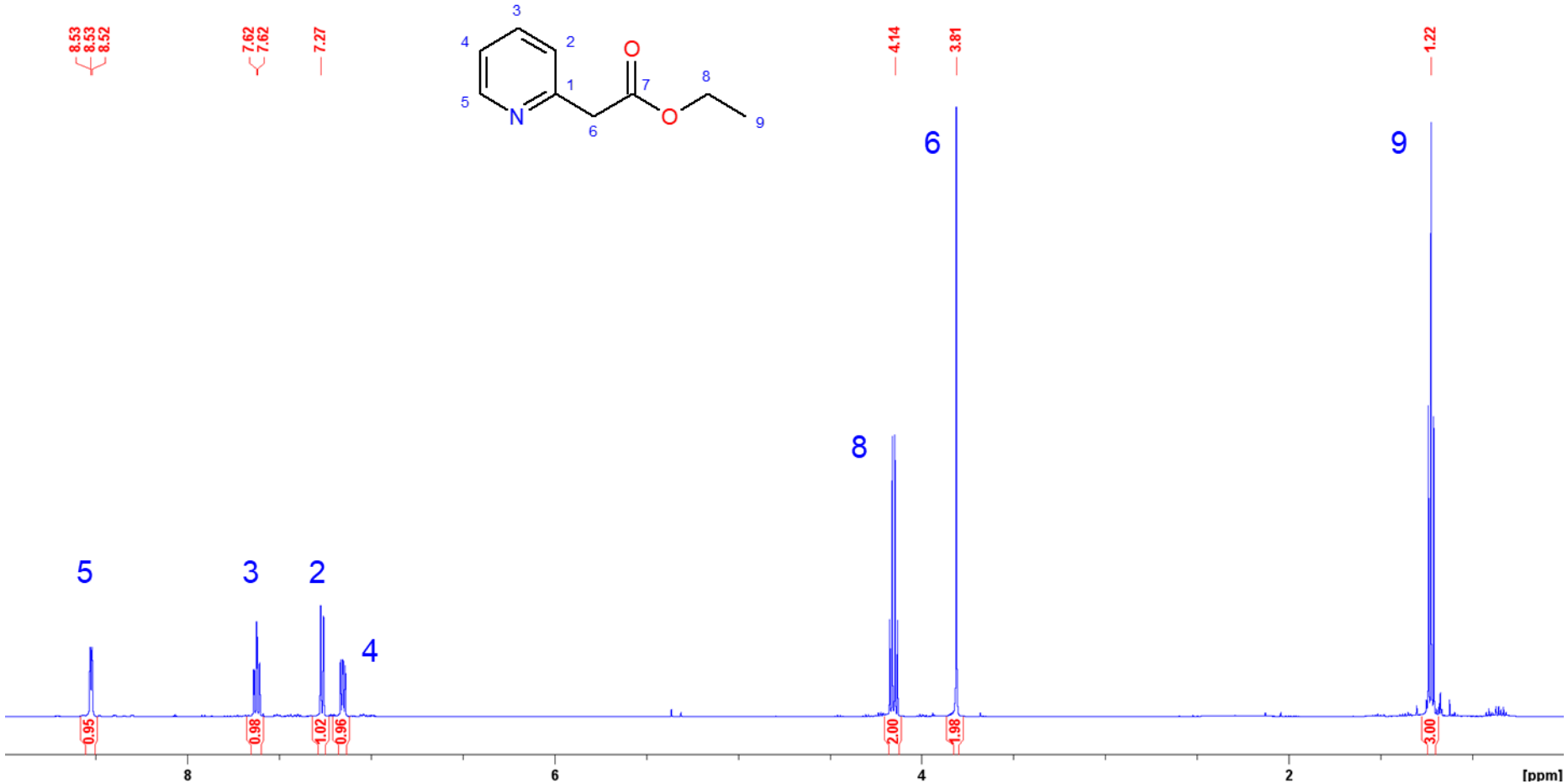

Figure S1. ^{1}H NMR of compound **1**, $CDCl_3$, 500 MHz, 298 K.

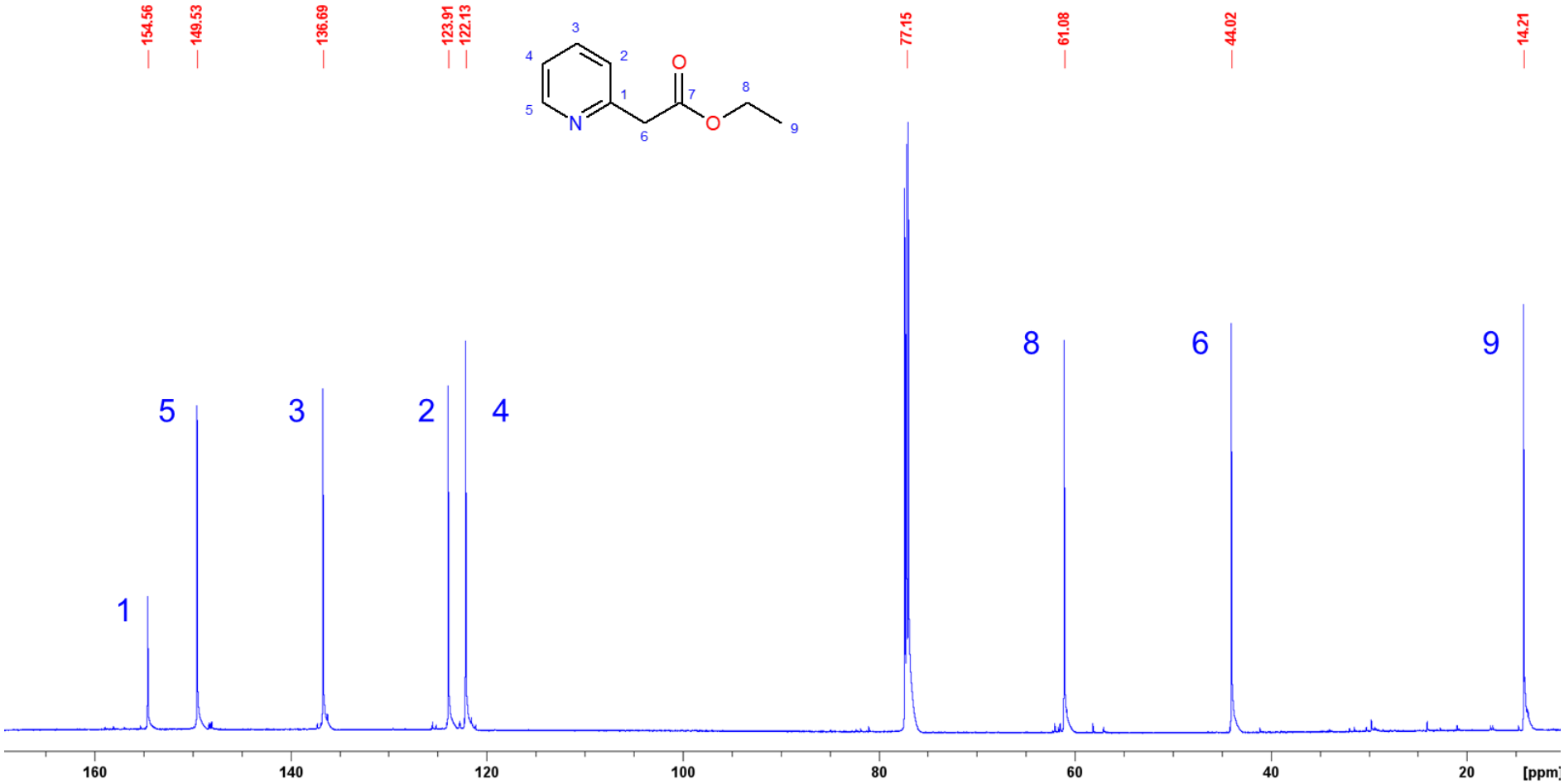

Figure S2. ^{13}C NMR of compound **1**, $CDCl_3$, 125 MHz, 298 K.

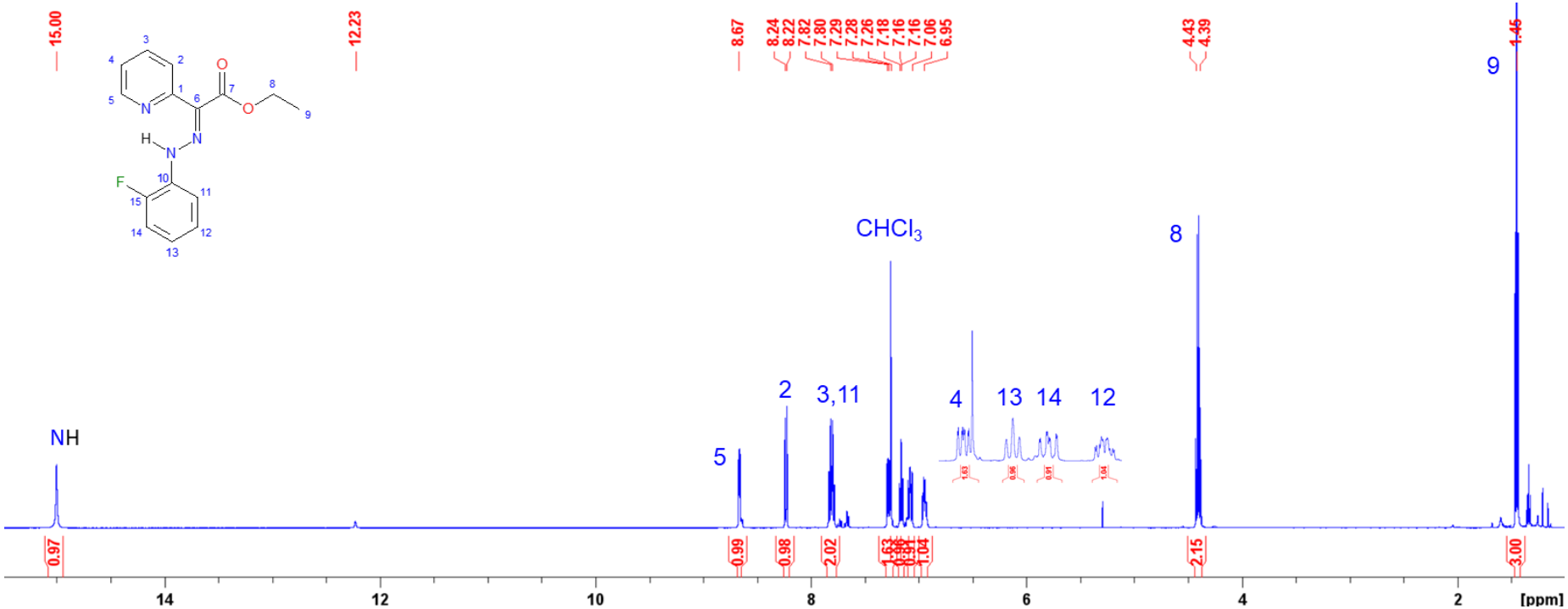

Figure S3. ^{1}H NMR spectrum of **2-F**, $CDCl_3$, 500 MHz, 298 K.

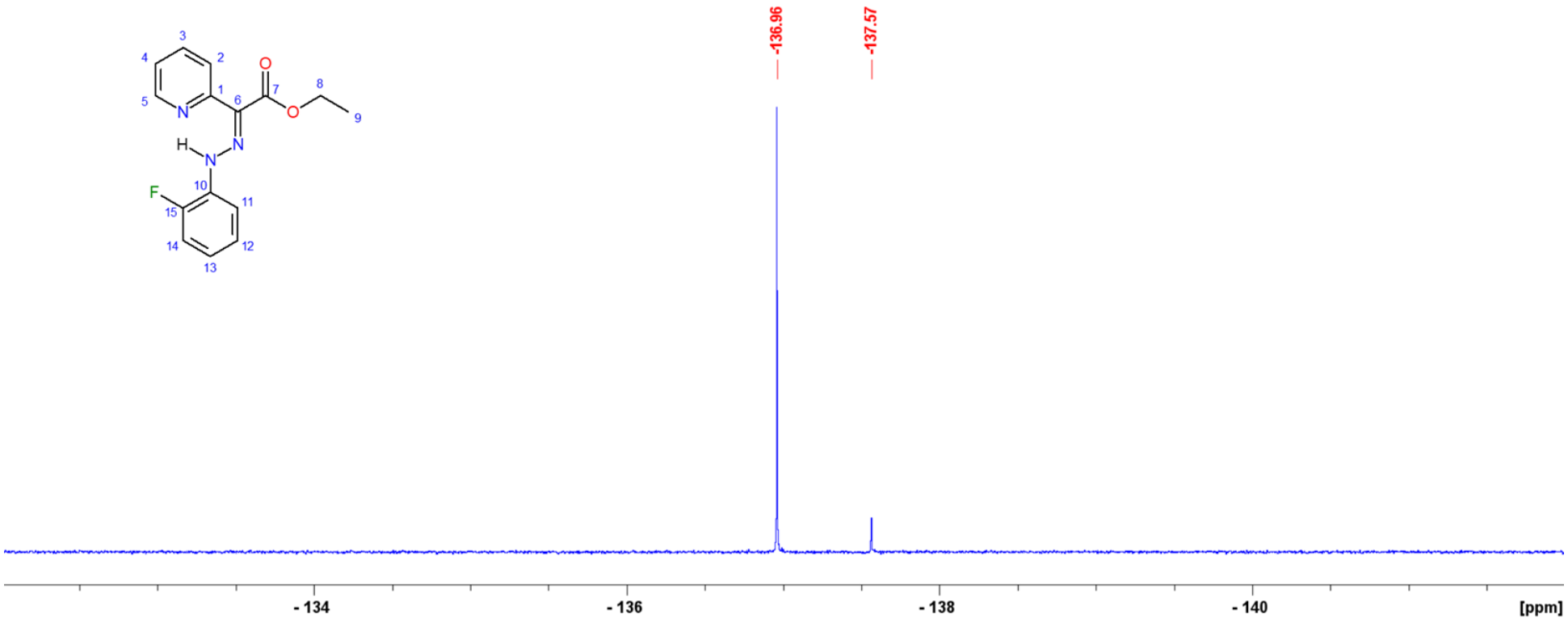

Figure S4. ^{19}F NMR spectrum of **2-F**, $CDCl_3$, 470 MHz, 298 K, ref. CF_3COOH $\delta = -78.50$ ppm.

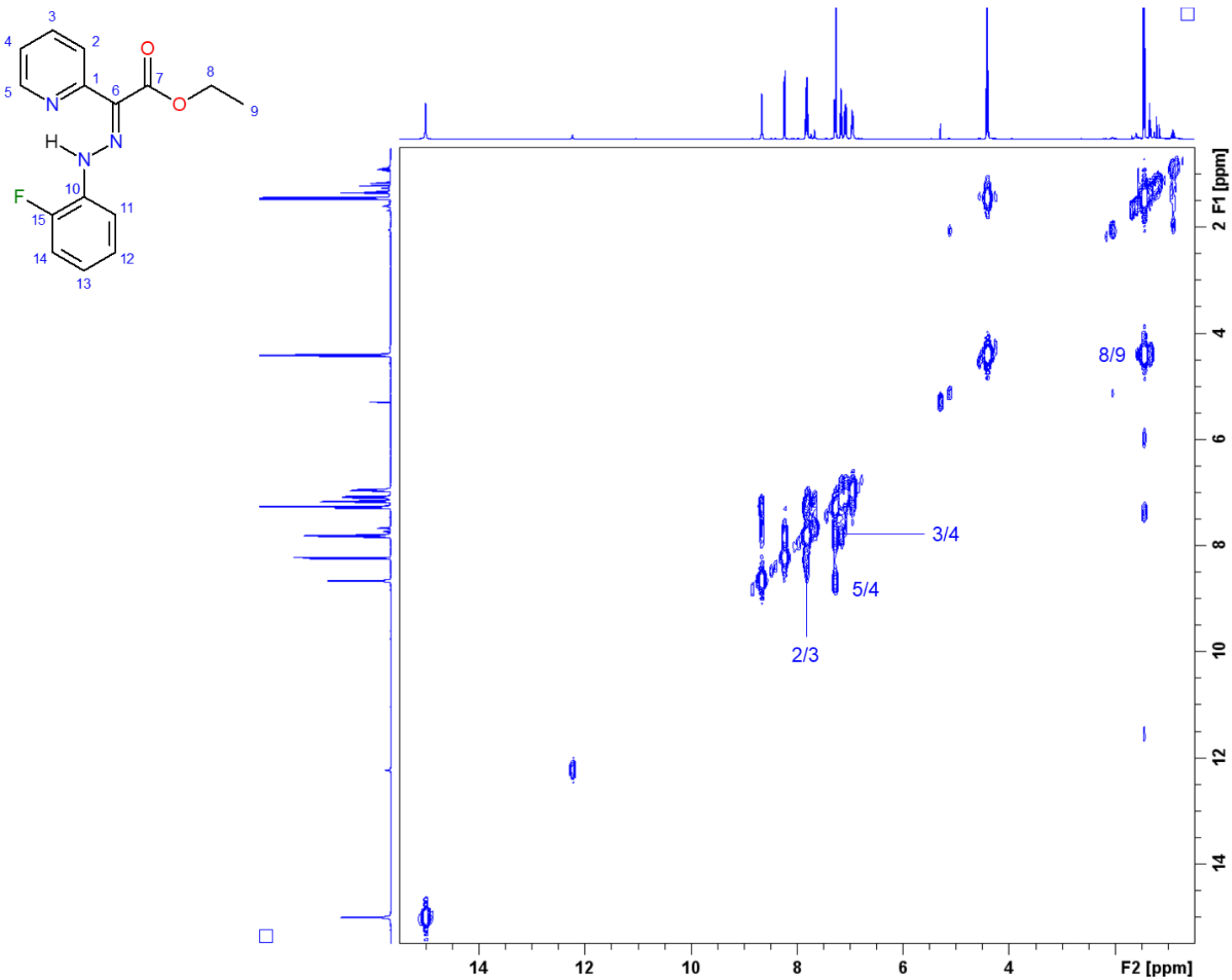

Figure S5. ^{1}H–^{1}H COSY correlation chart of **2-F**, $CDCl_3$, 500 MHz, 298 K.

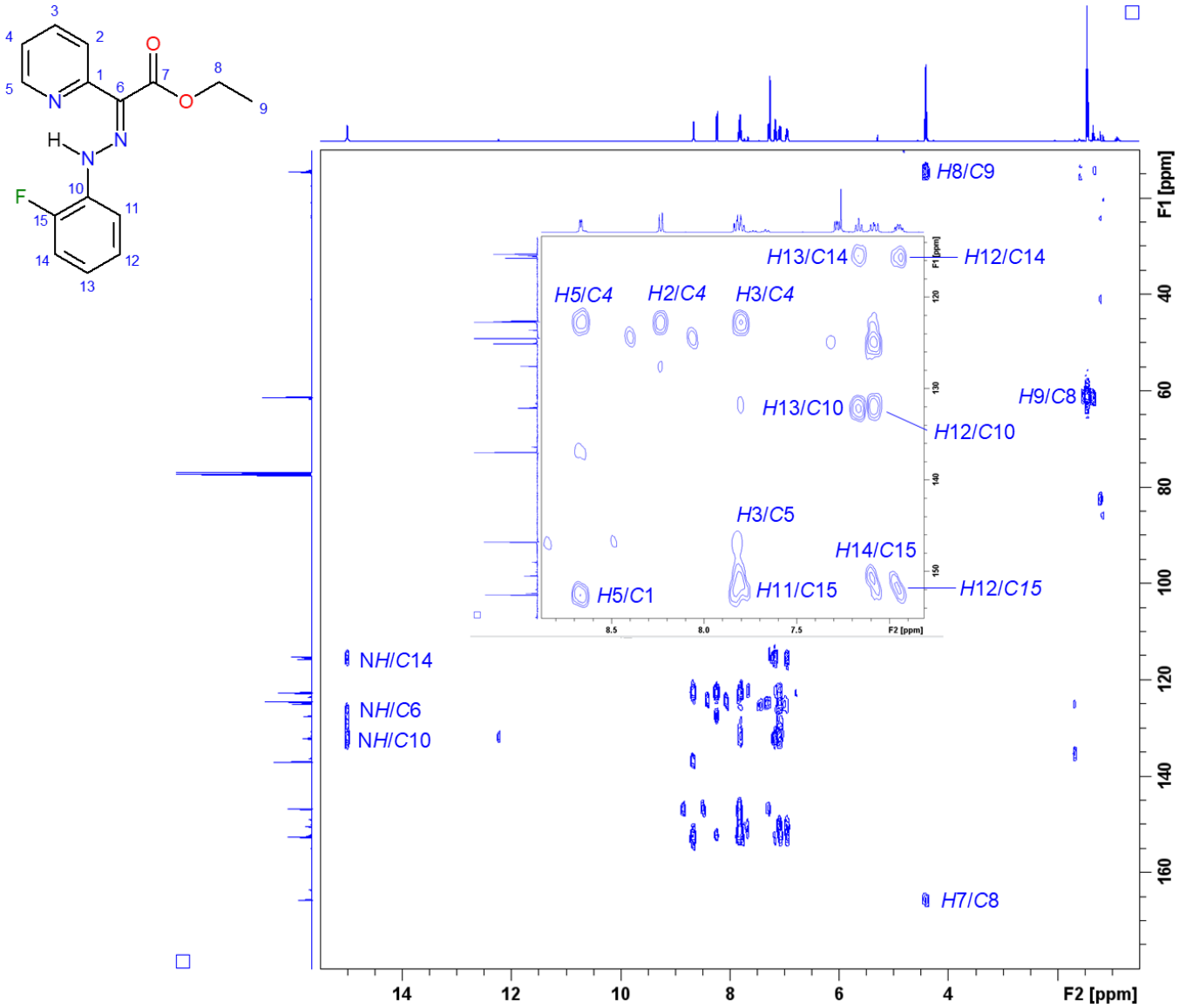

Figure S6. ^{13}C–^{1}H HMBC correlation chart of **2-F**, $CDCl_3$, 125 MHz–500 MHz, 298 K.

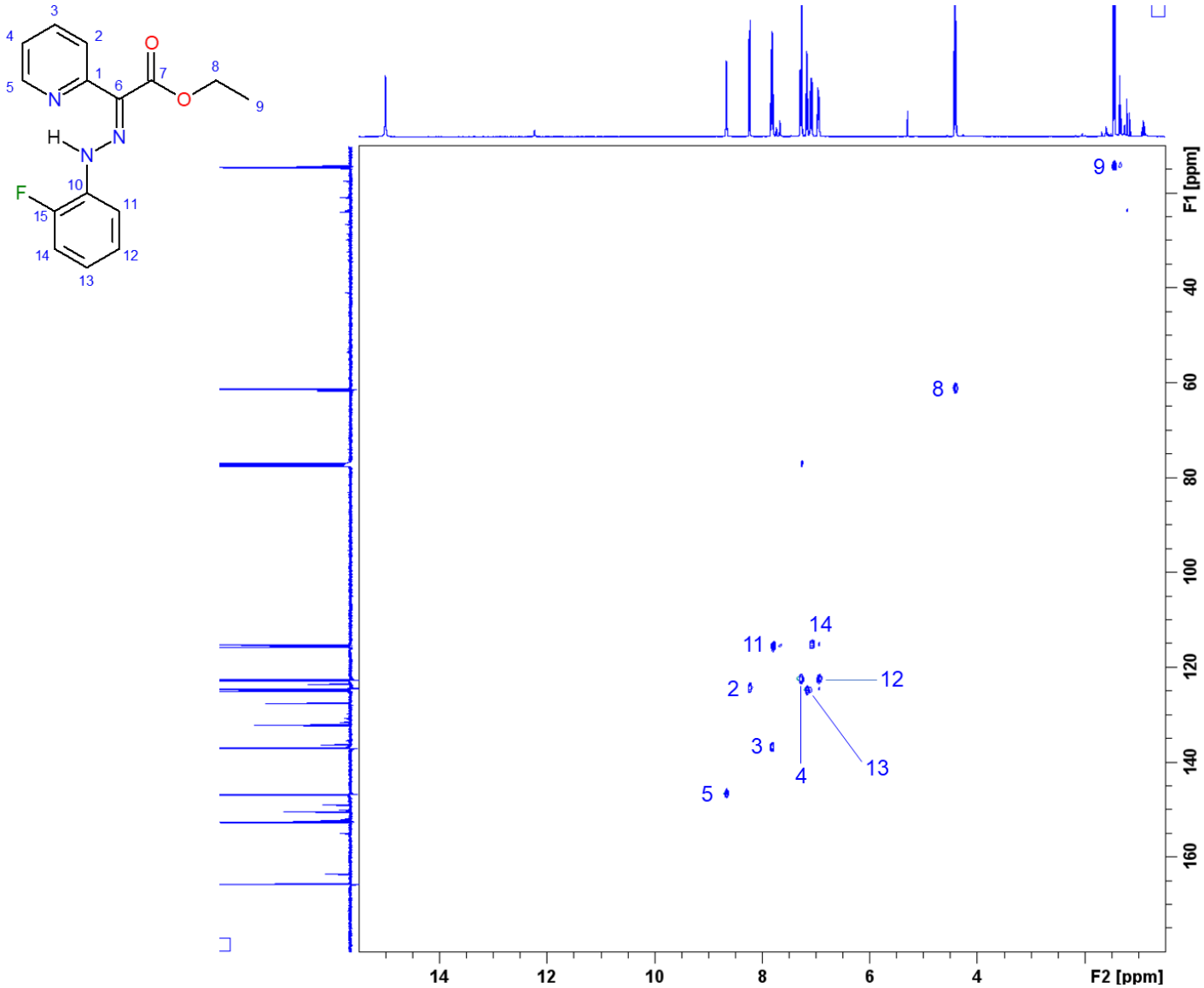

Figure S7. ^{13}C–^{1}H HSQC correlation chart of **2-F**, $CDCl_3$, 125 MHz–500 MHz, 298 K.

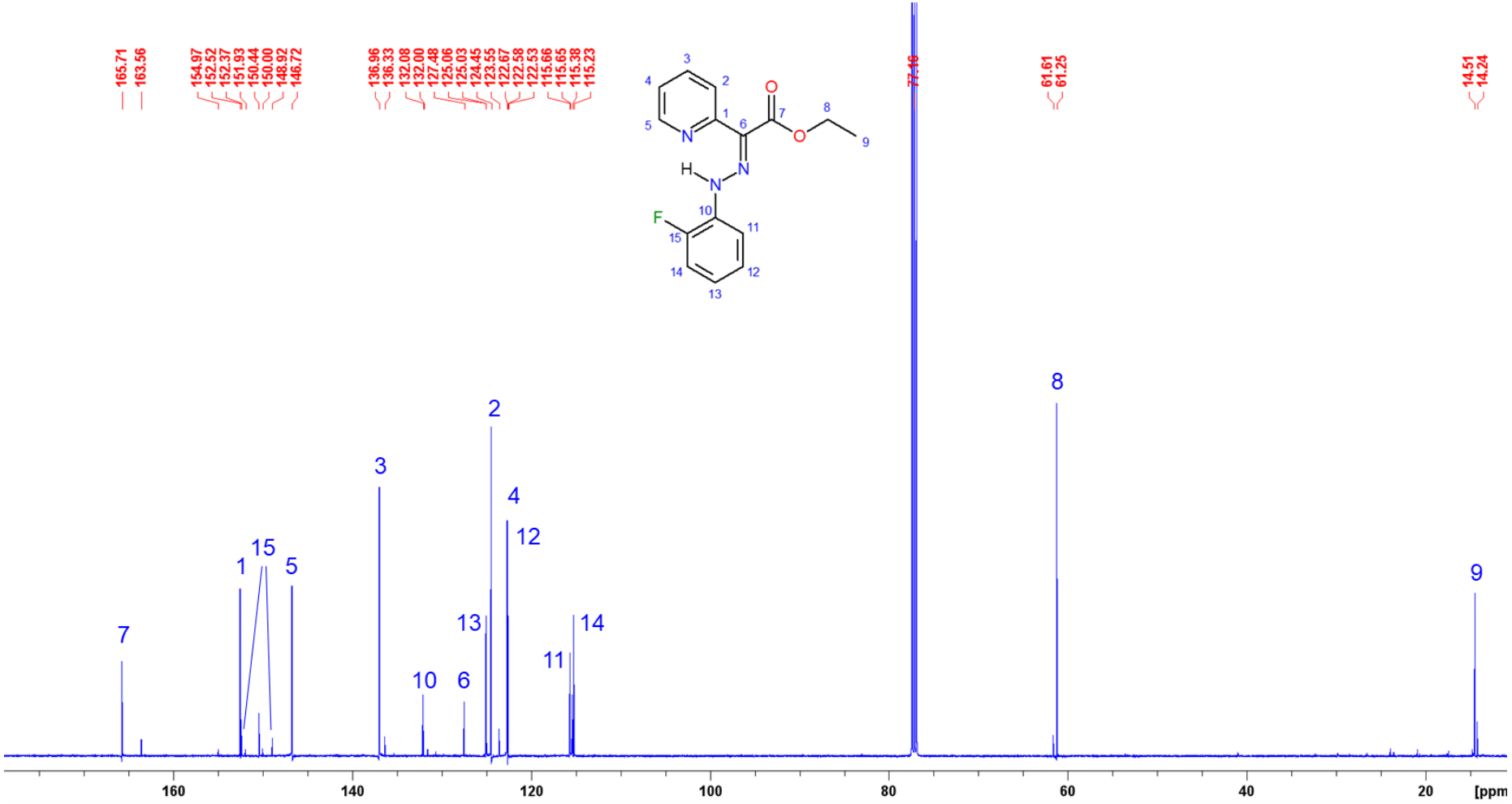

Figure S8. ^{13}C NMR spectrum of **2-F**, $CDCl_3$, 125 MHz, 298 K.

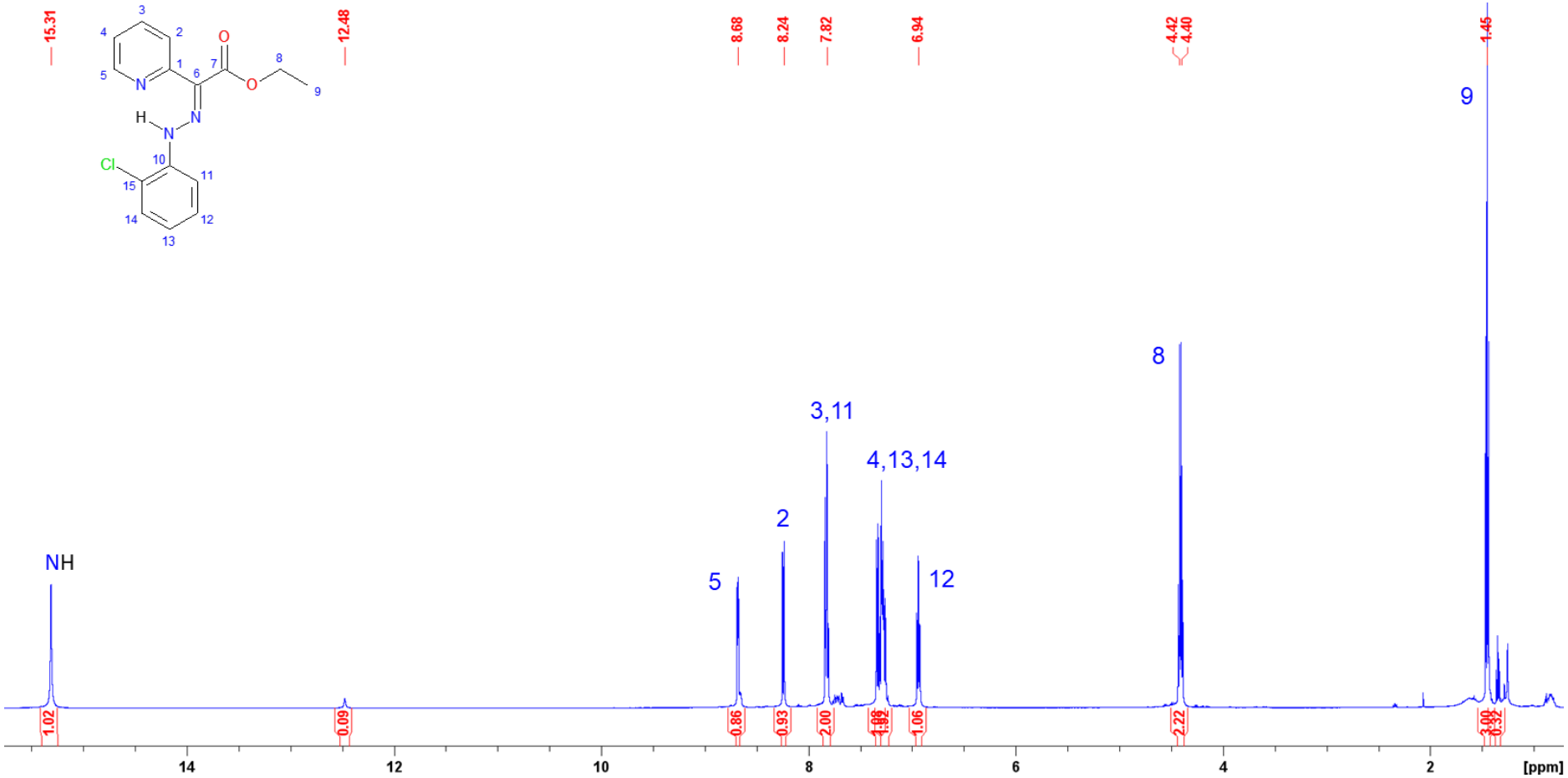

Figure S9. ^{1}H NMR spectrum of **2-Cl**, $CDCl_3$, 500 MHz, 298 K.

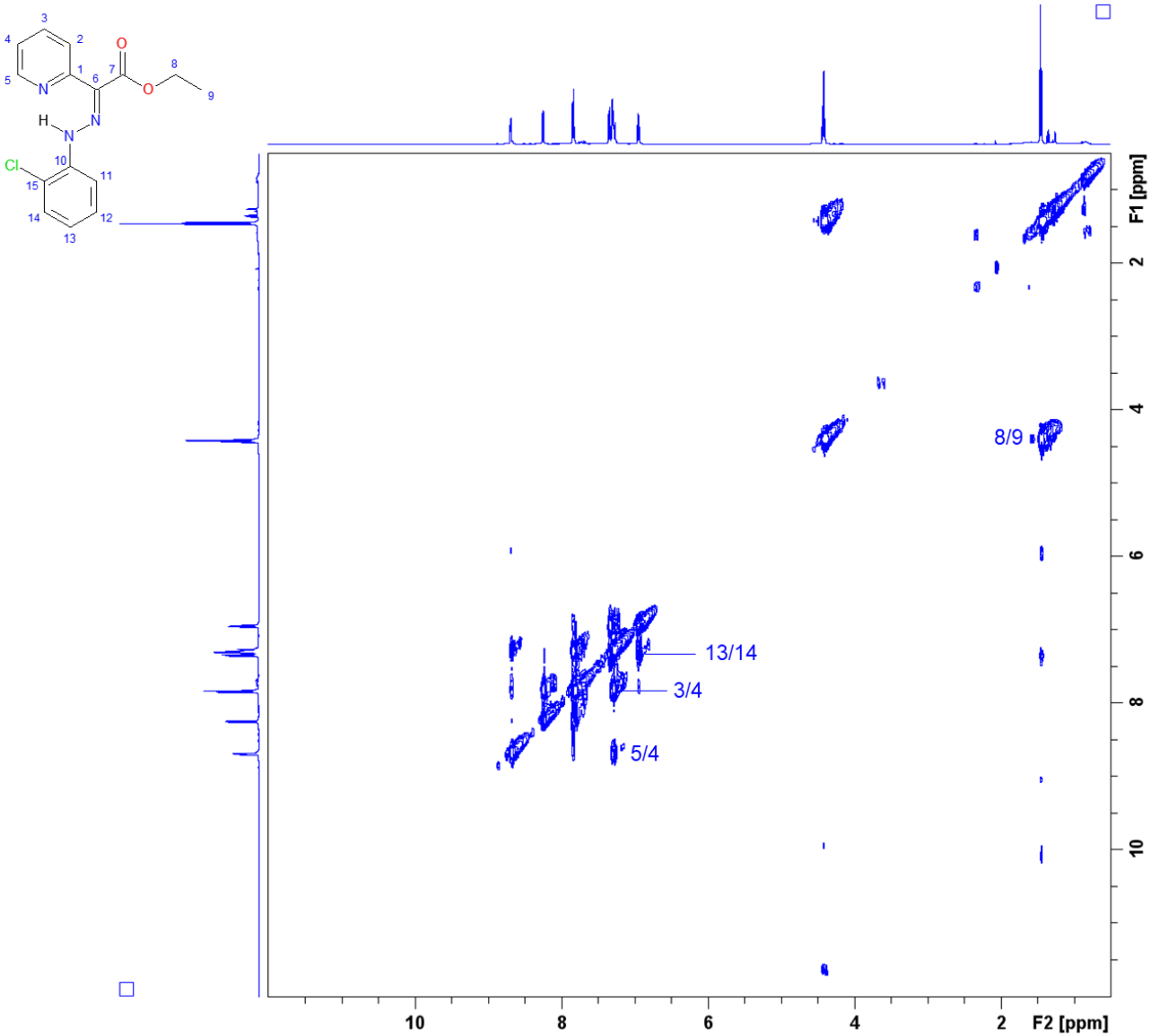

Figure S10. ^{1}H–^{1}H COSY correlation chart of **2-Cl**, $CDCl_3$, 500 MHz, 298 K.

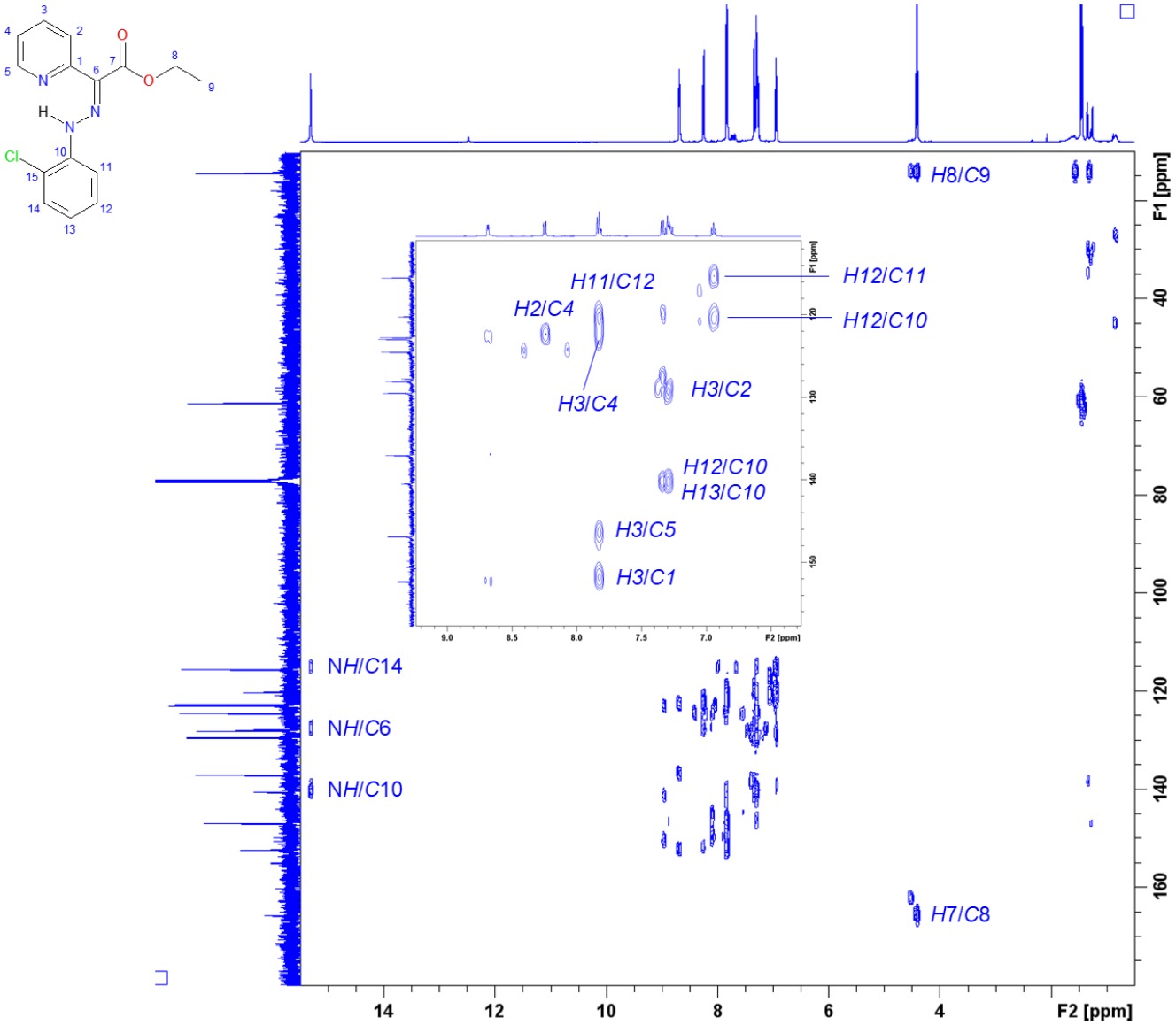

Figure S11. ^{13}C–^{1}H HMBC correlation chart of **2-Cl**, $CDCl_3$, 125 MHz–500 MHz, 298 K.

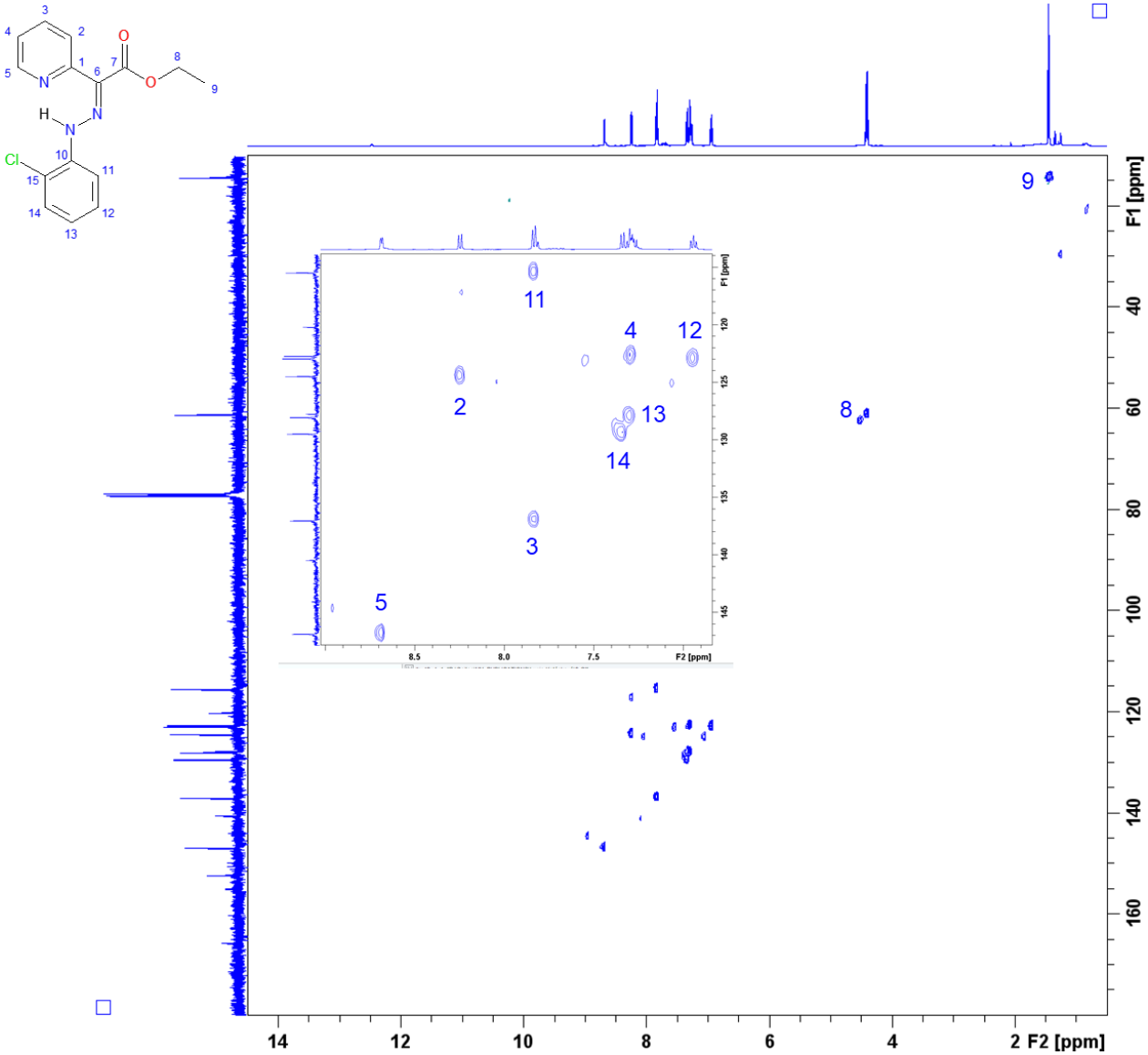

Figure S12. ^{13}C–^{1}H HSQC correlation chart of **2-Cl**, $CDCl_3$, 125 MHz–500 MHz, 298 K.

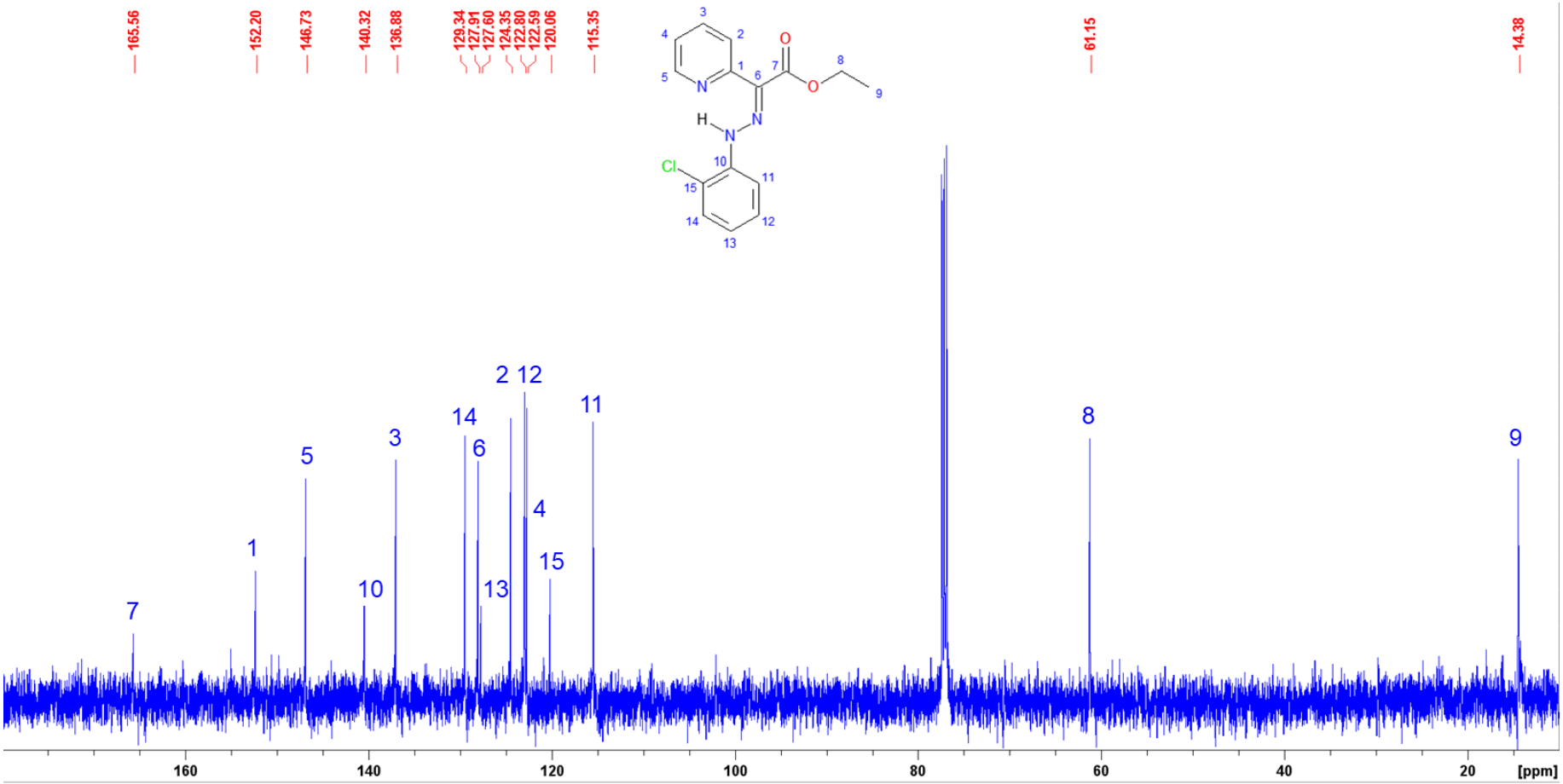

Figure S13. ^{13}C NMR spectrum of **2-Cl**, $CDCl_3$, 125 MHz, 298 K.

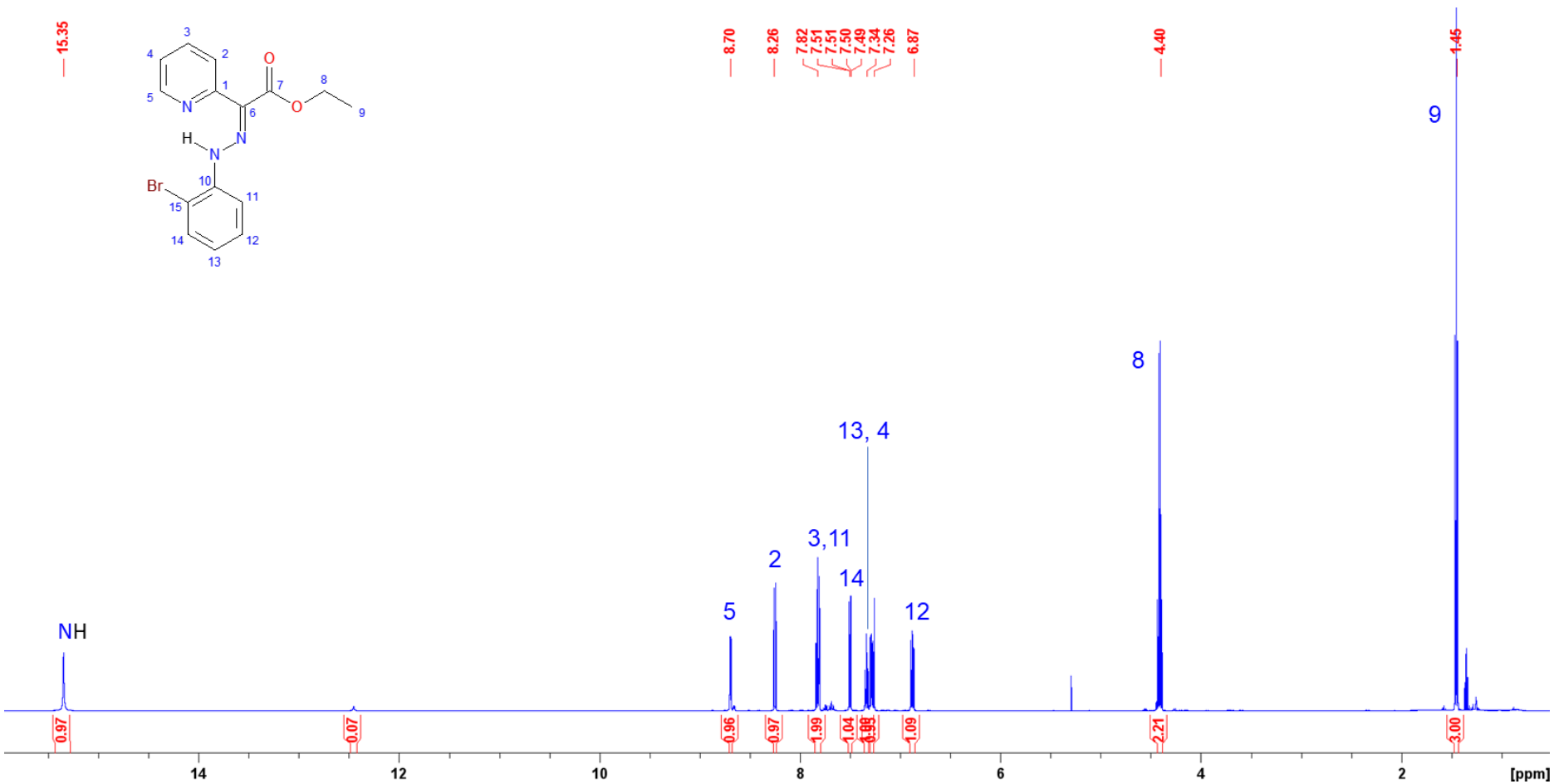

Figure S14. ^{1}H NMR spectrum of **2-Br**, $CDCl_3$, 500 MHz, 298 K.

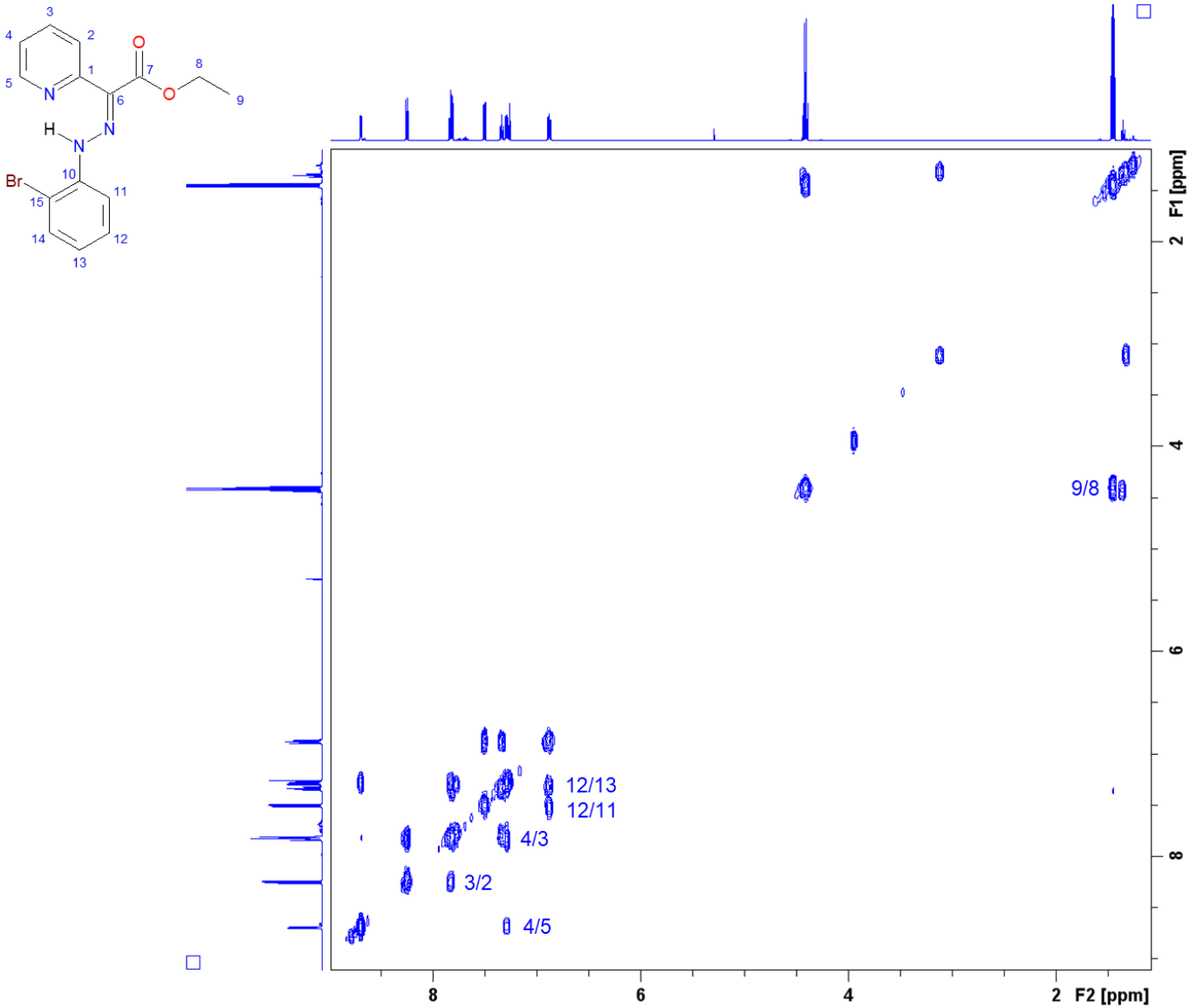

Figure S15. ^{1}H–^{1}H COSY correlation chart of **2-Br**, $CDCl_3$, 500 MHz, 298 K.

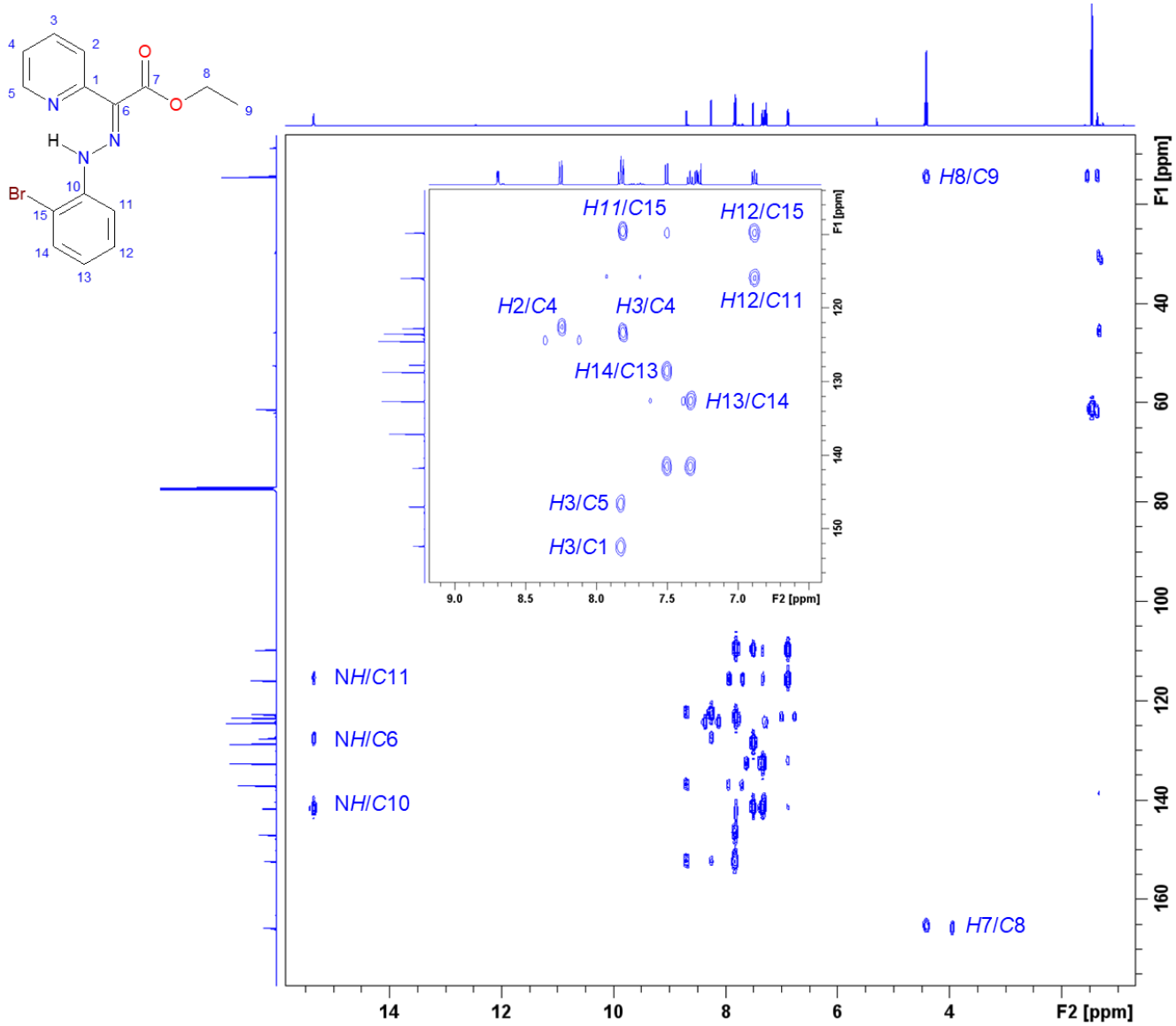

Figure S16. ^{13}C–^{1}H HMBC correlation chart of **2-Br**, $CDCl_3$, 125 MHz–500 MHz, 298 K.

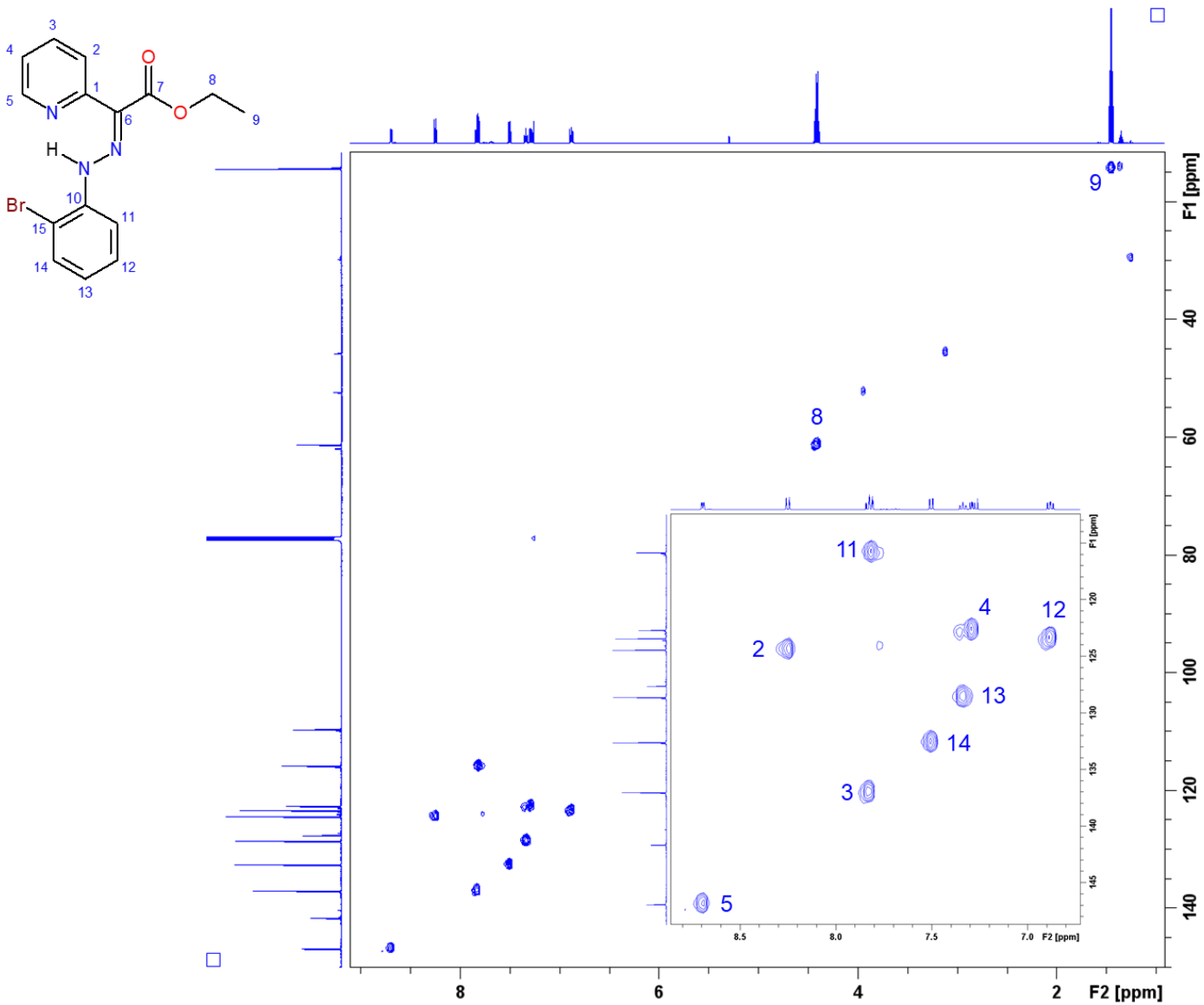

Figure S17. ^{13}C–^{1}H HSQC correlation chart of **2-Br**, $CDCl_3$, 125 MHz–500 MHz, 298 K.

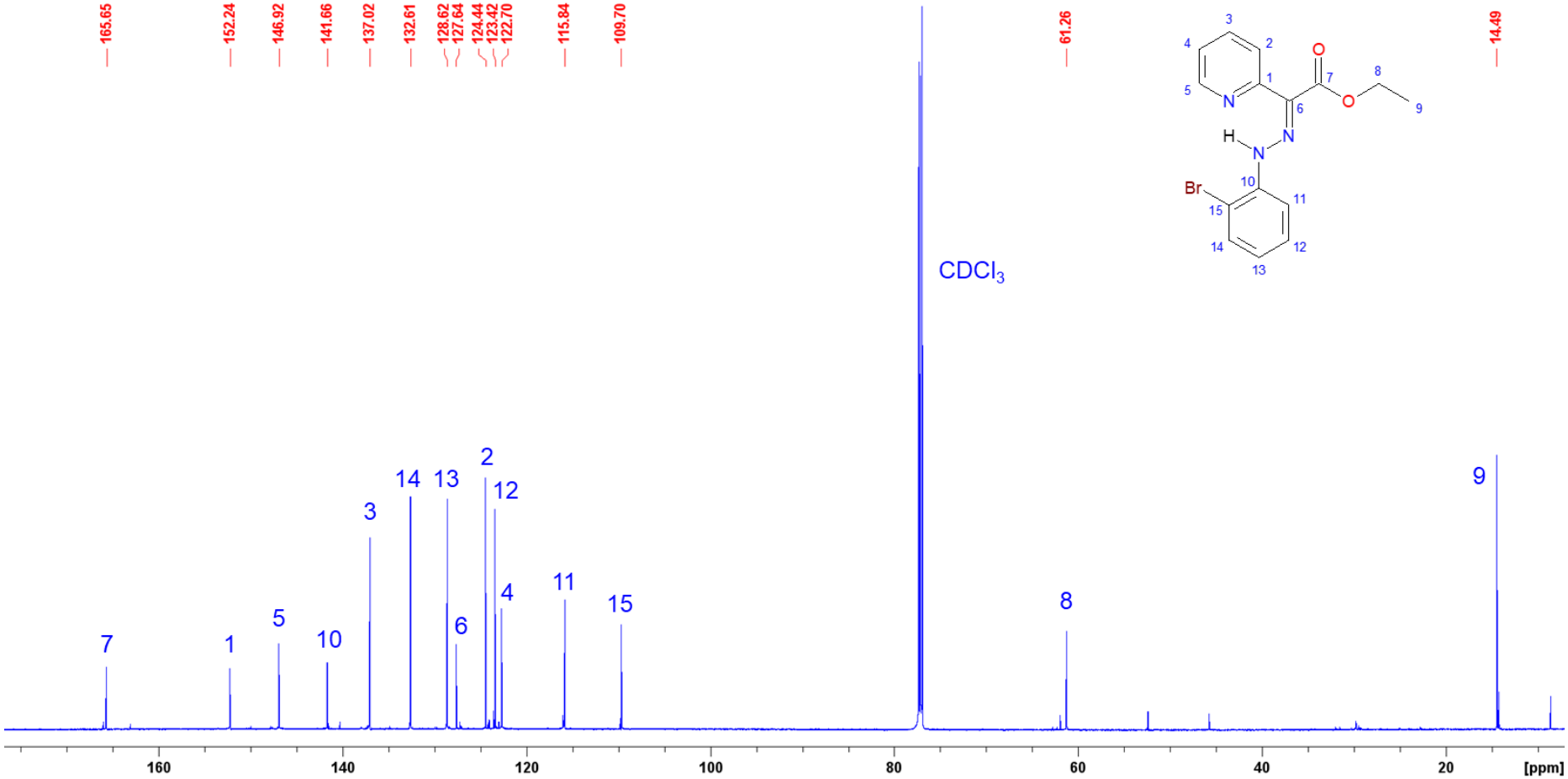

Figure S18. ^{13}C NMR spectrum of **2-Br**, $CDCl_3$, 125 MHz, 298 K.

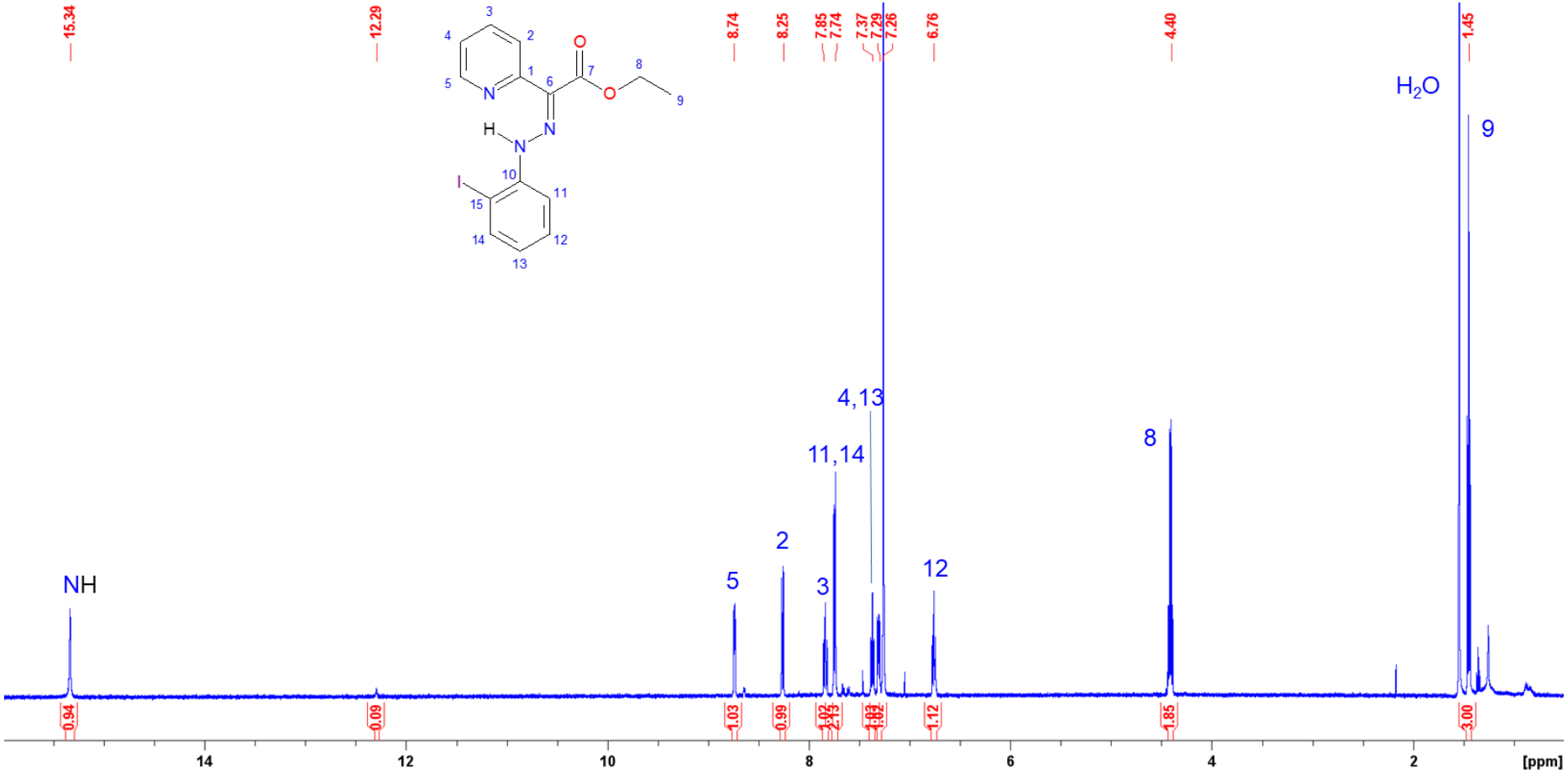

Figure S19. ^{1}H NMR spectrum of **2-I**, $CDCl_3$, 500 MHz, 298 K.

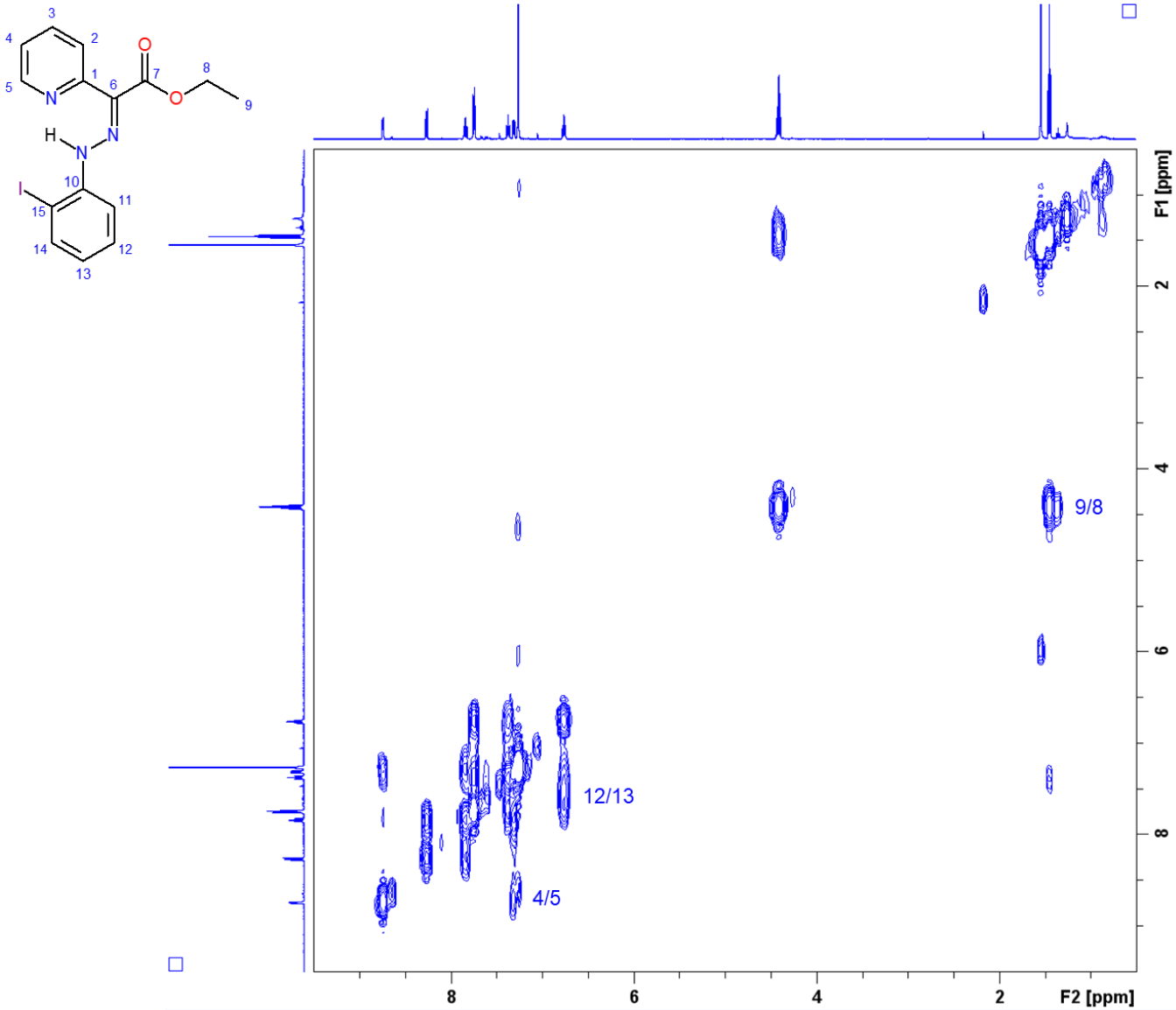

Figure S20. ^{1}H–^{1}H COSY correlation chart of **2-I**, $CDCl_3$, 500 MHz, 298 K.

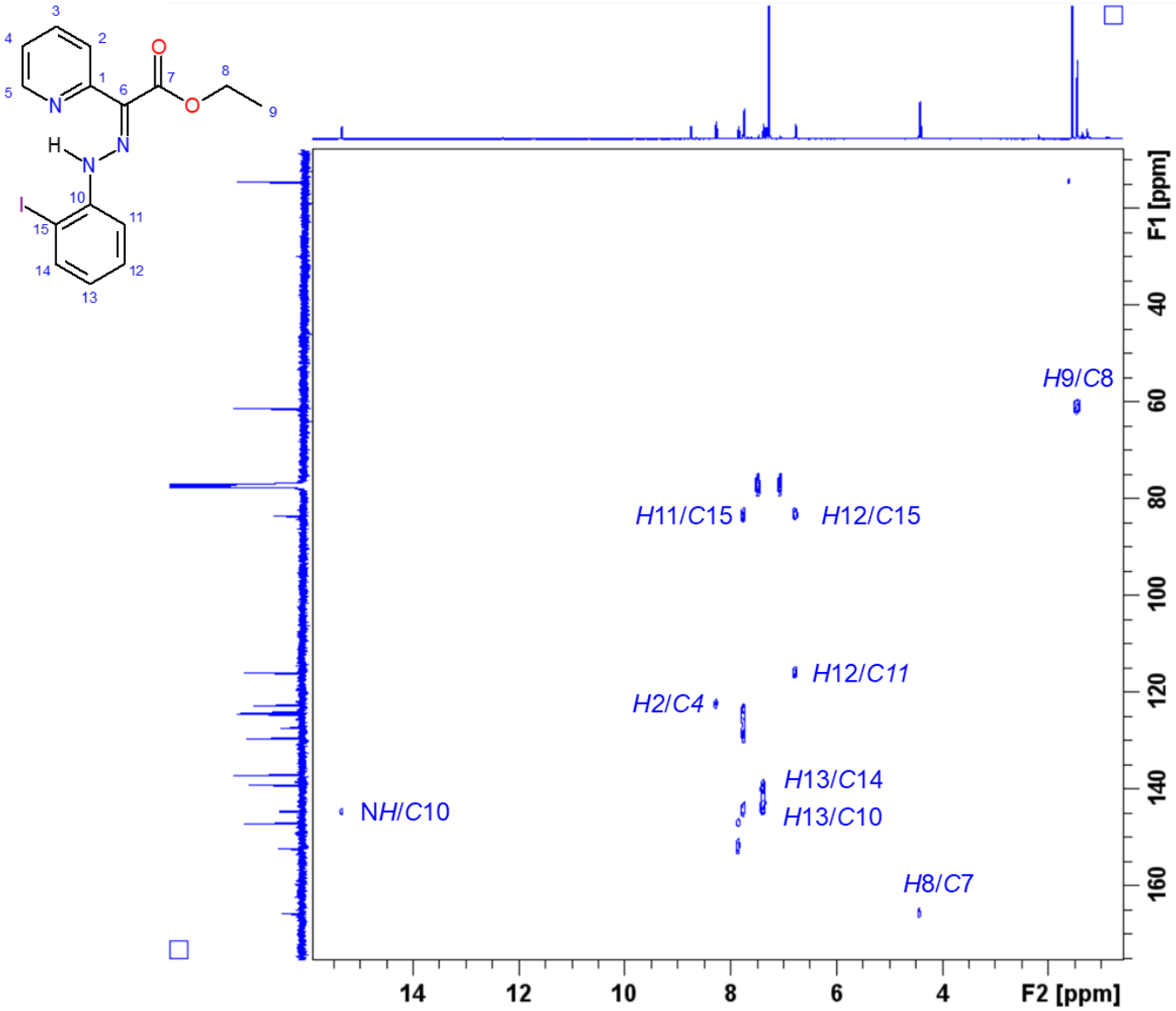

Figure S21. ^{13}C–^{1}H HMBC correlation chart of **2-I**, $CDCl_3$, 125 MHz–500 MHz, 298 K.

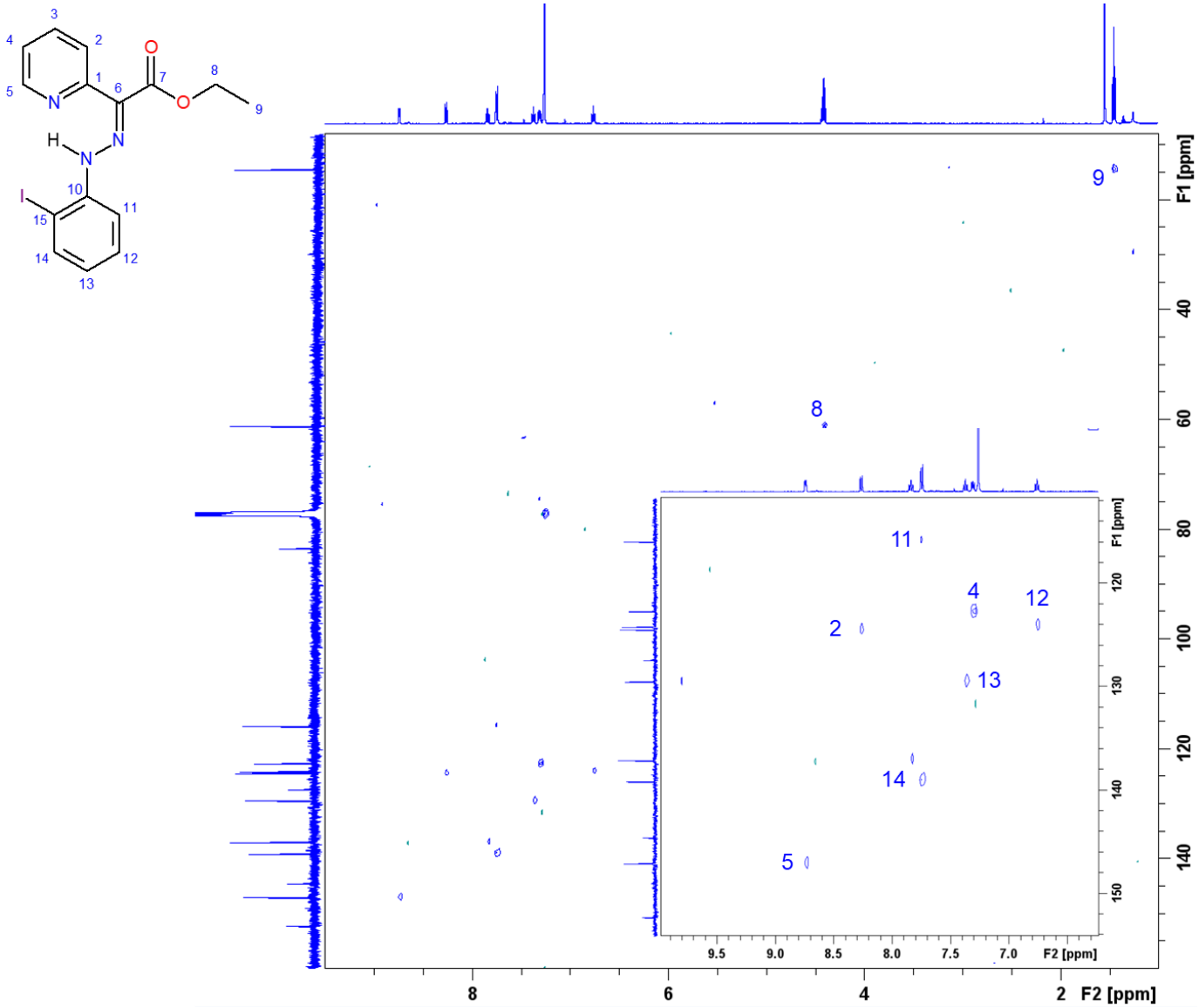

Figure S22. ^{13}C–^{1}H HSQC correlation chart of **2-I**, $CDCl_3$, 125 MHz–500 MHz, 298 K.

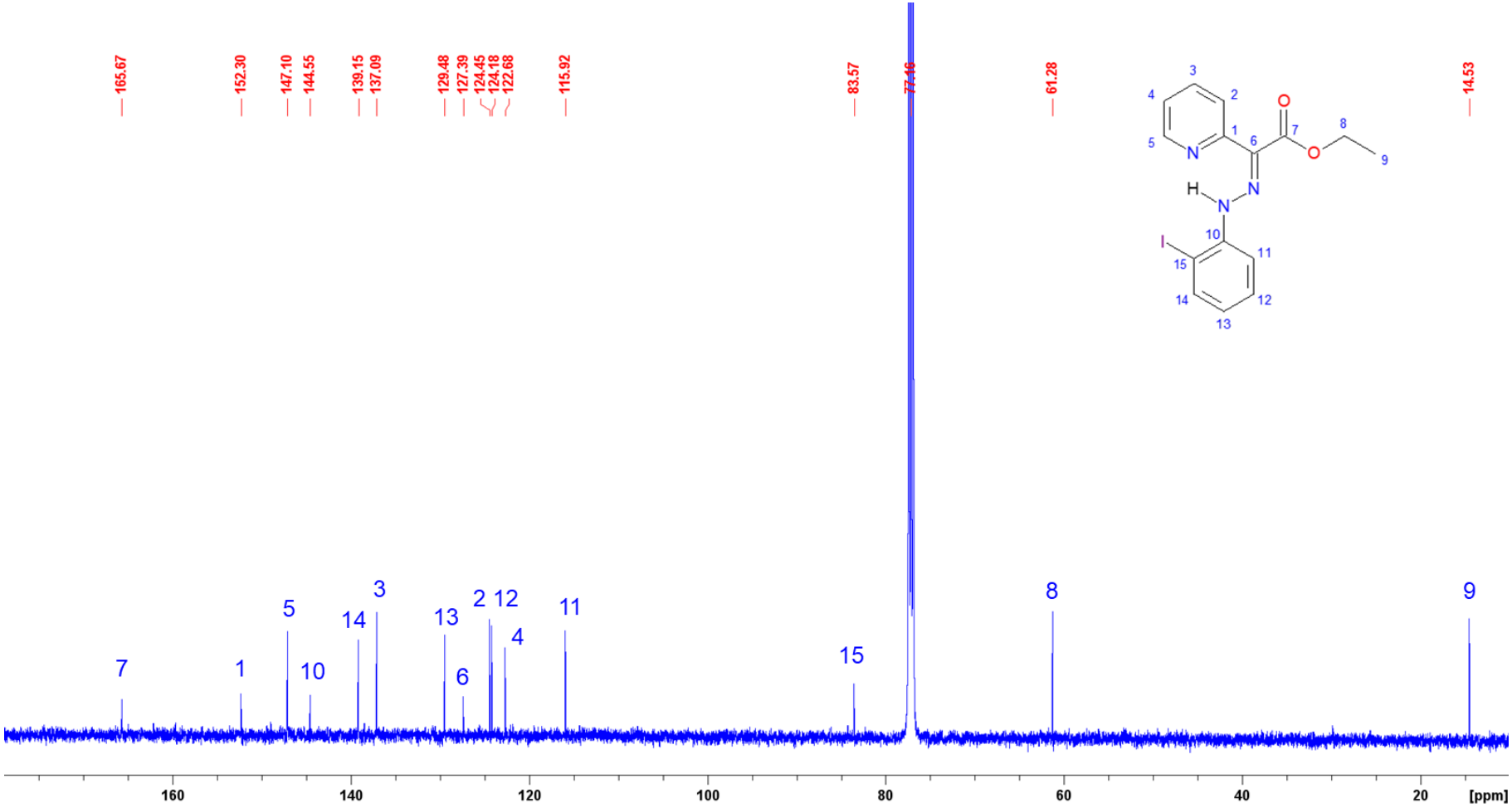

Figure S23. ^{13}C NMR spectrum of **2-I**, $CDCl_3$, 125 MHz, 298 K.

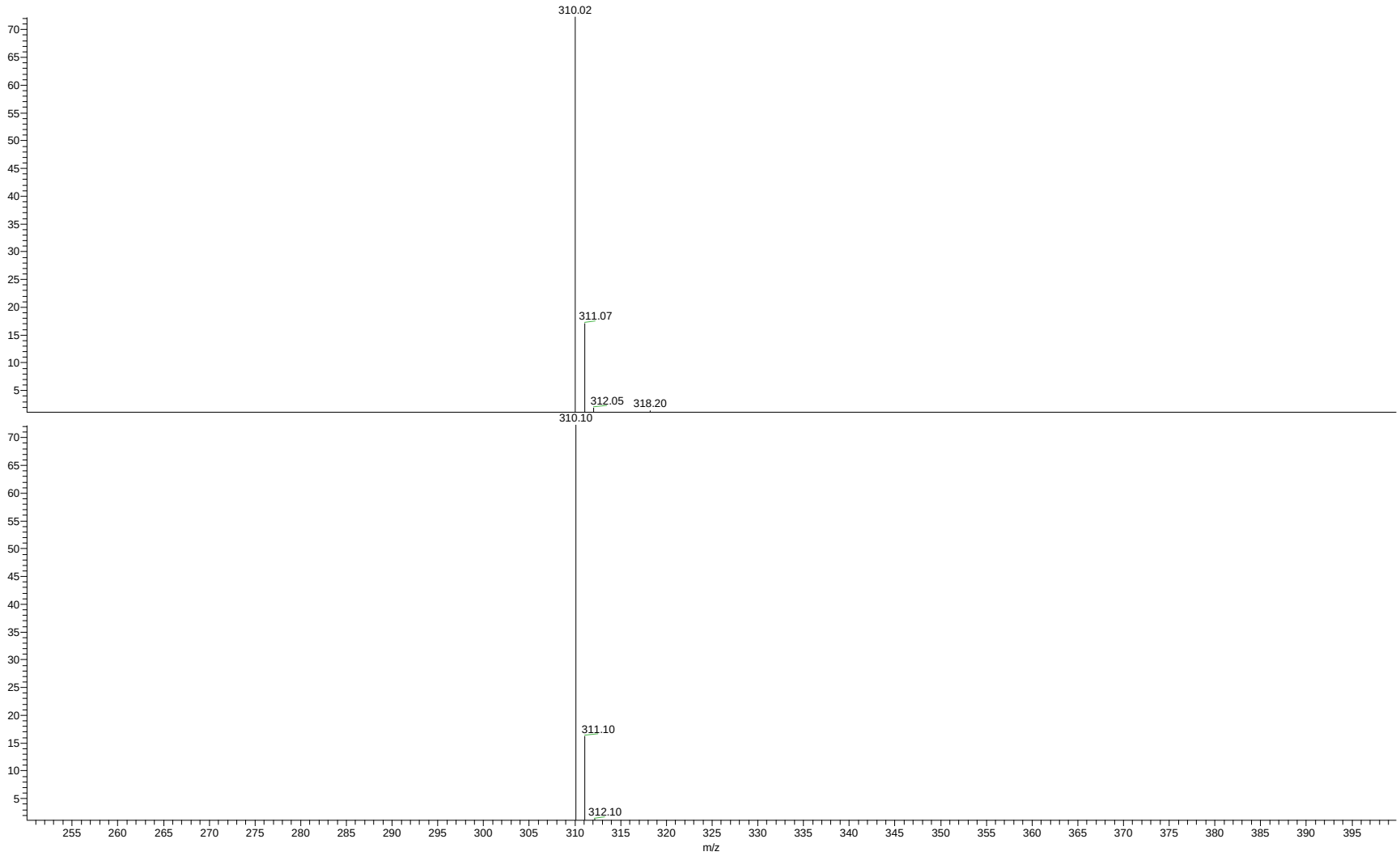

Figure S24. MS spectrum of **2-F** in MeOH ($[C_{15}H_{14}N_3O_2F+Na]^+$ ion, top) and simulated spectrum (bottom).

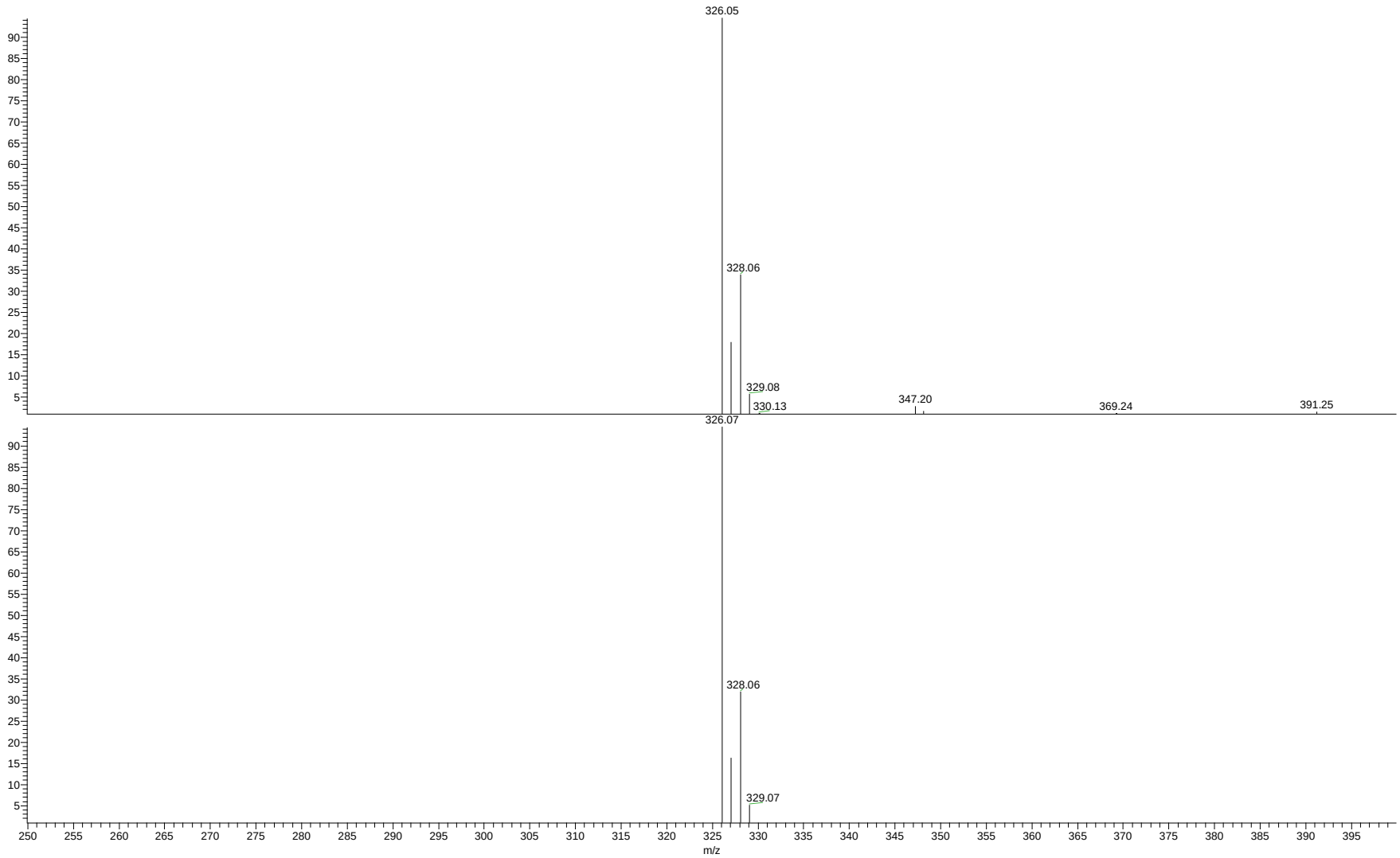

Figure S25. MS spectrum of **2-Cl** in MeOH ($[C_{15}H_{14}N_3O_2Cl+Na]^+$ ion, top) and simulated spectrum (bottom).

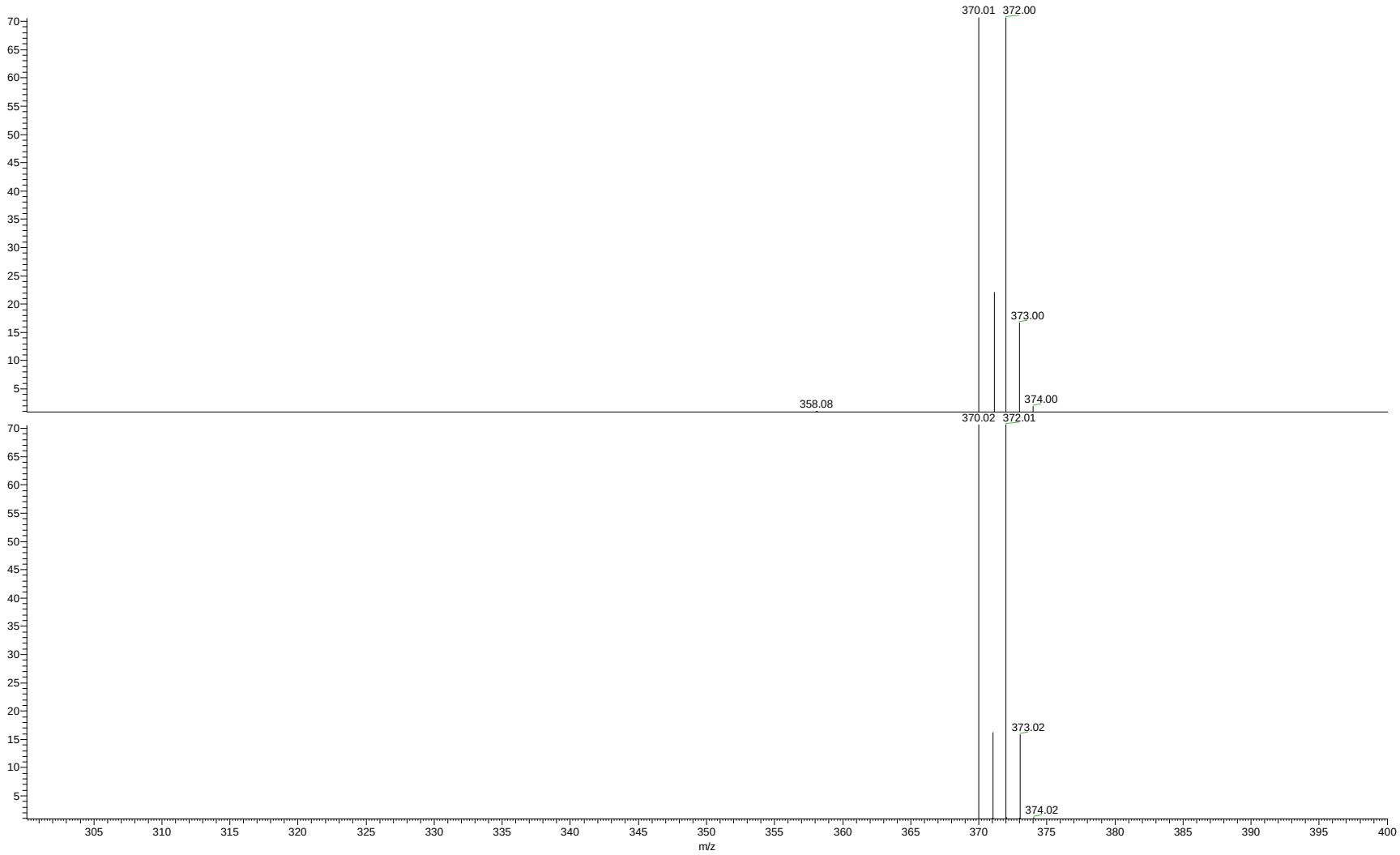

Figure S26. MS spectrum of **2-Br** in MeOH ($[C_{15}H_{14}N_3O_2Br+Na]^+$ ion, top) and simulated spectrum (bottom).

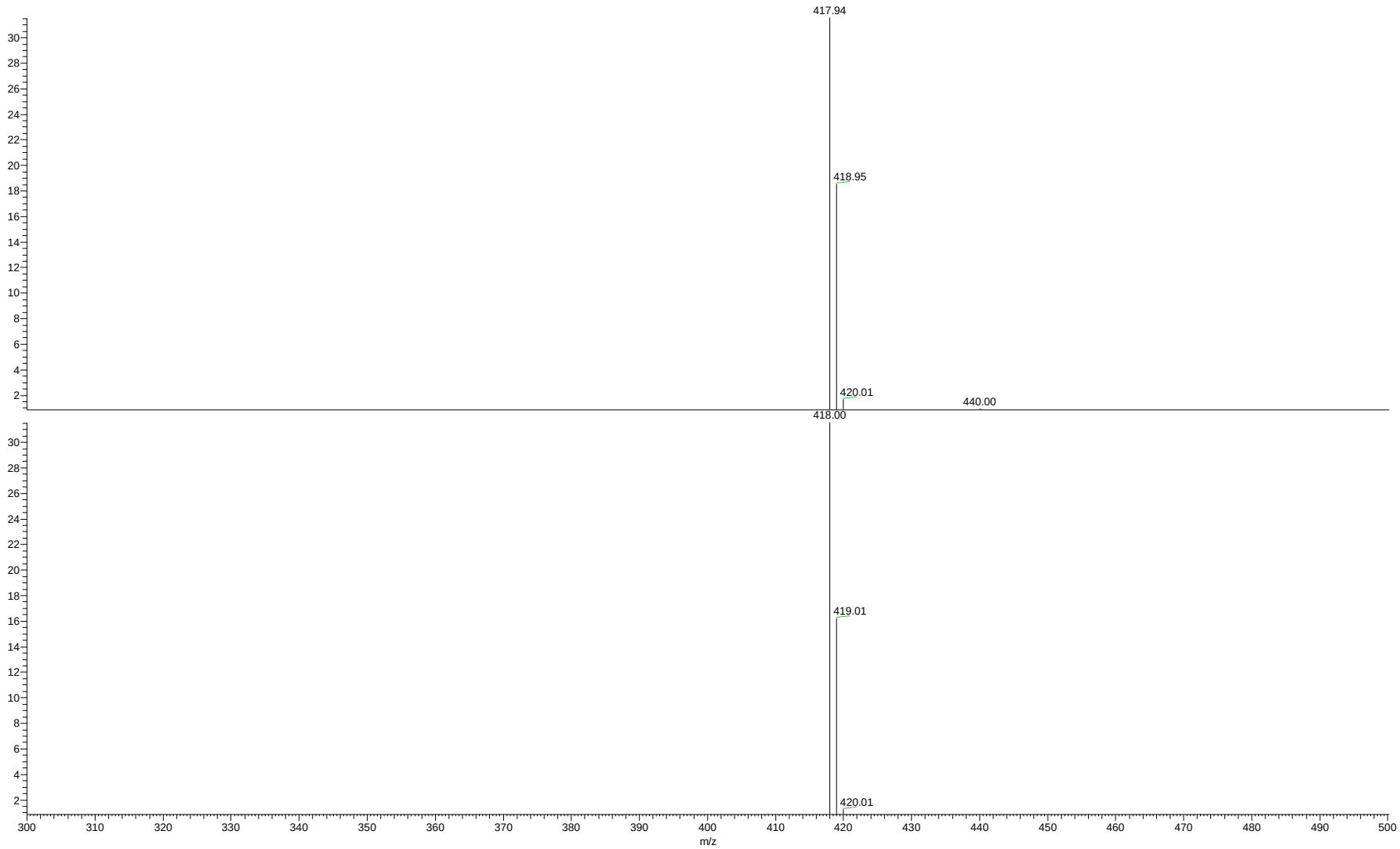

Figure S27. MS spectrum of **2-I** in MeOH ($[C_{15}H_{14}N_3O_2I+Na]^+$ ion, top) and simulated spectrum (bottom).

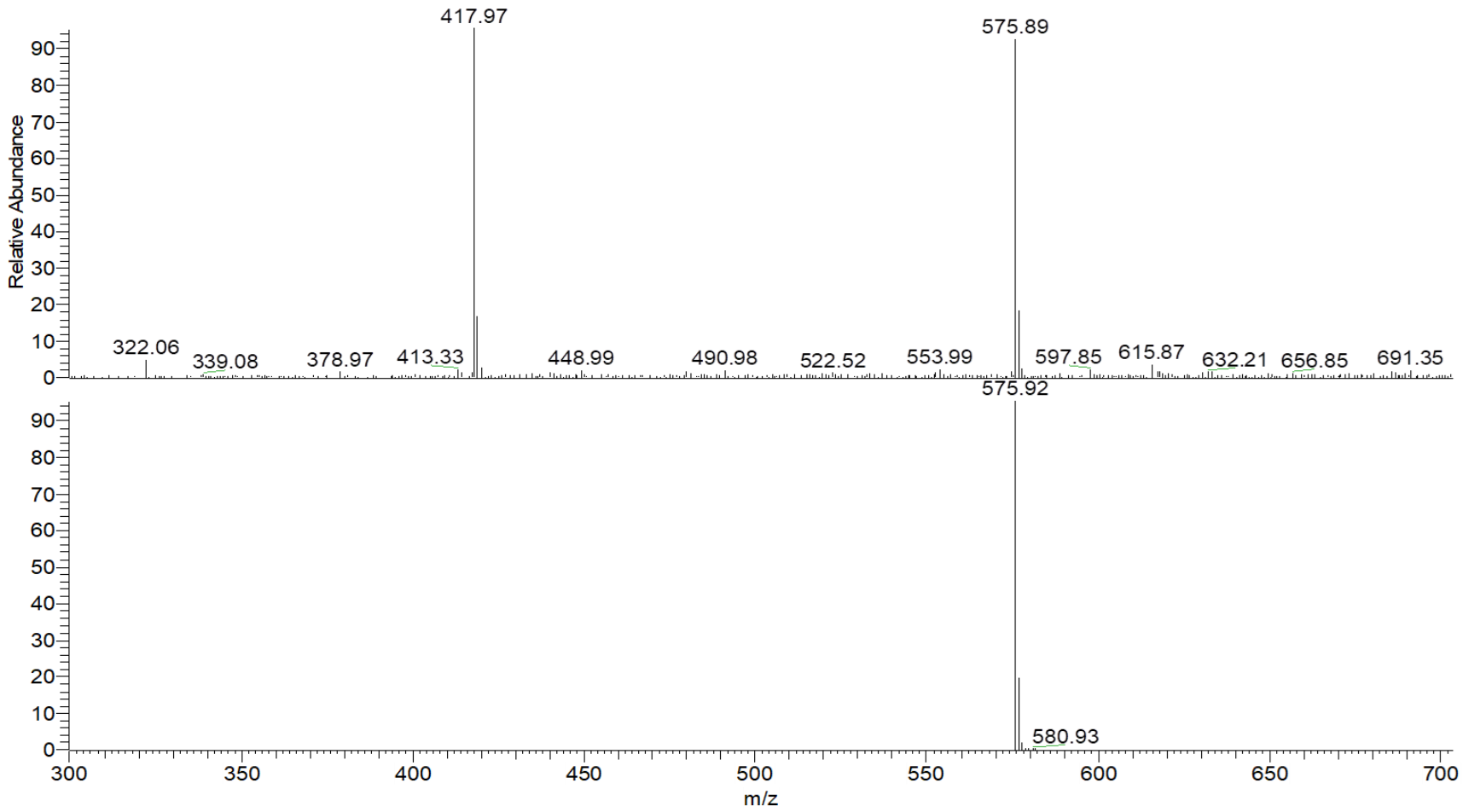

Figure S28. Top – MS spectrum of mixture of compounds **2-I** ($[C_{15}H_{14}N_3O_2I+Na]^+$ ion) and **2-I_azo** ($[C_{18}H_{13}N_5I_2+Na]^+$ ion) in MeOH. Bottom – simulated spectrum for **2-I_azo**.

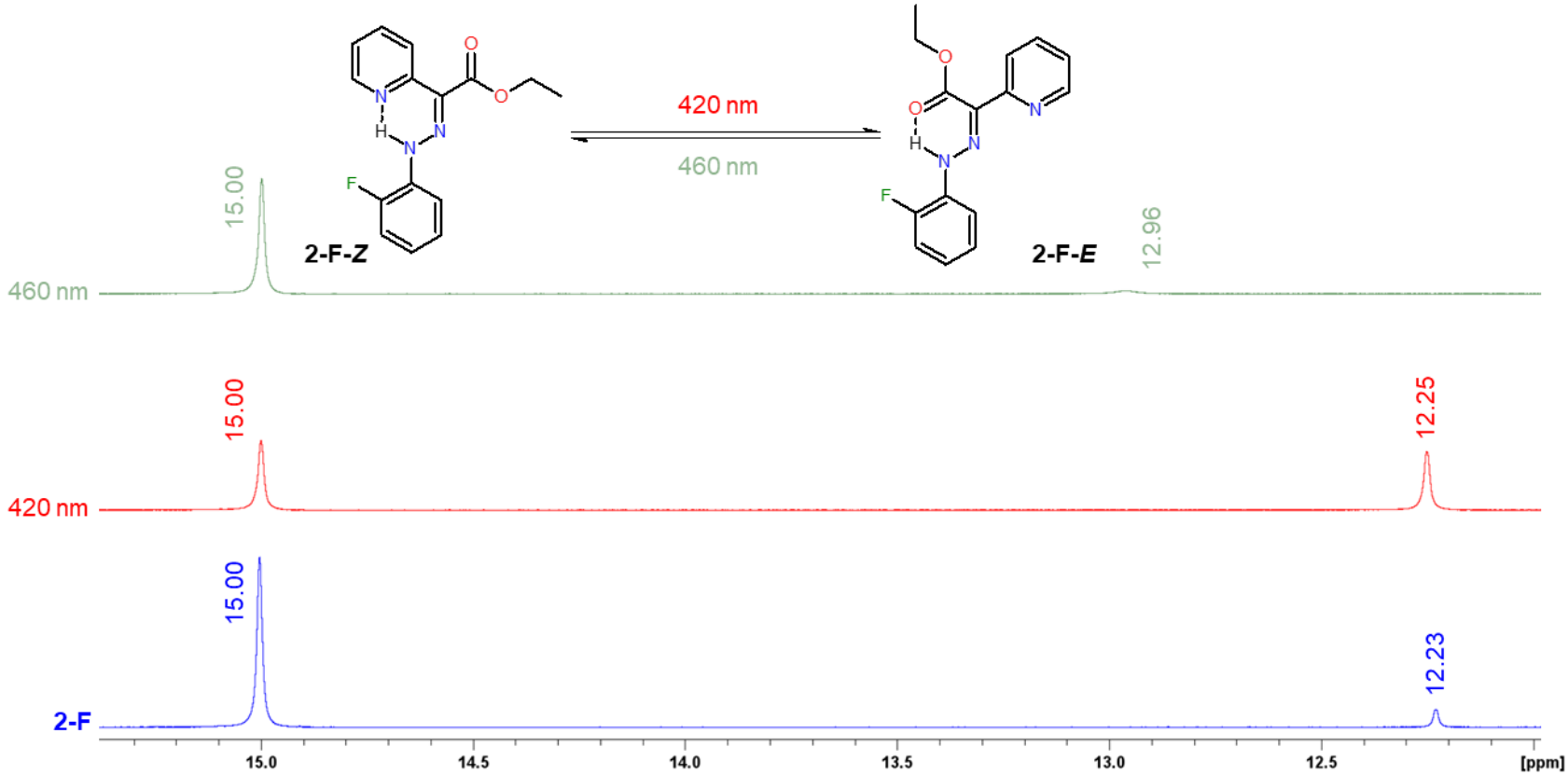

Figure S29. Comparison of N–*H* shift (ppm) of **2-F**. ^{1}H NMR spectrum of obtained **2-F** in blue. ^{1}H NMR spectrum after 420 nm/30 min. ^{1}H NMR spectrum after 460 nm/30 min. in green. $CDCl_3$, 500 MHz, 298 K.

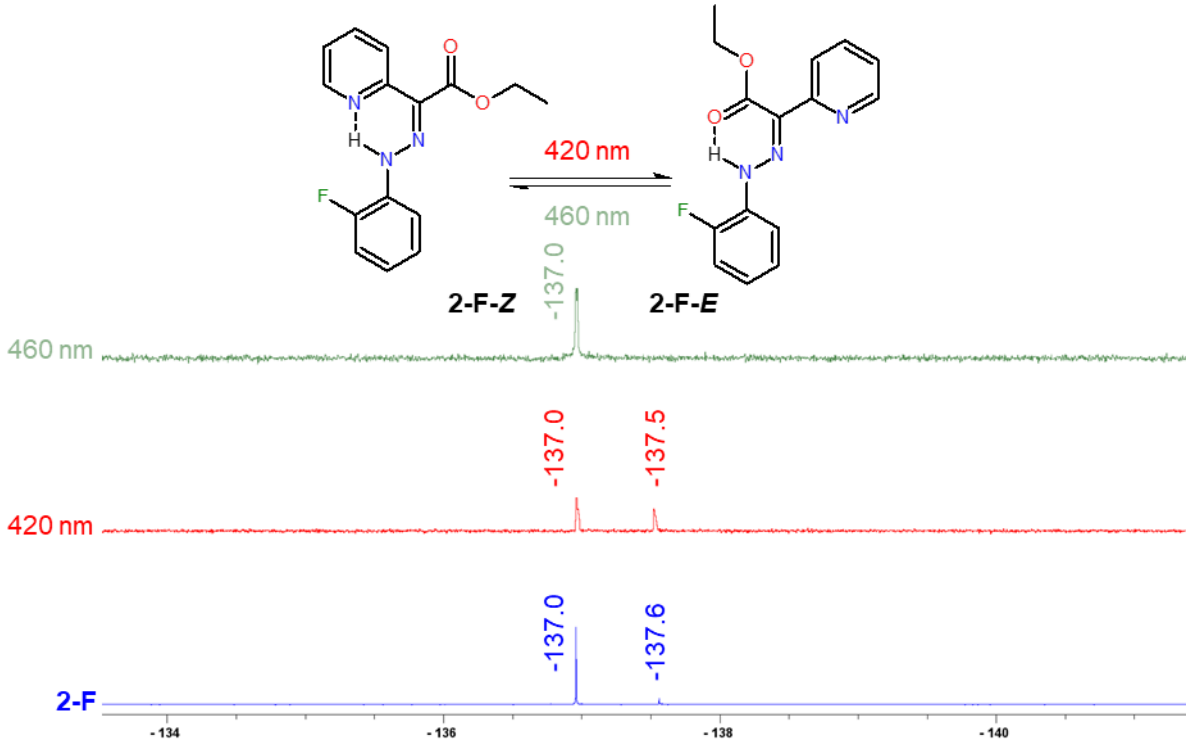

Figure S30. Comparison of C–*F* shift (ppm) of **2-F**. ^{19}F NMR spectrum of obtained **2-F** (blue). ^{19}F NMR spectrum after 420 nm/30 min (red). ^{19}F NMR spectrum after 460 nm/30 min. (green). $CDCl_3$, 470 MHz, 298 K, ref. CF_3COOH $\delta = -78.50$ ppm.

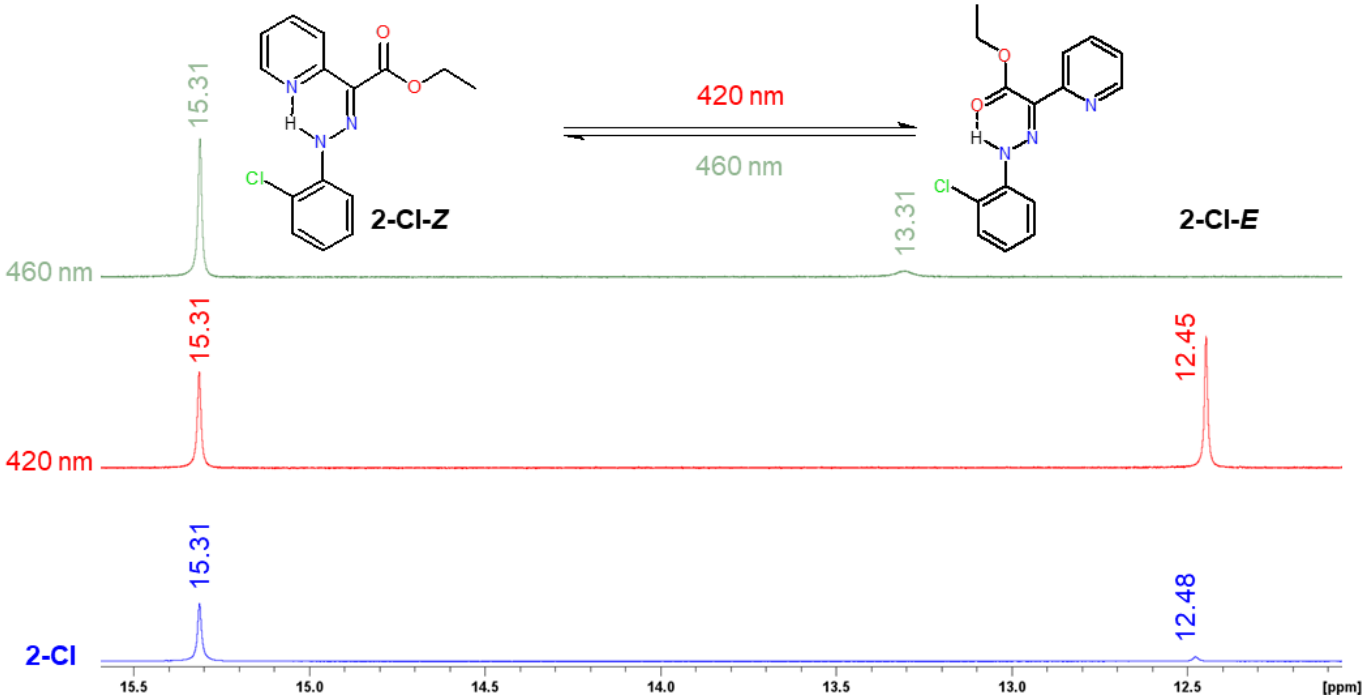

Figure S31. Comparison of N–*H* shift (ppm) of **2-Cl.** ^{1}H NMR spectrum of obtained **2-Cl** (blue). ^{1}H NMR spectrum after 420 nm/30 min (red). ^{1}H NMR spectrum after 460 nm/30 min. (green). $CDCl_3$, 500 MHz, 298 K.

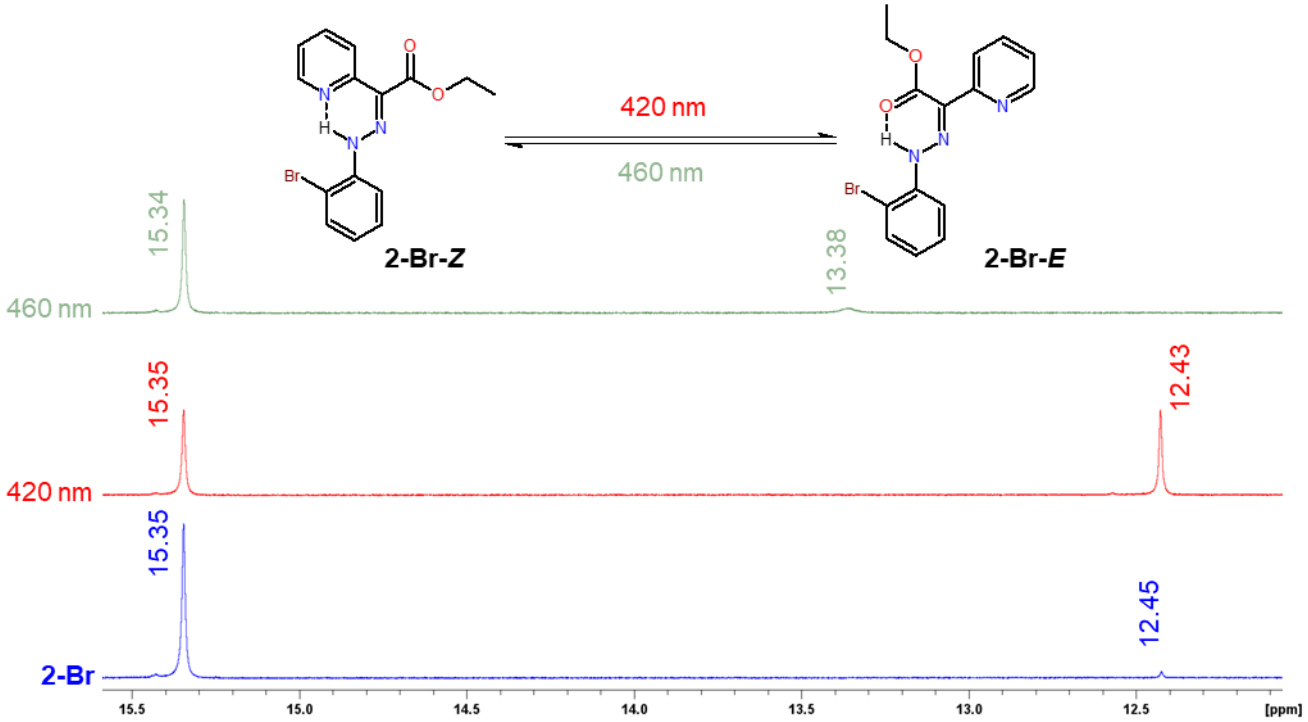

Figure S32. Comparison of N–*H* shift (ppm) of **2-Br**. ^{1}H NMR spectrum of obtained **2-Br** in blue. ^{1}H NMR spectrum after 420 nm/30 min. ^{1}H NMR spectrum after 460 nm/30 min. in green. $CDCl_3$, 500 MHz, 298 K.

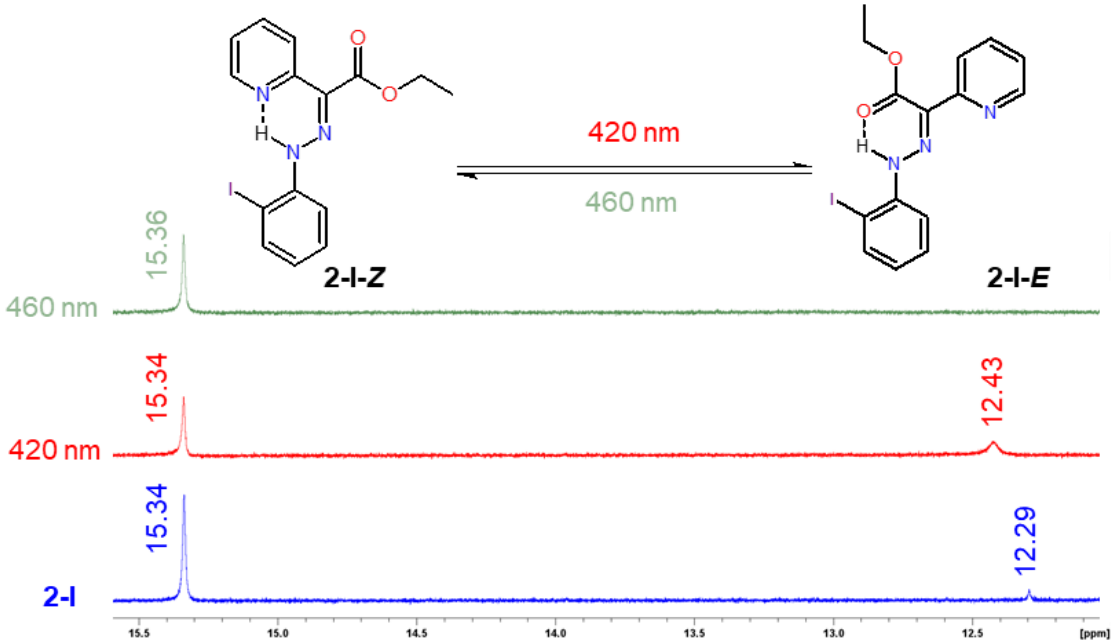

Figure S33. Comparison of N–*H* shift (ppm) of **2-I**. ^{1}H NMR spectrum of obtained **2-I** in blue. ^{1}H NMR spectrum after 420 nm/30 min. ^{1}H NMR spectrum after 460 nm/30 min. in green. $CDCl_3$, 500 MHz, 298 K.

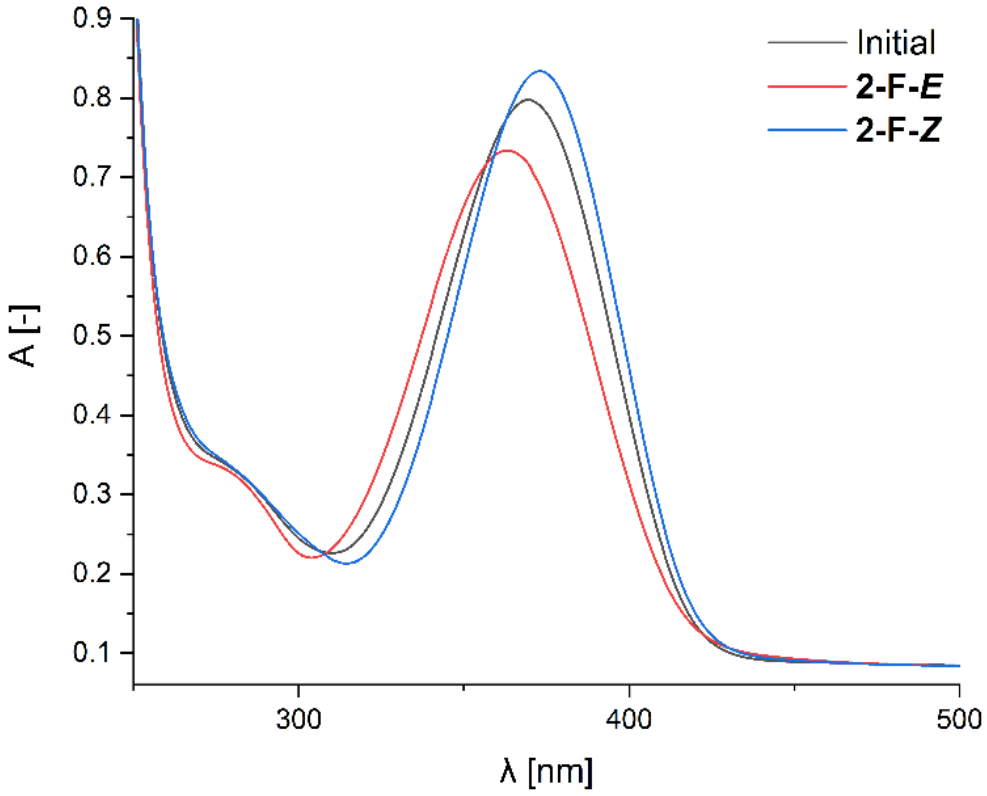

Figure S34. UV-VIS spectrum of compound **2-F** before (black line) and after irradiation at 420 nm (**2-F-*E***, red line) and 460 nm (**2-F-*Z***, blue line) for 30 minutes (2.73×10^{-5} M, $CHCl_3$).

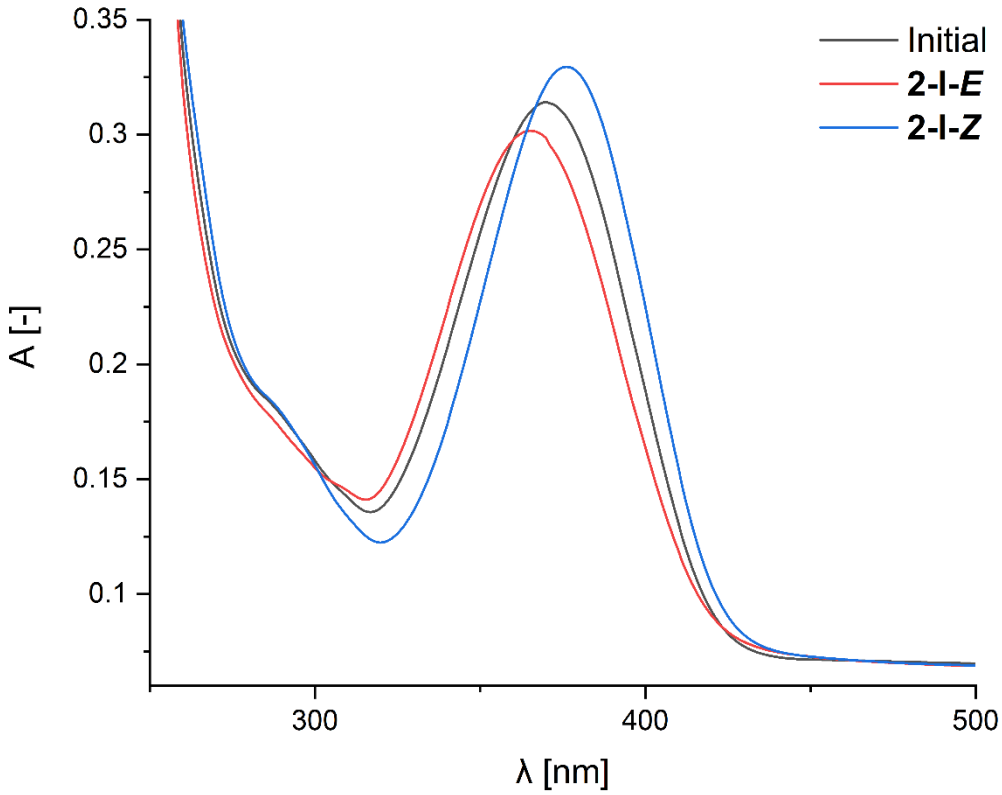

Figure S35. UV-VIS spectrum of compound **2-I** before (black line) and after irradiation at 420 nm (**2-I-*E***, red line) and 460 nm (**2-I-*Z***, blue line) for 30 minutes (1.36×10^{-5} M, $CHCl_3$).

Photoswitching efficiency

All compounds were irradiated for 1 minute at 420 nm ($Z \rightarrow E$) and for 3 minutes at 460 nm ($E \rightarrow Z$) in chloroform. The optimalization of irradiation conditions was performed for **2-Cl** and **2-Br**: 20 seconds at 420 nm ($Z \rightarrow E$) and 20 seconds at 365 nm ($E \rightarrow Z$). Compounds **2-F** and **2-Cl** were also photoswitched in toluene and acetonitrile.

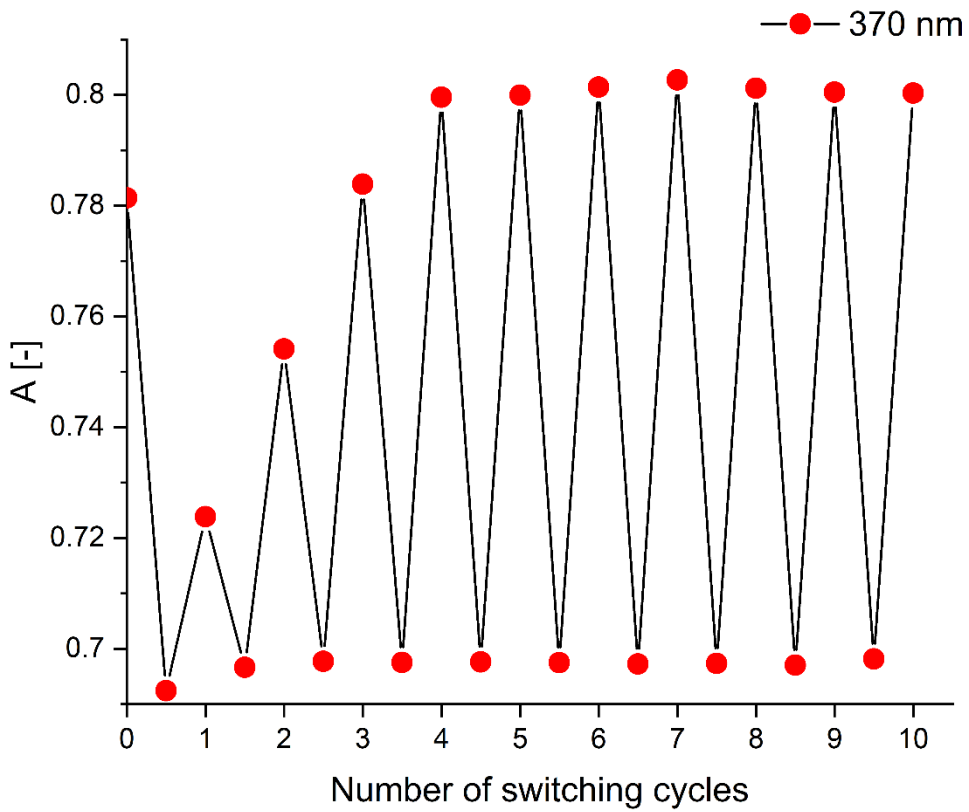

Figure S36. Isomerization cycles of **2-F** upon alternating irradiation at 420 nm for 1 min (bottom red dots) and 460 nm for 3 min (top red dots). The absorbances at 370 nm are plotted (2.73×10^{-5} M, $CHCl_3$).

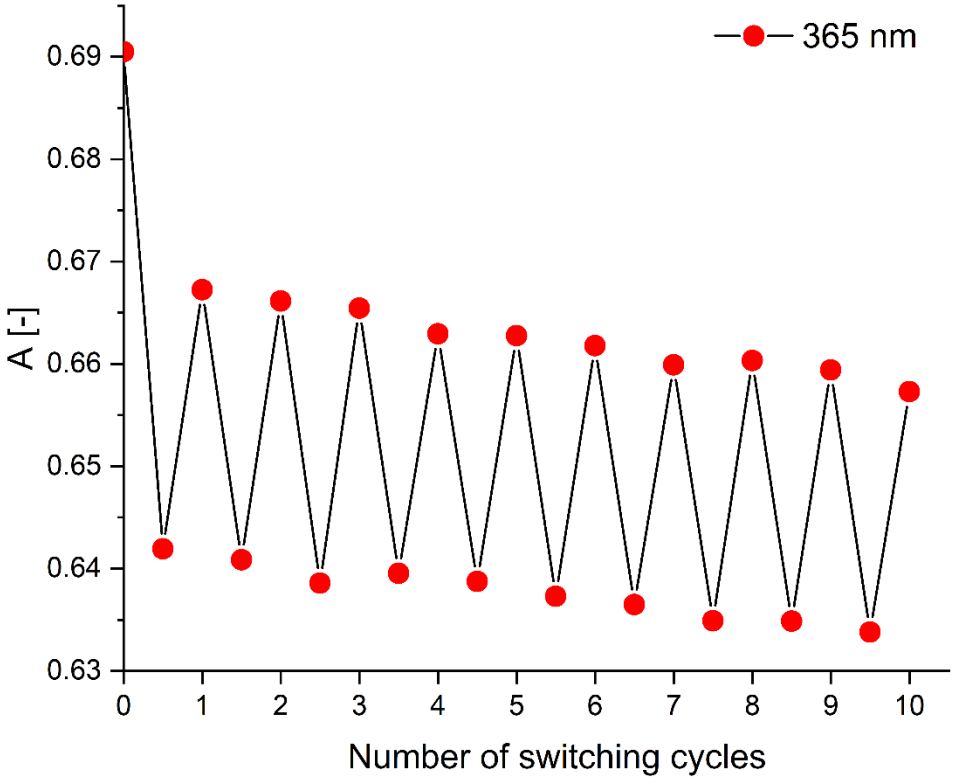

Figure S37. Isomerization cycles of **2-F** upon alternating irradiation at 420 nm for 20 s (bottom red dots) and 365 nm for 20 s (top red dots). The absorbances at 365 nm are plotted (2.41×10^{-5} M, toluene).

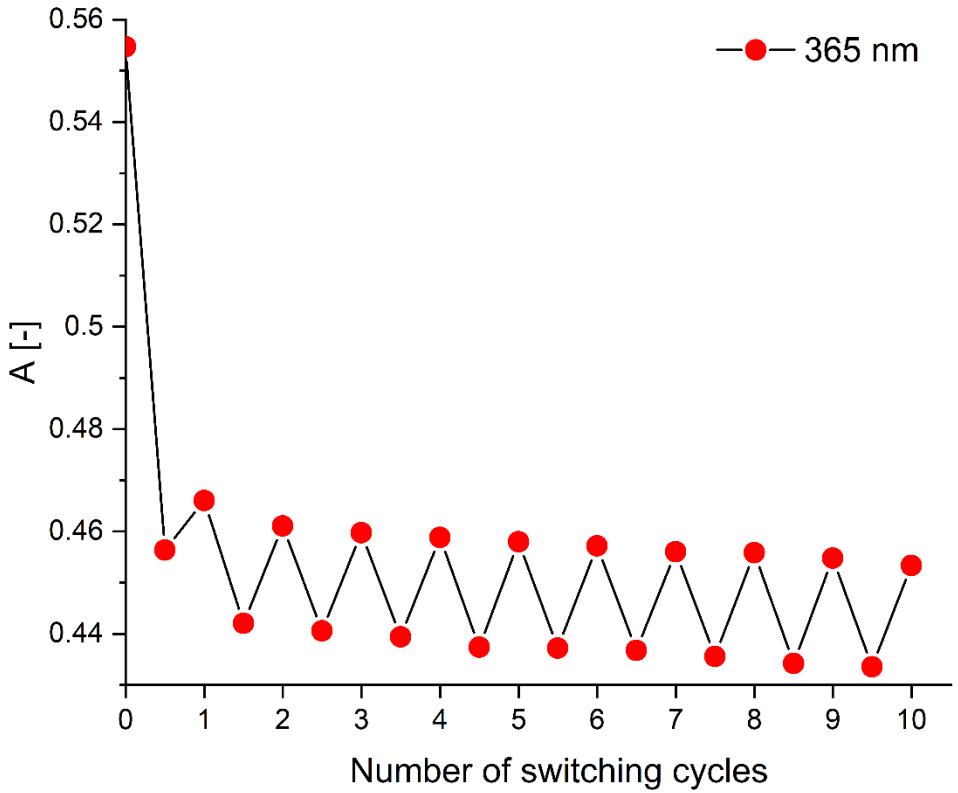

Figure S38. Isomerization cycles of **2-F** upon alternating irradiation at 420 nm for 20 s (bottom red dots) and 365 nm for 20 s (top red dots). The absorbances at 365 nm are plotted (1.92×10^{-5} M, acetonitrile).

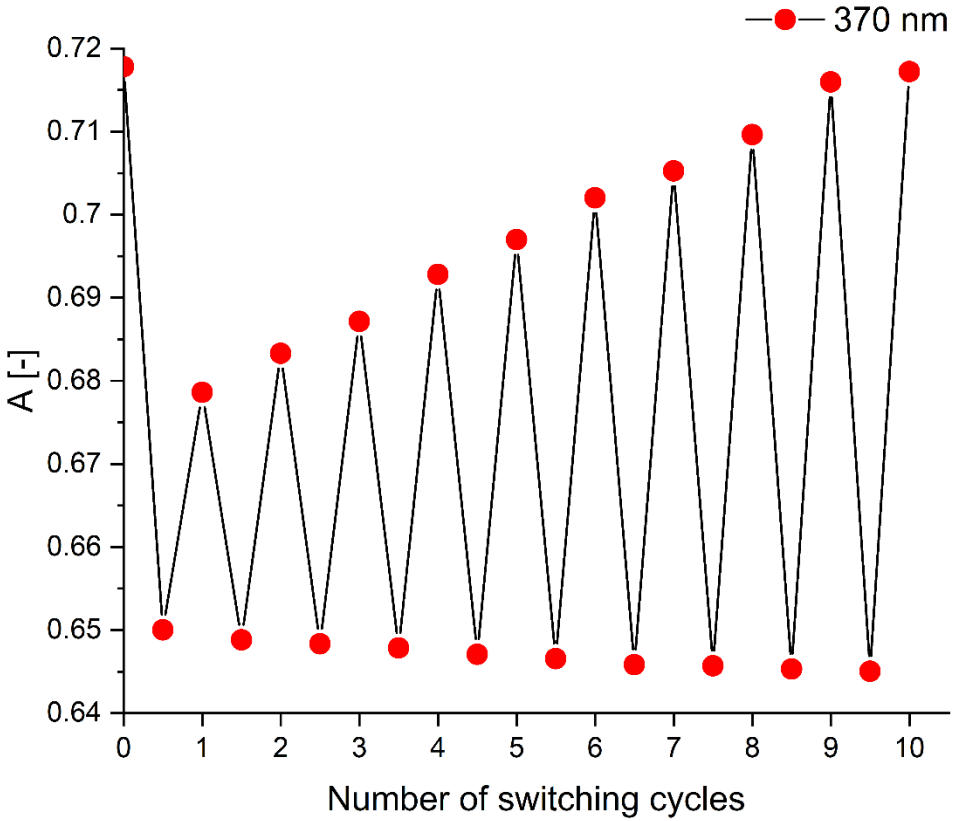

Figure S39. Isomerization cycles of **2-Cl** upon alternating irradiation at 420 nm for 1 min (bottom red dots) and 460 nm for 3 min (top red dots). The absorbances at 370 nm are plotted (2.73×10^{-5} M, $CHCl_3$).

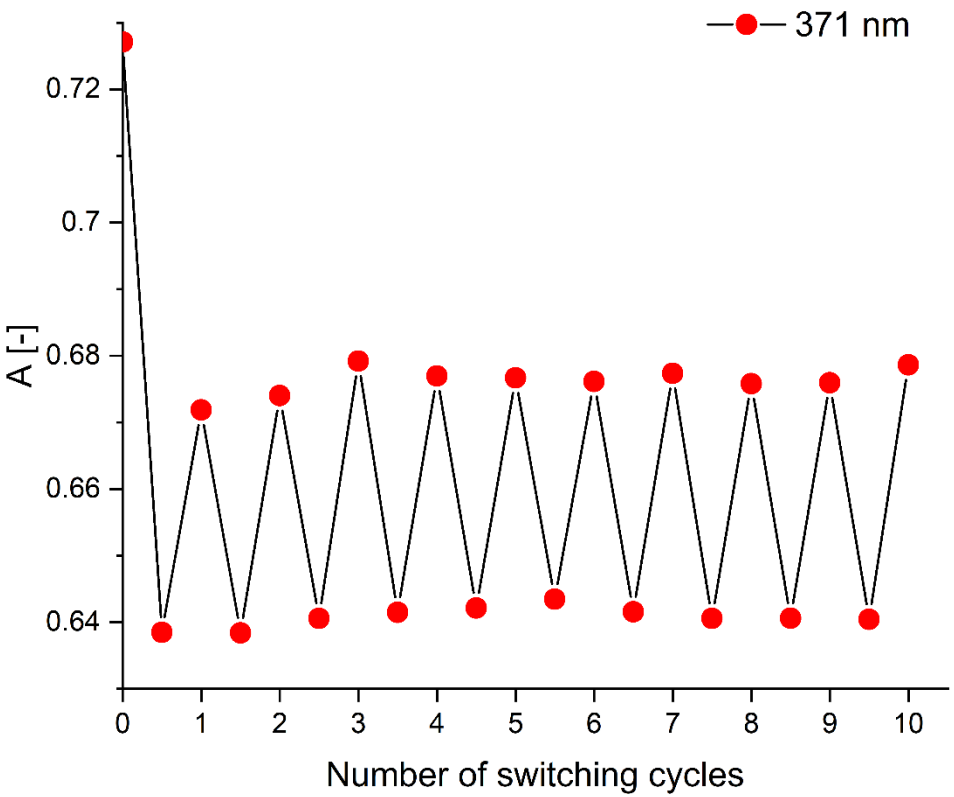

Figure S40. Isomerization cycles of **2-Cl** upon alternating irradiation at 420 nm for 20 s (bottom red dots) and 365 nm for 20 s (top red dots). The absorbances at 371 nm are plotted (2.73×10^{-5} M, $CHCl_3$).

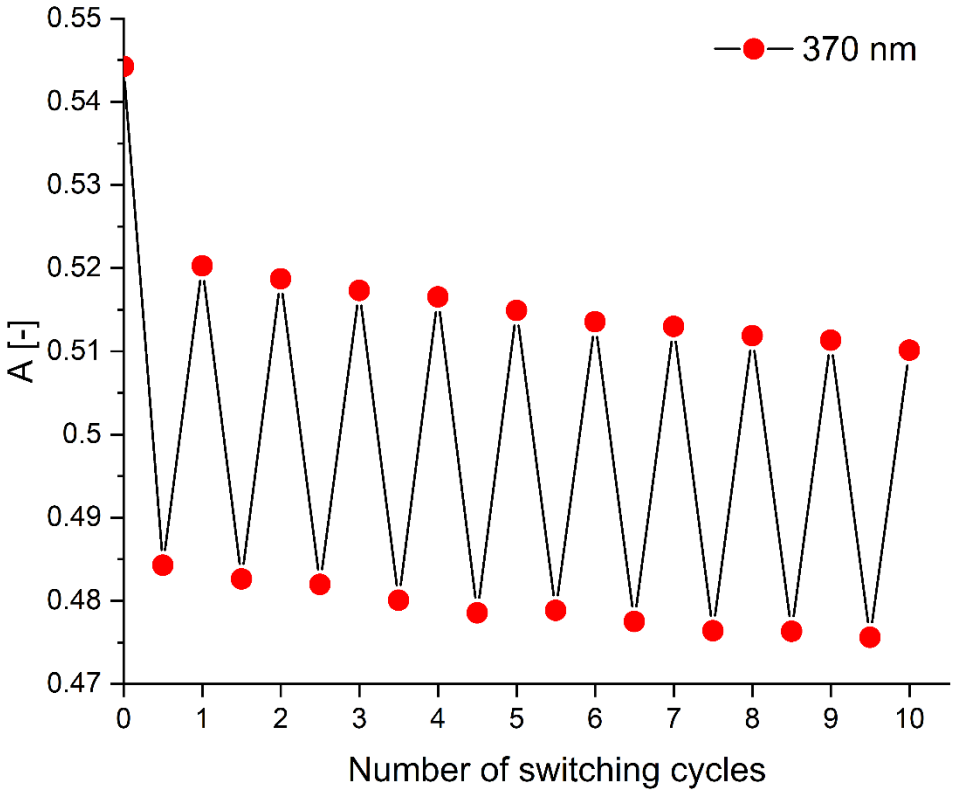

Figure S41. Isomerization cycles of **2-Cl** upon alternating irradiation at 420 nm for 20 s (bottom red dots) and 365 nm for 20 s (top red dots). The absorbances at 370 nm are plotted (2.05×10^{-5} M, toluene).

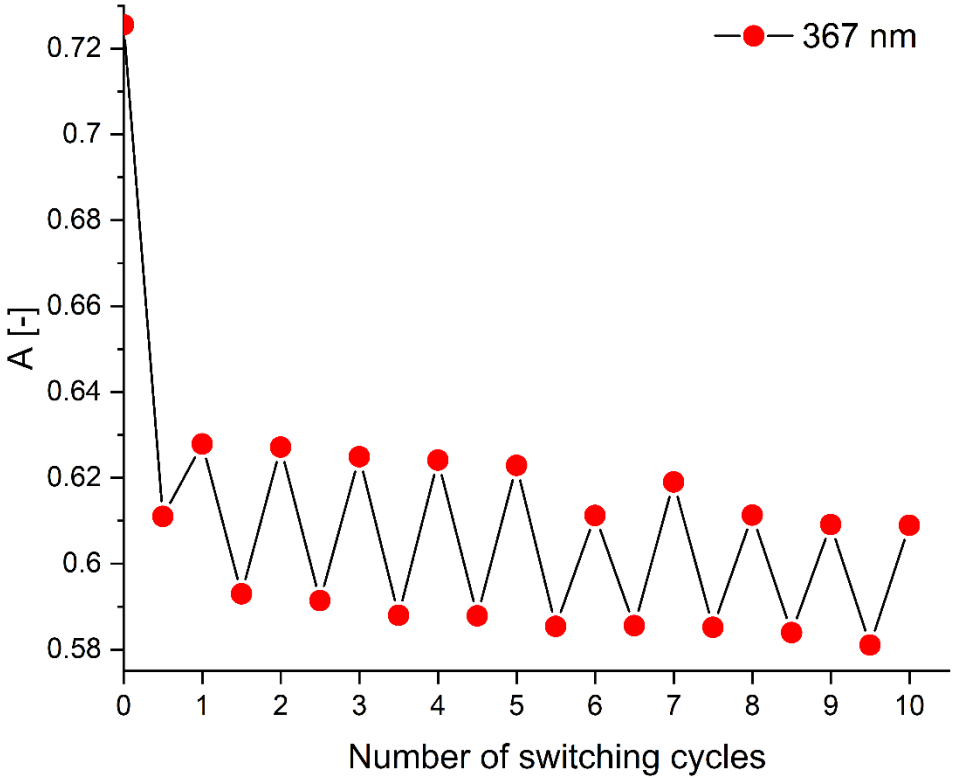

Figure S42. Isomerization cycles of **2-Cl** upon alternating irradiation at 420 nm for 20 s (bottom red dots) and 365 nm for 20 s (top red dots). The absorbances at 367 nm are plotted (2.78×10^{-5} M, acetonitrile).

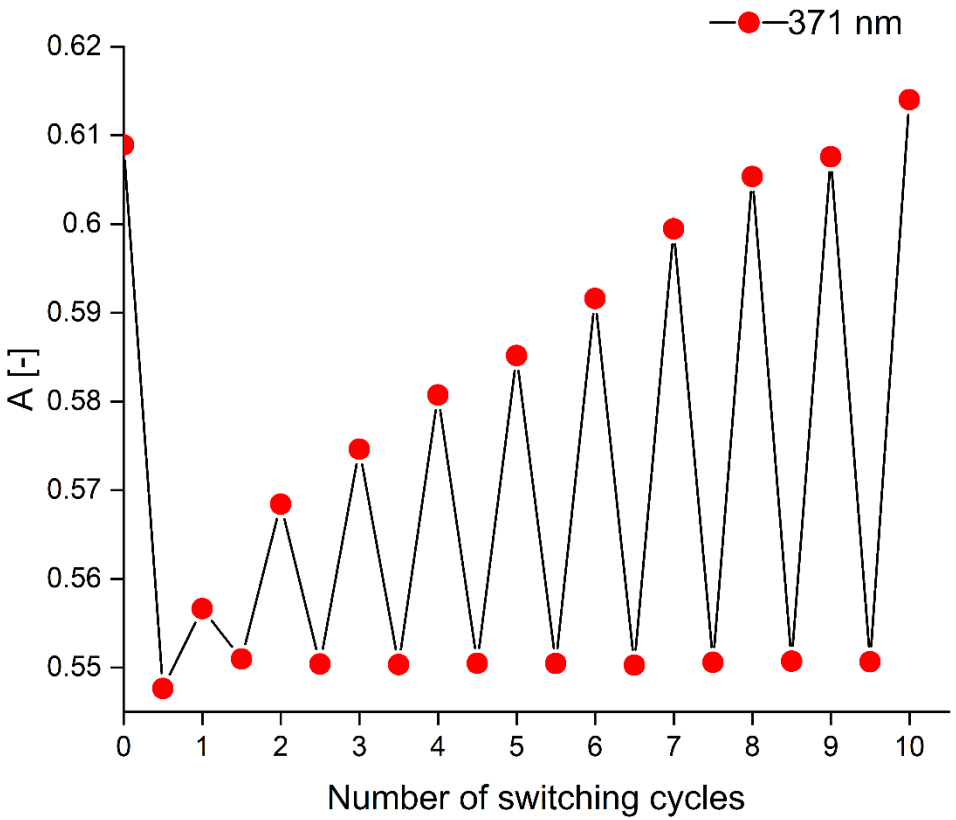

Figure S43. Isomerization cycles of **2-Br** upon alternating irradiation at 420 nm for 1 min (bottom red dots) and 460 nm for 1 min (top red dots). The absorbances at 371 nm are plotted (2.73×10^{-5} M, $CHCl_3$).

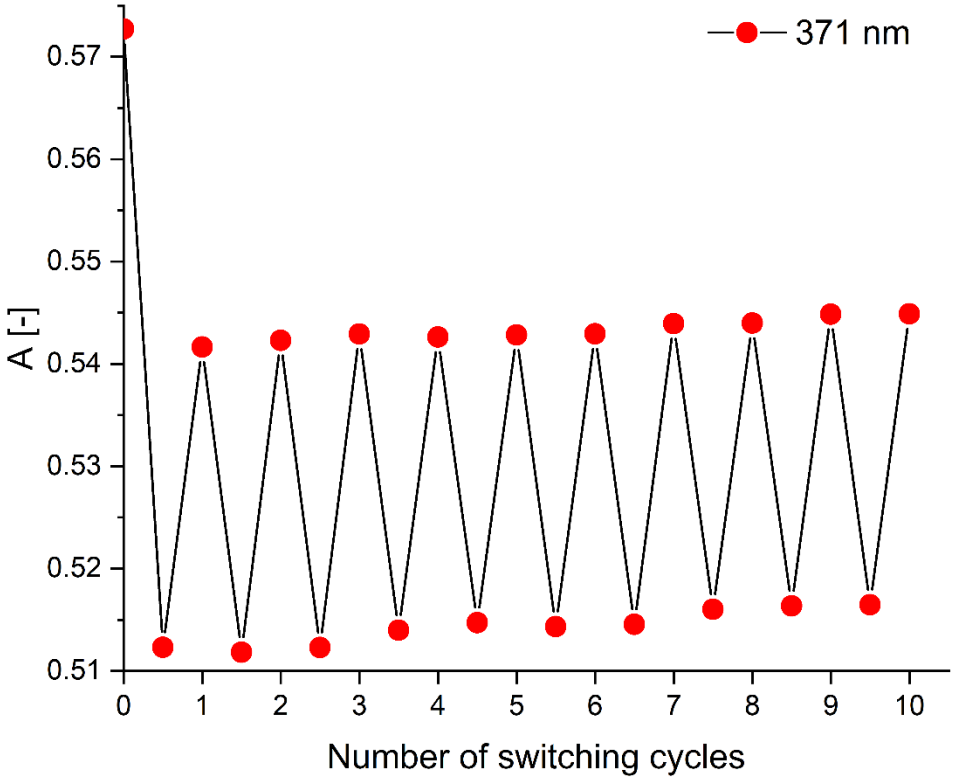

Figure S44. Isomerization cycles of **2-Br** upon alternating irradiation at 420 nm for 20 s (bottom red dots) and 365 nm for 20 s (top red dots). The absorbances at 371 nm are plotted (2.73×10^{-5} M, $CHCl_3$).

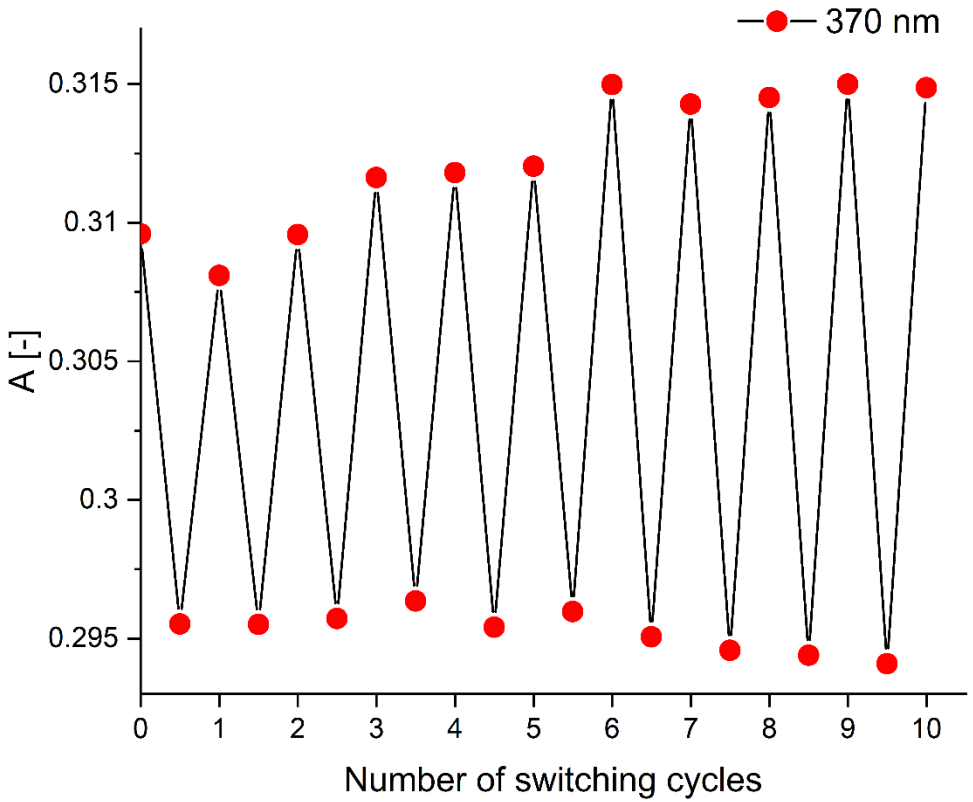

Figure S45. Isomerization cycles of **2-I** upon alternating irradiation at 420 nm for 1 min (bottom red dots) and 460 nm for 3 min (top red dots). The absorbances at 370 nm are plotted (1.36×10^{-5} M, $CHCl_3$).

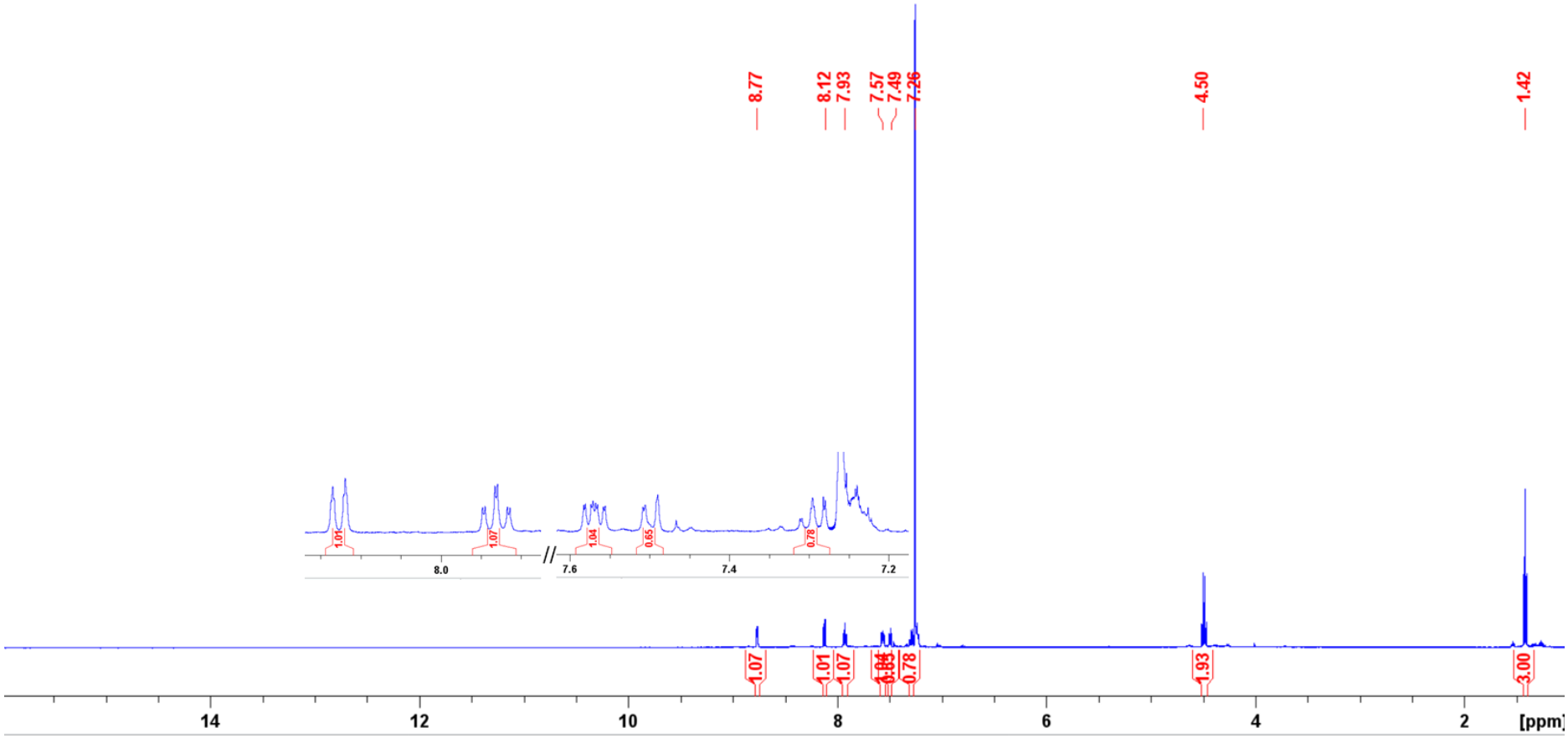

Figure S46. ^{1}H NMR spectrum of **2-Br** (c = 0.02 M) recorded after exposition on 460 nm over 3 hours, $CDCl_3$, 500 MHz, 298 K.

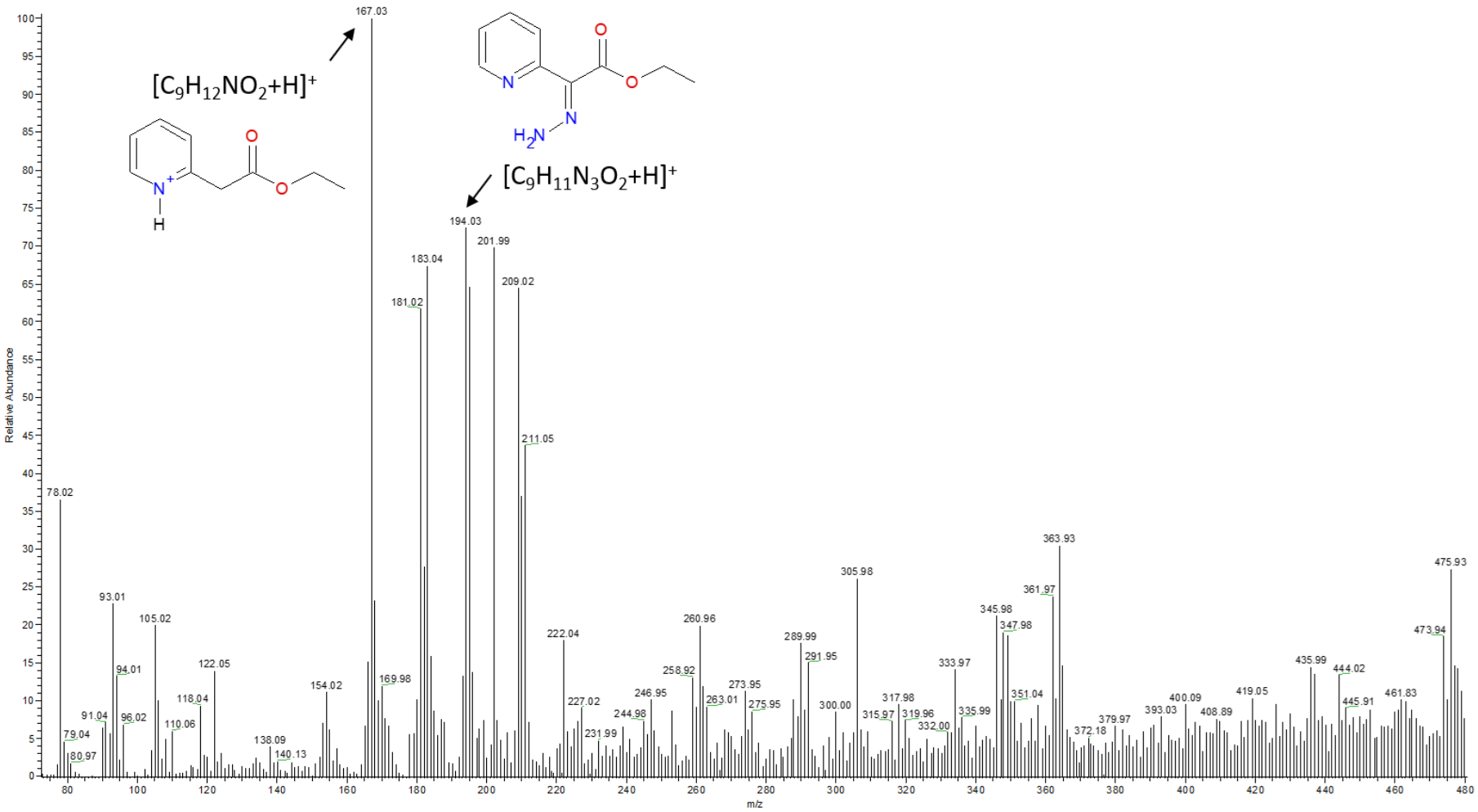

Figure S47. Positive ion mode MS spectrum of **2-Br** (in MeOH) after exposition to 460 nm irradiation for 3 hours at 0.02 M concentration.

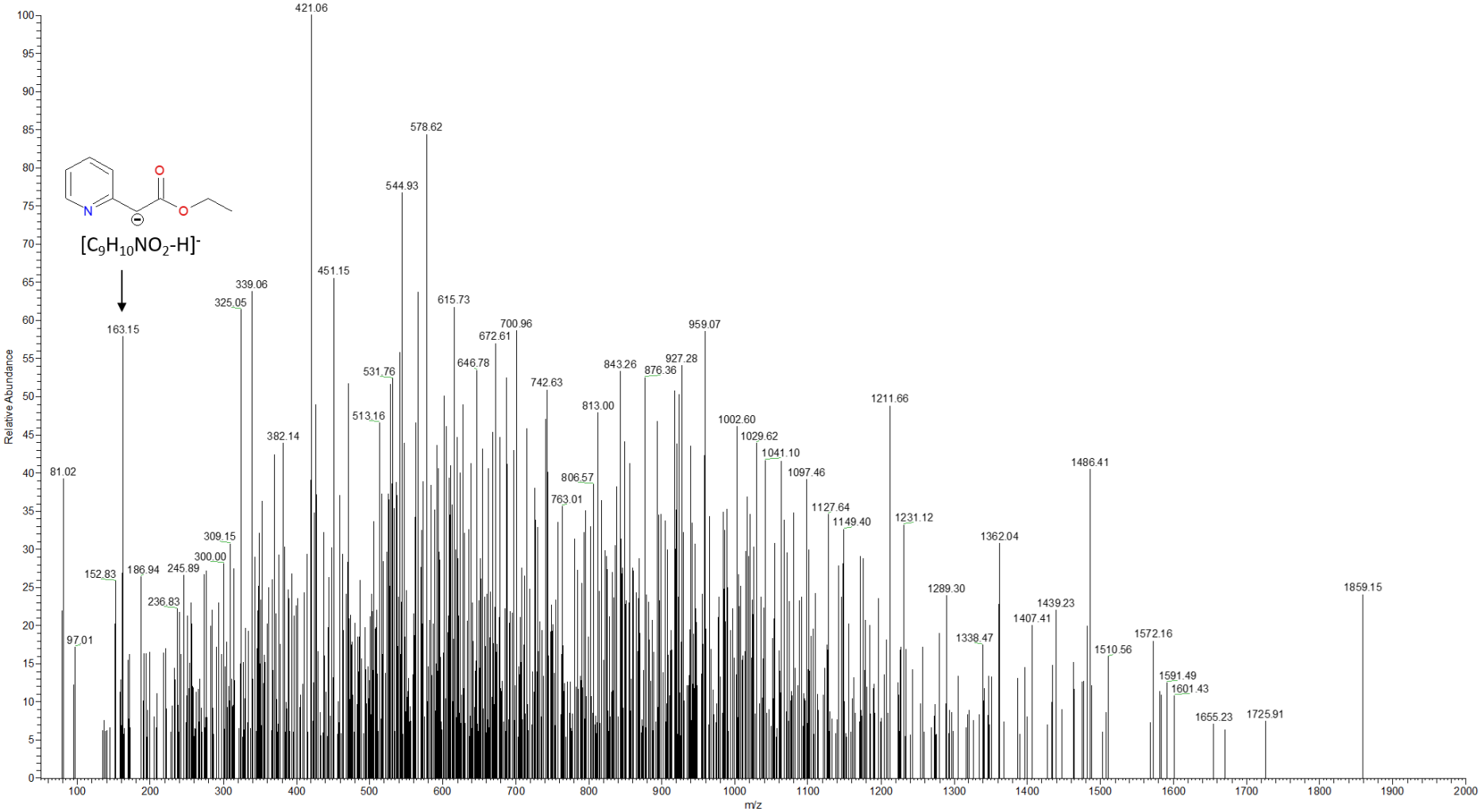

Figure S48. Negative ion mode MS spectrum of **2-Br** (in MeOH) after exposition to 460 nm irradiation for 3 hours at 0.02 M concentration.

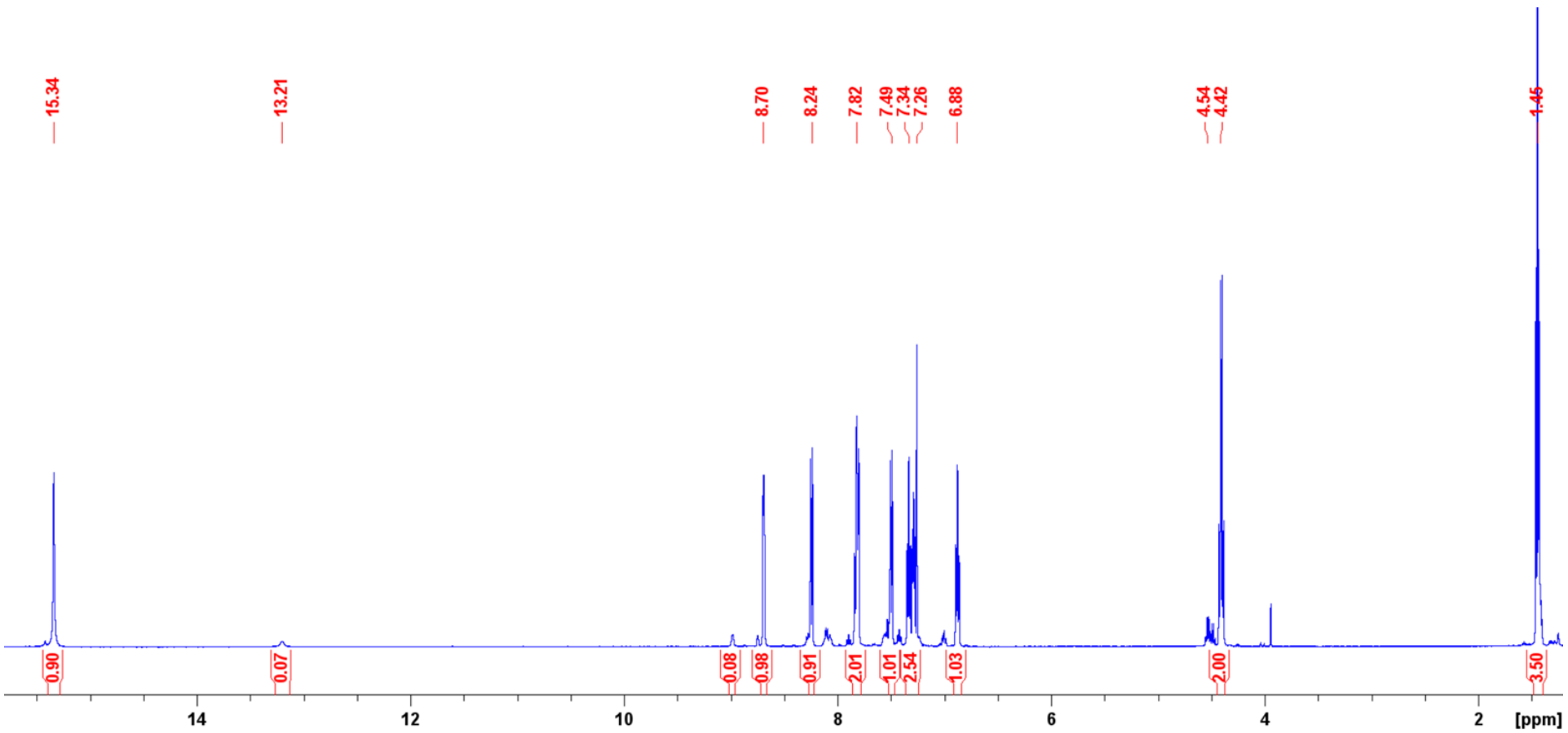

Figure S49. ^{1}H NMR spectrum of **2-Br** (c = 0.1 M) recorded after exposition on 460 nm over 3 hours, $CDCl_3$, 500 MHz, 298 K.

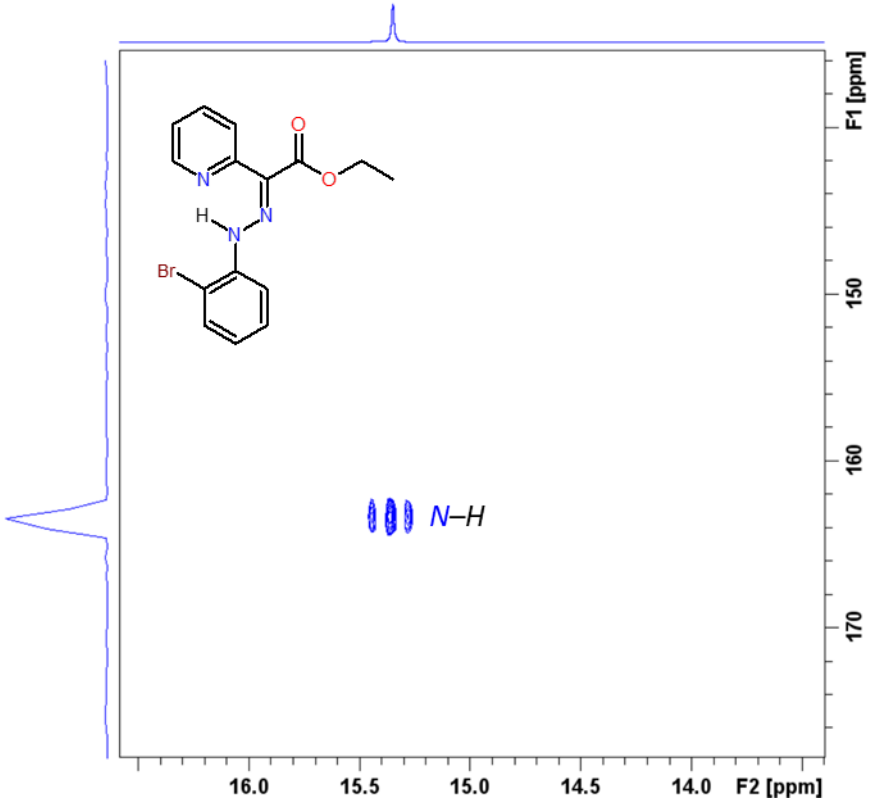

Figure S50. ^{15}N–^{1}H HSQC correlation chart of **2-Br** (c = 0.1 M), $CDCl_3$, 50 MHz–500 MHz, 298 K, ref. $NH_{3(liq.)}$ δ = 380.20 ppm.

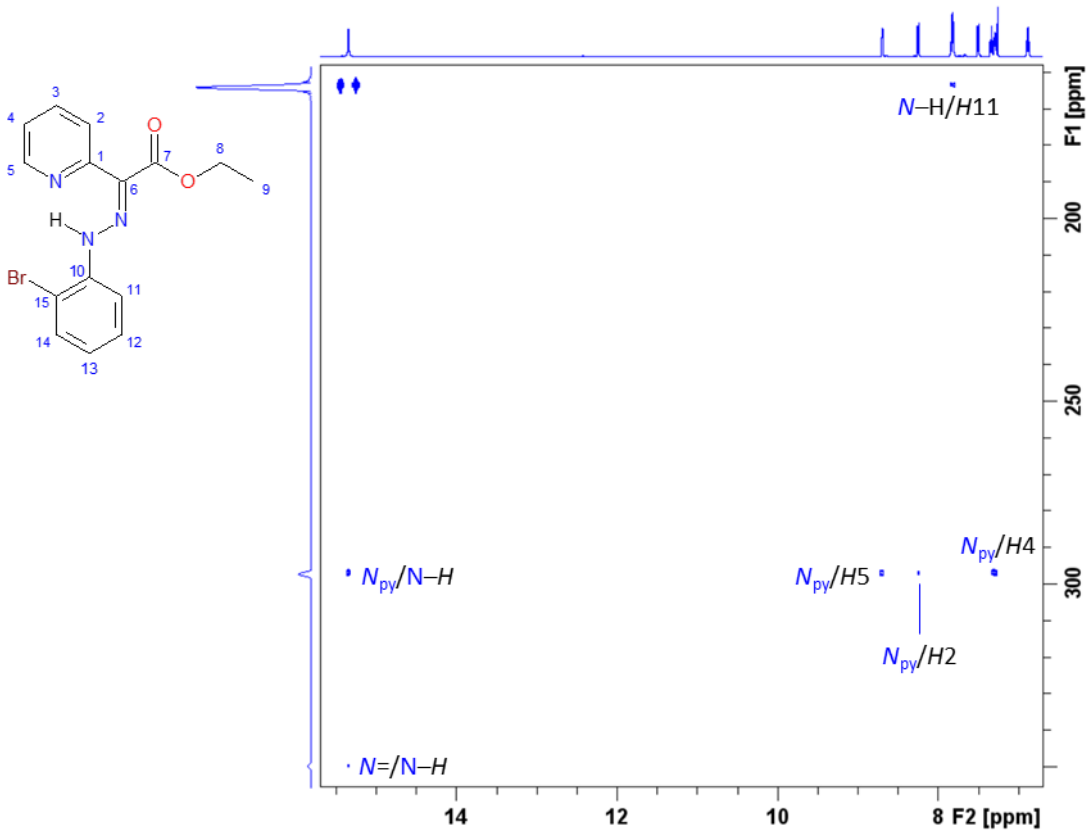

Figure S51. ^{15}N–^{1}H HMBC correlation chart of **2-Br** (c = 0.1 M), $CDCl_3$, 50 MHz–500 MHz, 298 K, ref. $NH_{3(liq.)}$ δ = 380.20 ppm.

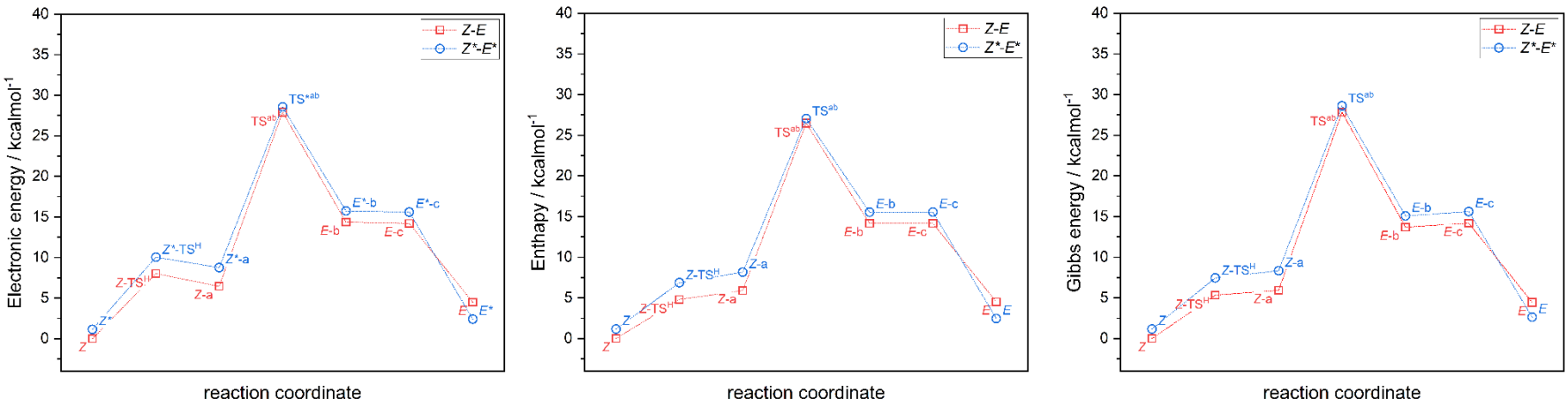

Figure S52. The minimal energy pathway for *Z-E* isomerization for **2-F** calculated with CAM-B3LYP+D4/def2-TZVP/C-CPCM($CHCl_3$): relative energies, enthalpies, and Gibbs energies.

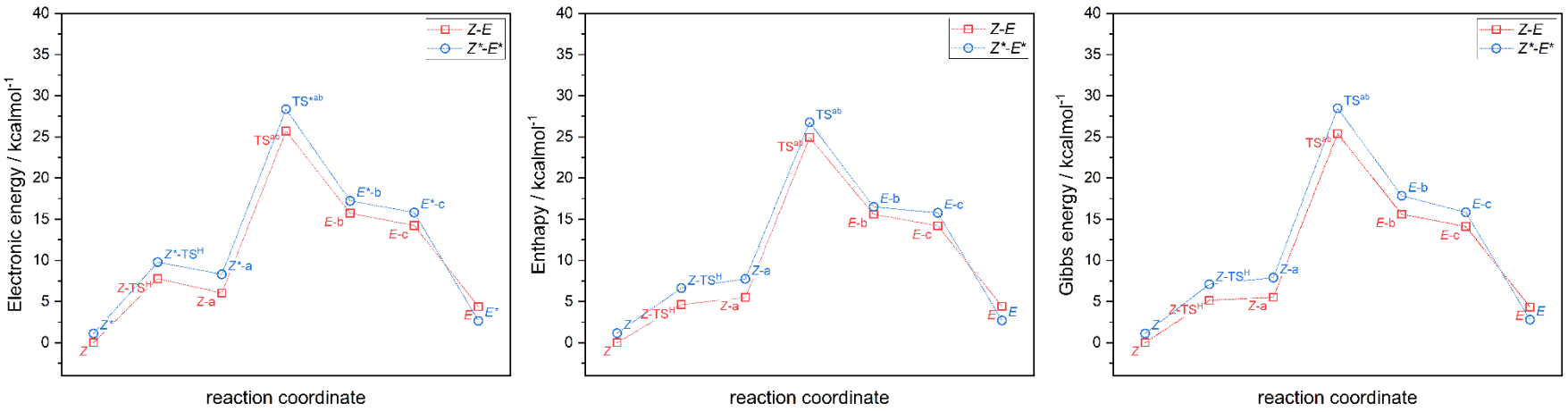

Figure S53. The minimal energy pathway for *Z-E* isomerization for **2-Br** calculated with CAM-B3LYP+D4/def2-TZVP/C-CPCM($CHCl_3$): relative energies, enthalpies, and Gibbs energies.

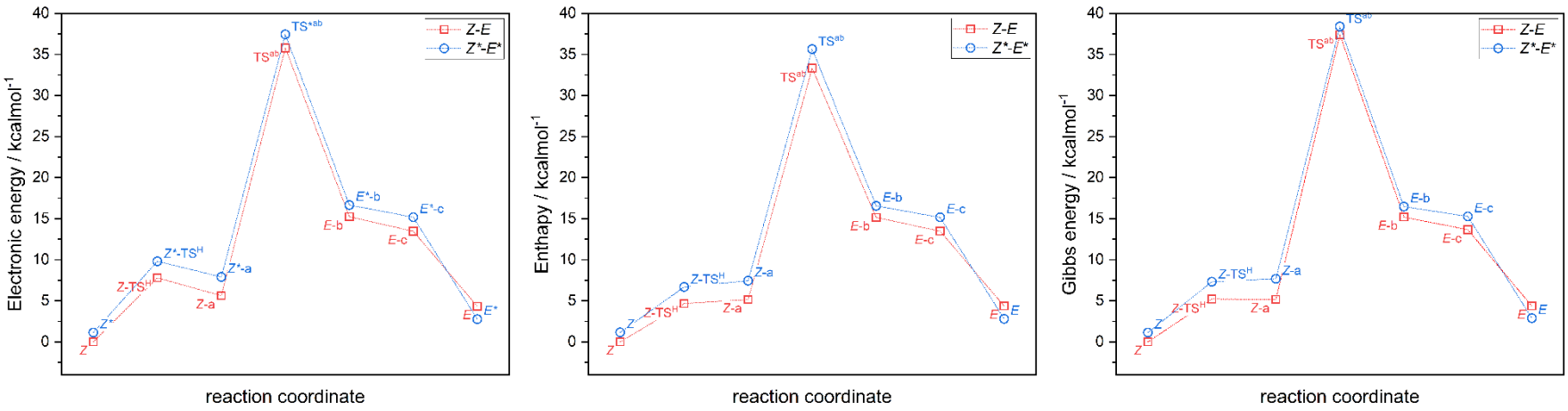

Figure S54. The minimal energy pathway for *Z*-*E* isomerization for **2-I** calculated with CAM-B3LYP+D4/def2-TZVP/C-CPCM($CHCl_3$): relative energies, enthalpies, and Gibbs energies.

Table S1. Crystal data and structure refinement for **2-Br** and **2-I**.

	2-Br	**2-I**
Formula	$C_{15}H_{14}BrN_3O_2$	$C_{15}H_{14}IN_3O_2$
M_r	348.201	395.202
Crystal system	monoclinic	monoclinic
Space group	$P2_1/c$	$P2_1/c$
T/K	150.00(10)	100.00(10)
a (Å)	4.7716(1)	4.6839(2)
b (Å)	18.2538(5)	18.5687(8)
c (Å)	16.7147(4)	16.9966(6)
α (°)	90	90
β (°)	97.171(2)	95.506(4)
γ (°)	90	90
V (Å^3)	1444.46(6)	1471.44(10)
Z	4	4
λ (Å), Cu Kα	1.54184	1.54184
D_{calc} (g·cm^{-3})	1.601	1.784
μ (mm^{-1})	3.956	17.179
F (000)	703.4	779.0
Reflections collected	10145	7046
R_{int}, R_{sigma}	0.0414, 0.0353	0.0441, 0.0390
Data/restraints/parameters	2653/0/191	2730/0/191
Goodness-of-fit on F^2	1.033	1.040
Final R indices [$I > 2\sigma(I)$]	R_1 = 0.0336 wR_2 = 0.0918	R_1 = 0.0550 wR_2 = 0.1458
Final R indices (all data)	R_1 = 0.0370 wR_2 = 0.0945	R_1 = 0.0583 wR_2 = 0.1492
Larg. d. peak/hole / e Å^{-3}	0.75/-0.60	1.22/-2.12
CCDC no.	2335394	2335397

Table S2. The CAM-B3LYP calculated values of $\Delta H_{iso}^{E\rightarrow Z}$ for **2-X**.

	kcal/mol	kcal/mol		kJ/mol	kJ/mol
X=	H(E)-H(Z)	H(E*)-H(Z*)		H(E*)-H(Z*)	G(E)-G(Z)
F	4.52	1.30		18.90	5.43
Cl	4.45	1.47		18.61	6.16
Br	4.42	1.54		18.50	6.44
I	4.37	1.64		18.27	6.87

Table S3. The CAM-B3LYP calculated values of $\Delta G^{\ddagger\, E\rightarrow Z}$ for **2-X**.

	kcal/mol	kcal/mol		kJ/mol	kJ/mol
X=	G(TS)-G(E)	G(TS*)-G(E*)		G(TS)-G(E)	G(TS*)-G(E*)
F	23.38	25.98		97.84	108.71
Cl	28.08	30.49		117.50	127.59
Br	21.07	25.67		88.14	107.41
I	33.02	35.51		138.14	148.57

Table S4. The isomer shifts of ^{1}H NMR relative to TMS together with atom numbering scheme, calculated with CAM-B3LYP/PCSSEG-2/C-PCM($CHCl_3$), for **2-F**.

	Atom	shift[ppm]	rel.intensity	
Z	2	15.65	1.00	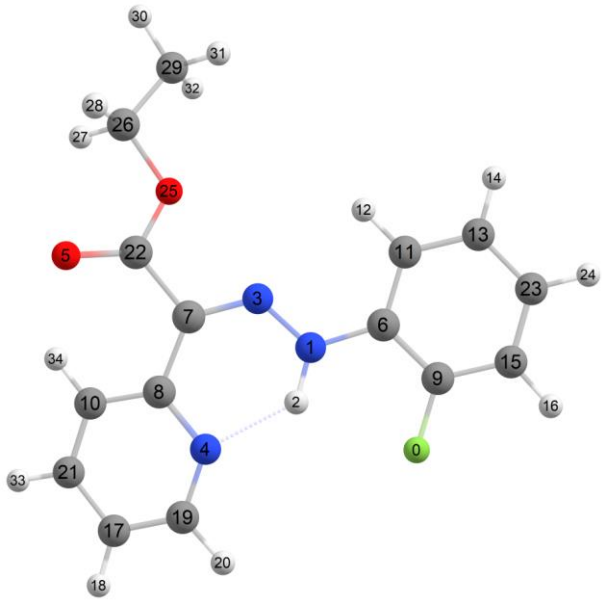
	12	8.43	1.00	
	14	7.72	1.00	
	16	7.70	1.00	
	18	7.78	1.00	
	20	9.16	1.00	
	24	7.47	1.00	
	27	4.38	1.00	
	28	4.30	1.00	
	30	1.47	1.00	
	31	1.72	1.00	
	32	1.64	1.00	
	33	8.39	1.00	
	34	8.71	1.00	
Z-a	2	20.32	1.00	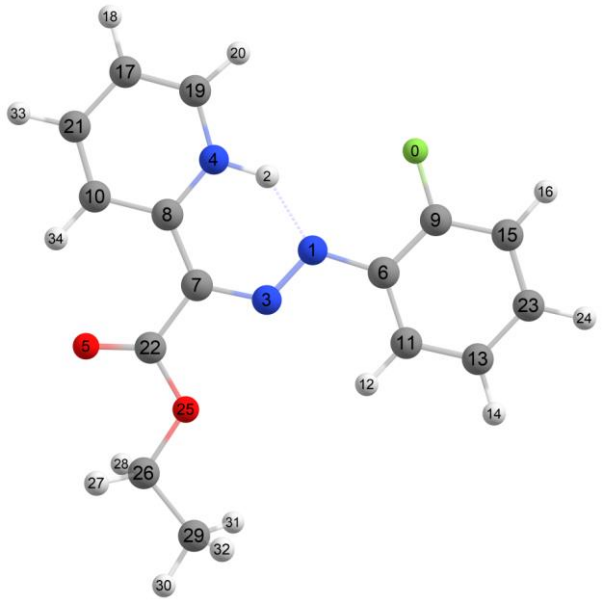
	12	8.60	1.00	
	14	7.68	1.00	
	16	7.72	1.00	
	18	7.58	1.00	
	20	8.47	1.00	
	24	7.61	1.00	
	27	4.31	1.00	
	28	4.28	1.00	
	30	1.45	1.00	
	31	1.67	1.00	
	32	1.65	1.00	
	33	8.54	1.00	
	34	9.81	1.00	

E-b	2	12.47	1.00	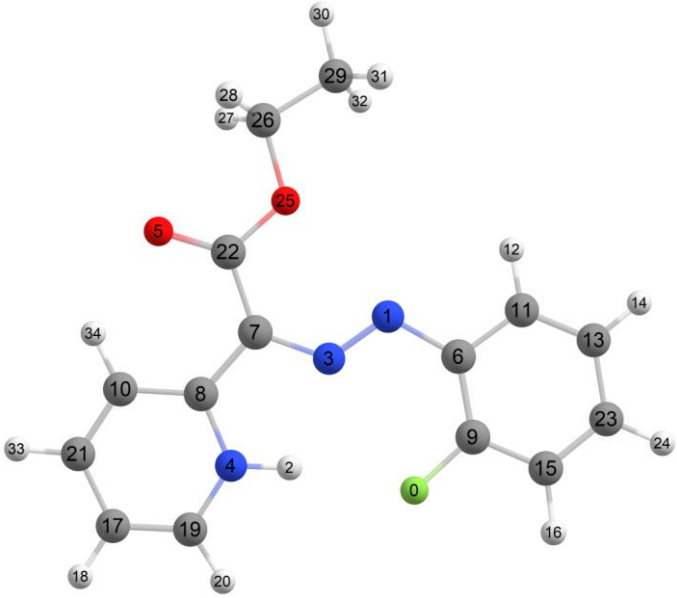
	12	8.37	1.00	
	14	7.76	1.00	
	16	7.68	1.00	
	18	7.21	1.00	
	20	8.24	1.00	
	24	7.60	1.00	
	27	4.27	1.00	
	28	4.27	1.00	
	30	1.39	1.00	
	31	1.69	1.00	
	32	1.62	1.00	
	33	8.36	1.00	
	34	9.50	1.00	
E-c	11	7.83	1.00	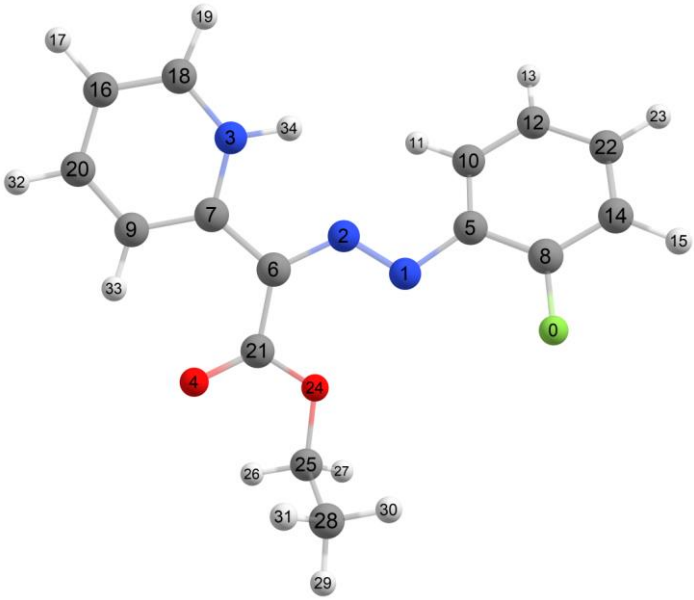
	13	7.63	1.00	
	15	7.68	1.00	
	17	7.15	1.00	
	19	8.14	1.00	
	23	7.66	1.00	
	26	5.10	1.00	
	27	3.93	1.00	
	29	1.12	1.00	
	30	1.47	1.00	
	31	1.63	1.00	
	32	8.29	1.00	
	33	9.15	1.00	
	34	12.38	1.00	
E	11	8.30	1.00	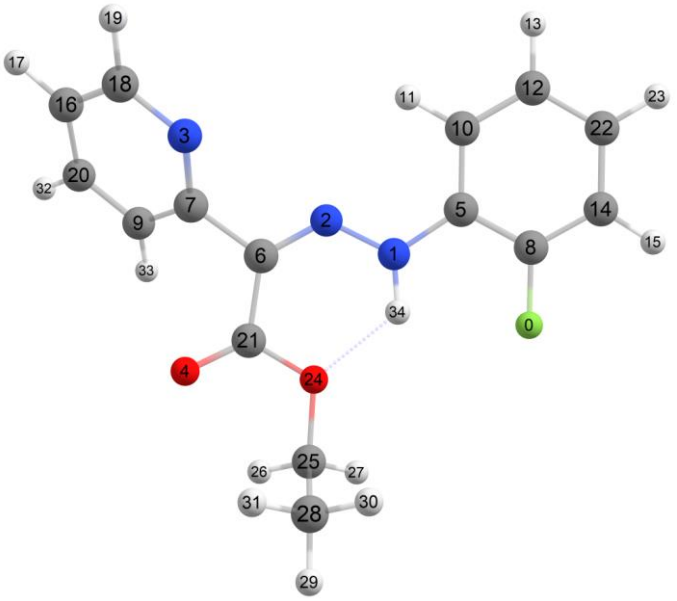
	13	7.70	1.00	
	15	7.67	1.00	
	17	7.72	1.00	
	19	9.11	1.00	
	23	7.45	1.00	
	26	5.23	1.00	
	27	4.37	1.00	
	29	1.26	1.00	
	30	1.43	1.00	
	31	1.64	1.00	
	32	8.23	1.00	
	33	8.02	1.00	
	34	11.66	1.00	

*Z**	2	15.05	1.00
	12	8.40	1.00
	14	7.70	1.00
	16	7.67	1.00
	18	7.78	1.00
	20	9.18	1.00
	24	7.43	1.00
	27	4.46	1.00
	28	4.31	1.00
	30	1.38	1.00
	31	1.40	1.00
	32	1.52	1.00
	33	8.37	1.00
	34	8.18	1.00
*Z**-a	2	20.76	1.00
	12	8.66	1.00
	14	7.69	1.00
	16	7.70	1.00
	18	7.53	1.00
	20	8.48	1.00
	24	7.61	1.00
	27	4.48	1.00
	28	4.36	1.00
	30	1.49	1.00
	31	1.64	1.00
	32	1.71	1.00
	33	8.48	1.00
	34	9.08	1.00
*E**-b	2	12.34	1.00
	12	8.36	1.00
	14	7.75	1.00
	16	7.66	1.00
	18	7.12	1.00
	20	8.19	1.00
	24	7.59	1.00
	27	4.31	1.00
	28	4.22	1.00
	30	1.44	1.00
	31	1.55	1.00
	32	1.63	1.00
	33	8.27	1.00
	34	8.82	1.00

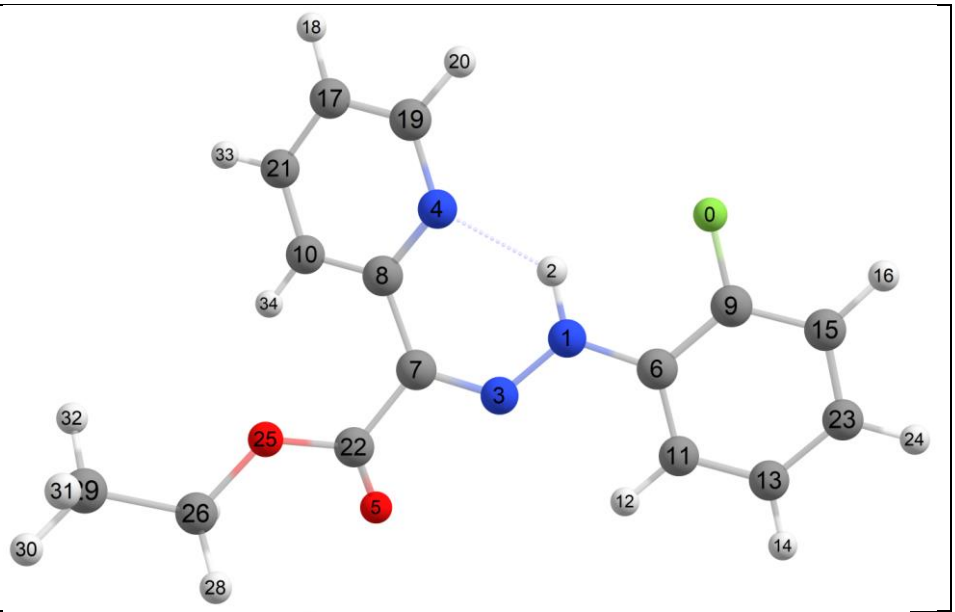

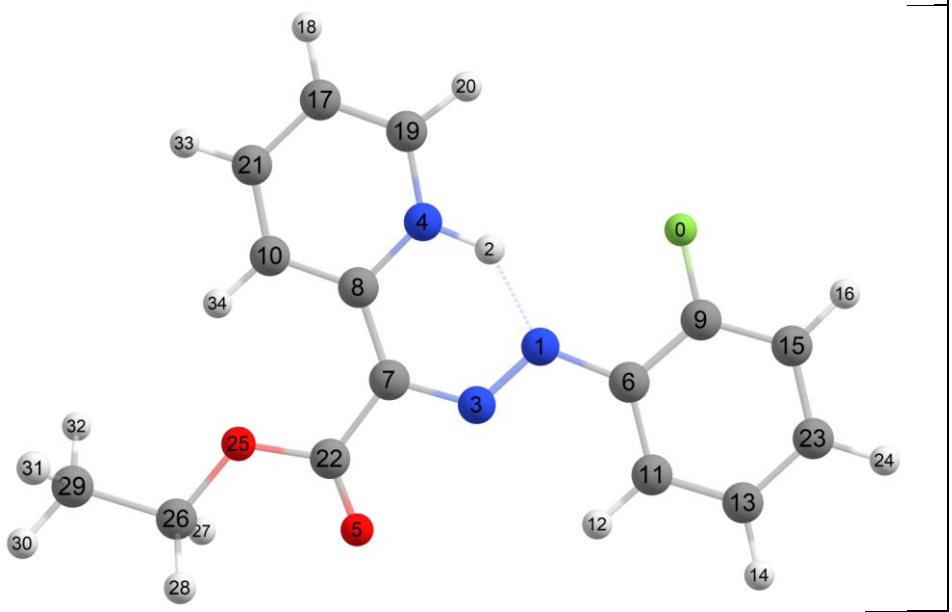

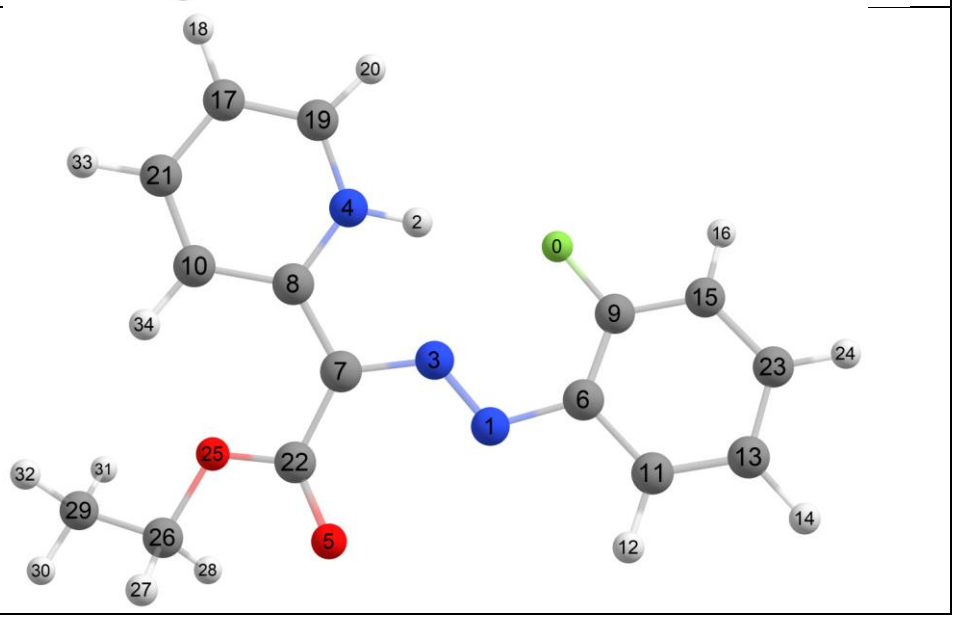

*E**-c	11	7.84	1.00	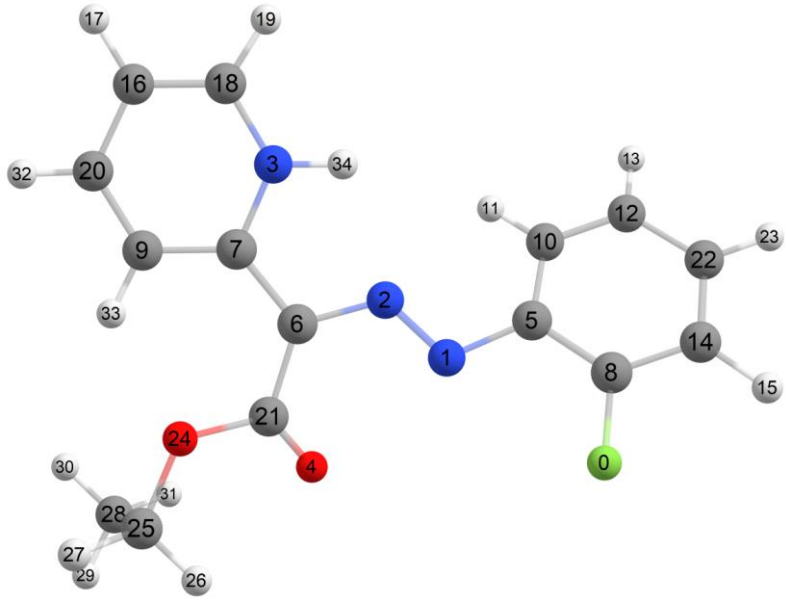
	13	7.60	1.00	
	15	7.65	1.00	
	17	7.04	1.00	
	19	8.07	1.00	
	23	7.65	1.00	
	26	5.14	1.00	
	27	3.95	1.00	
	29	1.21	1.00	
	30	1.43	1.00	
	31	1.67	1.00	
	32	8.17	1.00	
	33	8.52	1.00	
	34	12.08	1.00	
*E**	11	8.31	1.00	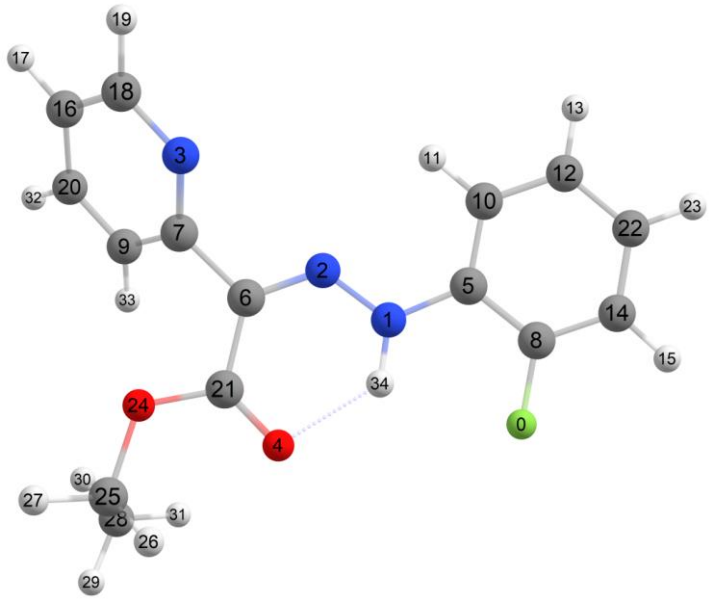
	13	7.68	1.00	
	15	7.67	1.00	
	17	7.72	1.00	
	19	9.11	1.00	
	23	7.46	1.00	
	26	5.04	1.00	
	27	3.95	1.00	
	29	1.26	1.00	
	30	1.48	1.00	
	31	1.78	1.00	
	32	8.24	1.00	
	33	8.02	1.00	
	34	13.34	1.00	

Table S5. The isomer shifts of ^{1}H NMR relative to TMS together with atom numbering scheme, calculated with CAM-B3LYP/PCSSEG-2/C-PCM($CHCl_3$), for **2-Cl**.

Z	Atom shift[ppm] rel.intensity 2 15.81 1.00 12 8.46 1.00 14 7.83 1.00 16 7.94 1.00 18 7.79 1.00 20 9.21 1.00 24 7.46 1.00 27 4.38 1.00 28 4.31 1.00 30 1.48 1.00 31 1.72 1.00 32 1.65 1.00 33 8.40 1.00 34 8.71 1.00	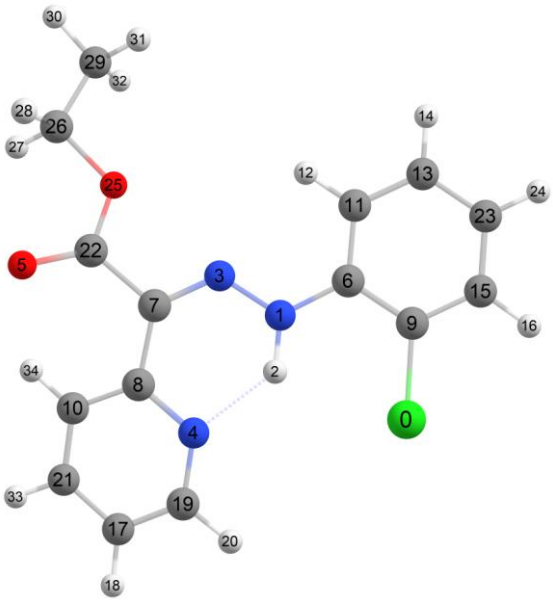
Z-a	2 20.48 1.00 12 8.59 1.00 14 7.80 1.00 16 8.00 1.00 18 7.61 1.00 20 8.56 1.00 24 7.58 1.00 27 4.32 1.00 28 4.29 1.00 30 1.45 1.00 31 1.65 1.00 32 1.66 1.00 33 8.57 1.00 34 9.83 1.00	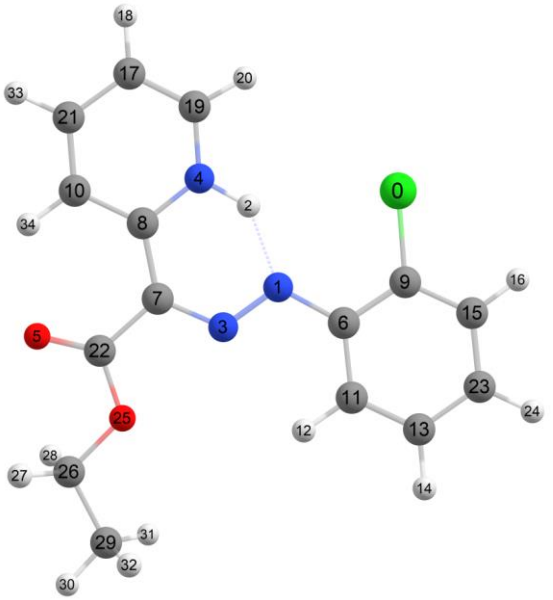

E-b	2	12.61	1.00	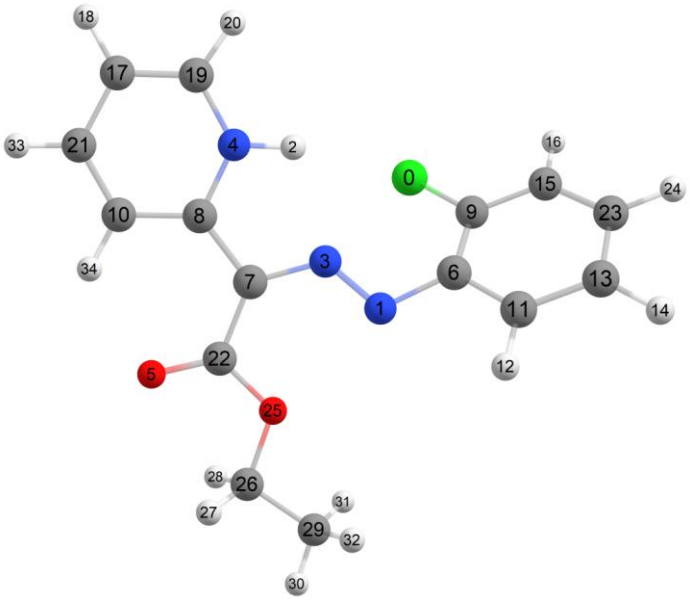
	12	7.89	1.00	
	14	7.81	1.00	
	16	7.94	1.00	
	18	7.21	1.00	
	20	8.13	1.00	
	24	7.56	1.00	
	27	4.26	1.00	
	28	4.24	1.00	
	30	1.34	1.00	
	31	1.49	1.00	
	32	1.60	1.00	
	33	8.37	1.00	
	34	9.60	1.00	
E-c	11	7.74	2.00	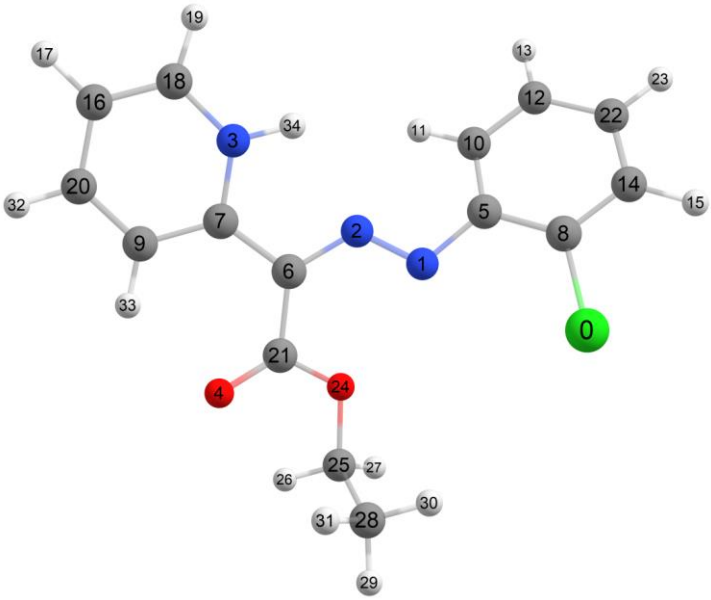
	15	7.96	1.00	
	17	7.17	1.00	
	19	8.15	1.00	
	23	7.60	1.00	
	26	5.13	1.00	
	27	3.96	1.00	
	29	1.13	1.00	
	30	1.53	1.00	
	31	1.63	1.00	
	32	8.31	1.00	
	33	9.18	1.00	
	34	12.43	1.00	
E	11	8.34	1.00	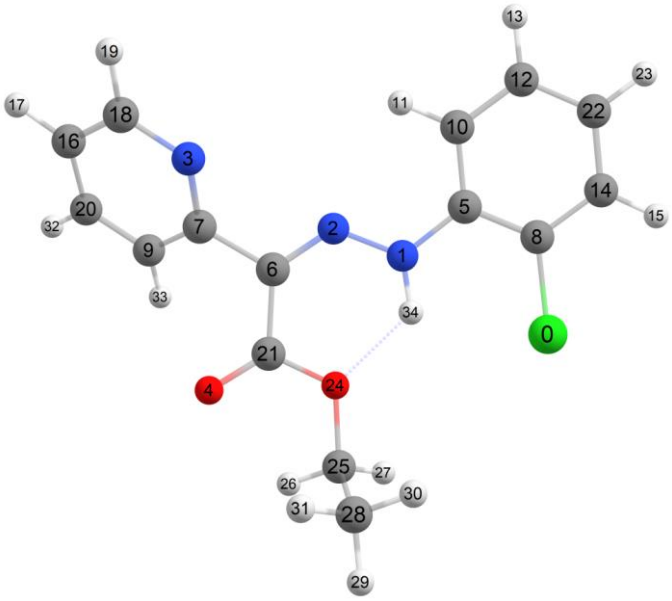
	13	7.83	1.00	
	15	7.92	1.00	
	17	7.72	1.00	
	19	9.11	1.00	
	23	7.44	1.00	
	26	5.30	1.00	
	27	4.39	1.00	
	29	1.27	1.00	
	30	1.50	1.00	
	31	1.63	1.00	
	32	8.23	1.00	
	33	7.99	1.00	
	34	11.92	1.00	

*Z**	2	15.18	1.00	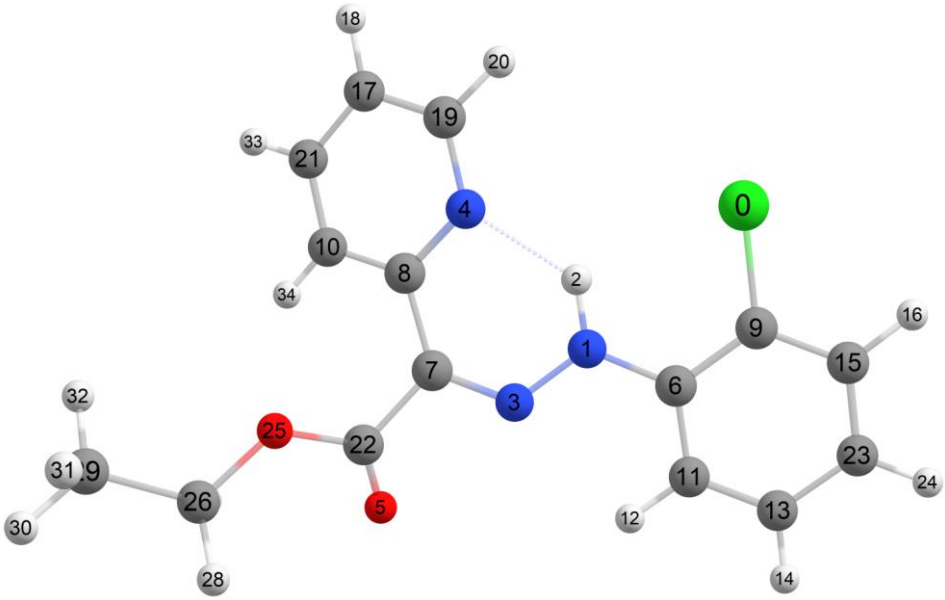
	12	8.44	1.00	
	14	7.82	1.00	
	16	7.92	1.00	
	18	7.79	1.00	
	20	9.22	1.00	
	24	7.42	1.00	
	27	4.47	1.00	
	28	4.31	1.00	
	30	1.38	1.00	
	31	1.40	1.00	
	32	1.52	1.00	
	33	8.39	1.00	
	34	8.19	1.00	
*Z**-a	2	20.88	1.00	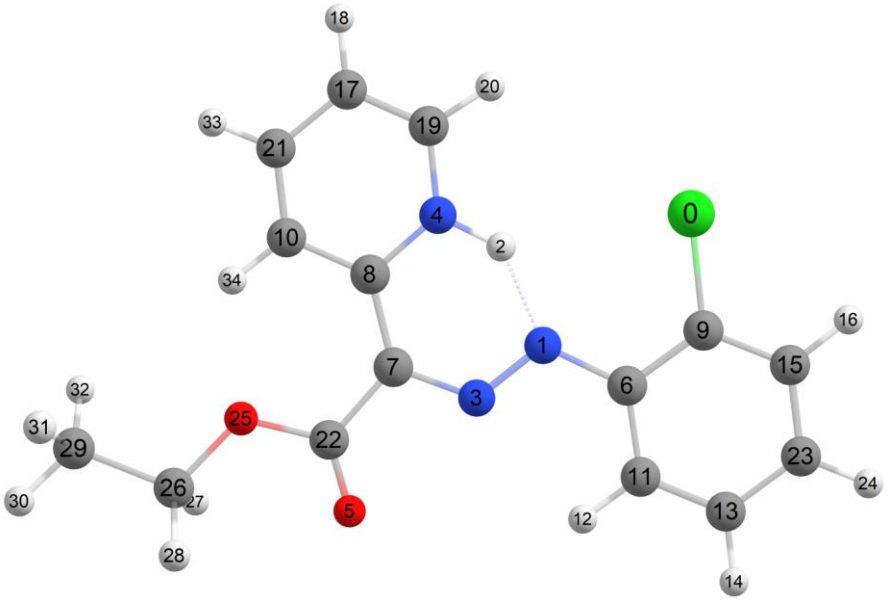
	12	8.68	1.00	
	14	7.81	1.00	
	16	7.99	1.00	
	18	7.56	1.00	
	20	8.58	1.00	
	24	7.57	1.00	
	27	4.49	1.00	
	28	4.36	1.00	
	30	1.49	1.00	
	31	1.63	1.00	
	32	1.72	1.00	
	33	8.50	1.00	
	34	9.07	1.00	
*E**-b	2	12.76	1.00	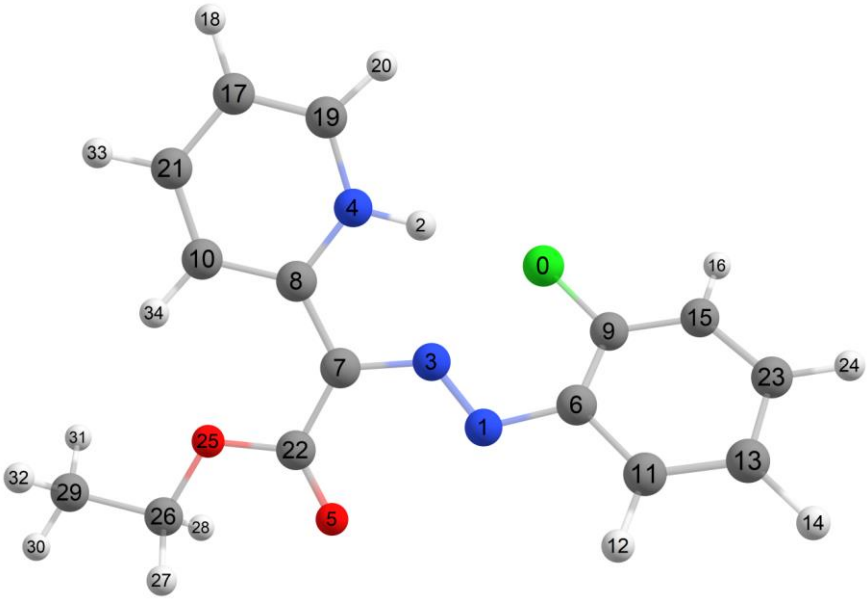
	12	7.95	1.00	
	14	7.82	1.00	
	16	7.93	1.00	
	18	7.18	1.00	
	20	8.14	1.00	
	24	7.57	1.00	
	27	4.29	1.00	
	28	4.23	1.00	
	30	1.47	1.00	
	31	1.63	1.00	
	32	1.64	1.00	
	33	8.34	1.00	
	34	9.07	1.00	

*E**-c	11	7.70	1.00	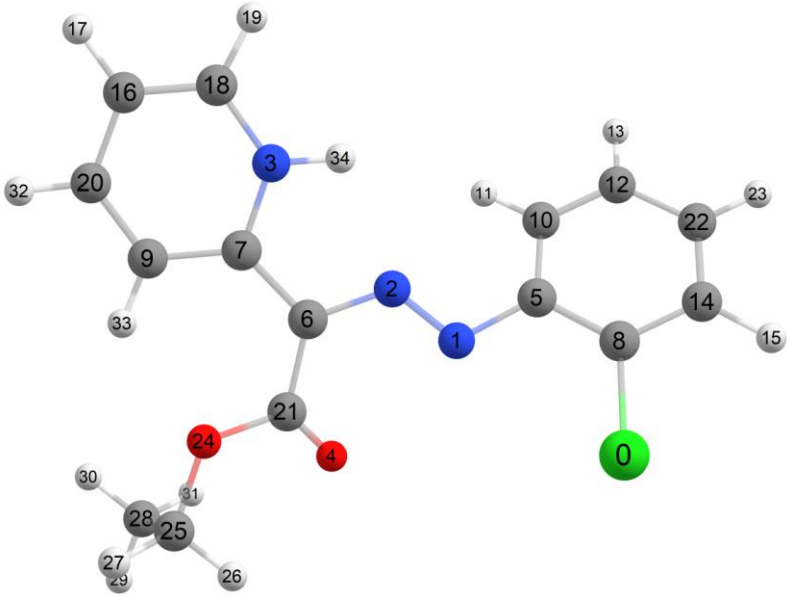
	13	7.72	1.00	
	15	7.93	1.00	
	17	7.05	1.00	
	19	8.07	1.00	
	23	7.60	1.00	
	26	5.15	1.00	
	27	3.96	1.00	
	29	1.22	1.00	
	30	1.43	1.00	
	31	1.68	1.00	
	32	8.19	1.00	
	33	8.53	1.00	
	34	12.10	1.00	
*E**	11	8.35	1.00	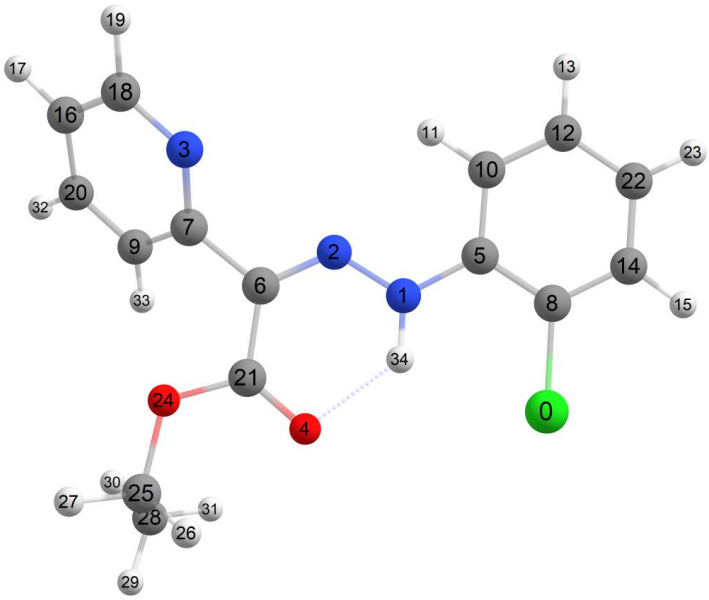
	13	7.79	1.00	
	15	7.92	1.00	
	17	7.73	1.00	
	19	9.11	1.00	
	23	7.45	1.00	
	26	5.05	1.00	
	27	3.97	1.00	
	29	1.27	1.00	
	30	1.49	1.00	
	31	1.80	1.00	
	32	8.25	1.00	
	33	8.02	1.00	
	34	13.50	1.00	

Table S6. The isomer shifts of ^{1}H NMR relative to TMS together with atom numbering scheme, calculated with CAM-B3LYP/PCSSEG-2/C-PCM($CHCl_3$), for **2-Br**.

	Atom shift[ppm] rel.intensity		
Z	2	15.85	1.00
	12	8.49	1.00
	14	7.88	1.00
	16	8.01	1.00
	18	7.79	1.00
	20	9.23	1.00
	24	7.44	1.00
	27	4.39	1.00
	28	4.31	1.00
	30	1.48	1.00
	31	1.72	1.00
	32	1.65	1.00
	33	8.40	1.00
	34	8.71	1.00
Z-a	2	20.29	1.00
	12	8.62	1.00
	14	7.84	1.00
	16	8.08	1.00
	18	7.62	1.00
	20	8.61	1.00
	24	7.56	1.00
	27	4.32	1.00
	28	4.29	1.00
	30	1.46	1.00
	31	1.65	1.00
	32	1.67	1.00
	33	8.58	1.00
	34	9.84	1.00

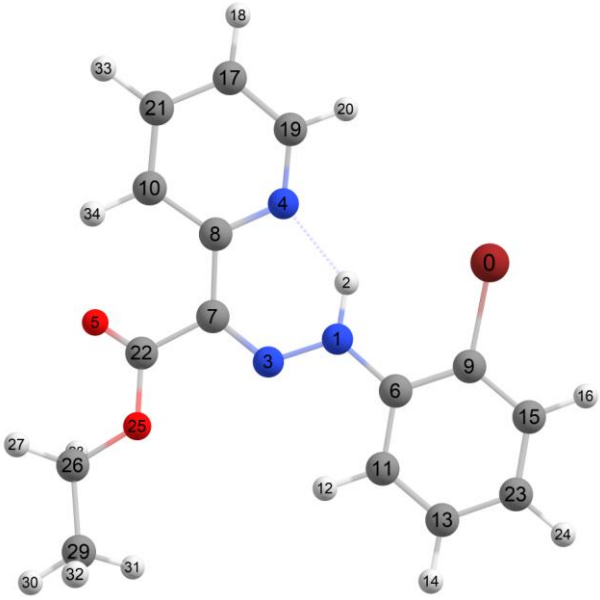

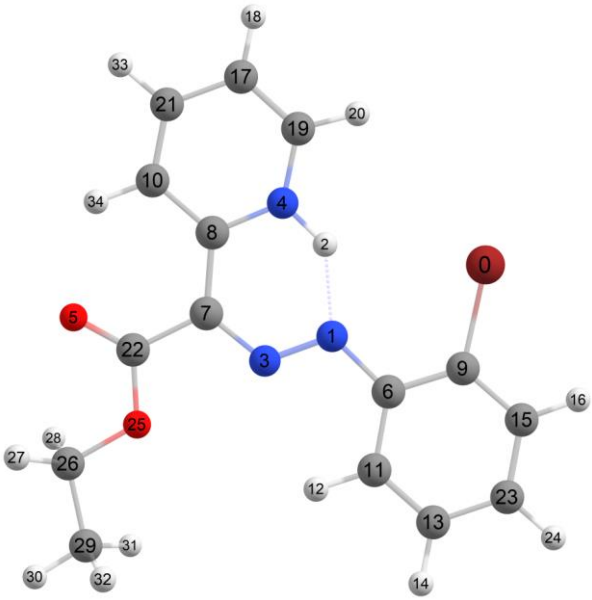

E-b	2	12.62	1.00	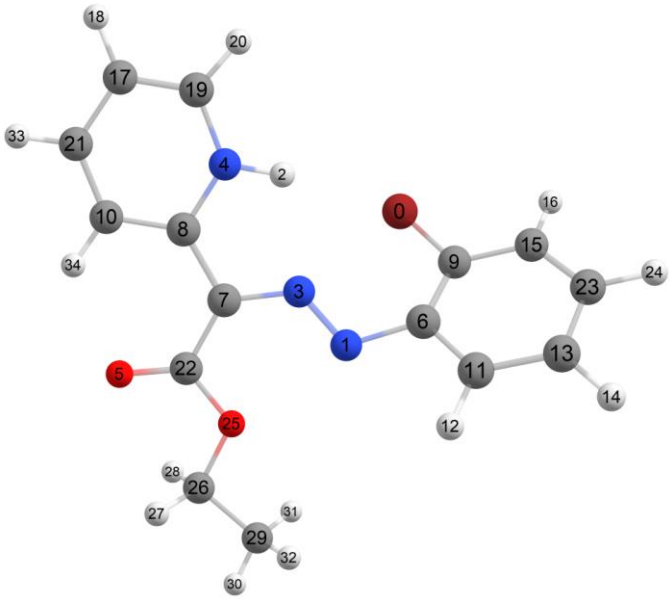
	12	7.86	1.00	
	14	7.85	1.00	
	16	8.02	1.00	
	18	7.21	1.00	
	20	8.13	1.00	
	24	7.56	1.00	
	27	4.26	1.00	
	28	4.25	1.00	
	30	1.33	1.00	
	31	1.48	1.00	
	32	1.59	1.00	
	33	8.37	1.00	
	34	9.59	1.00	
E-c	11	7.77	1.00	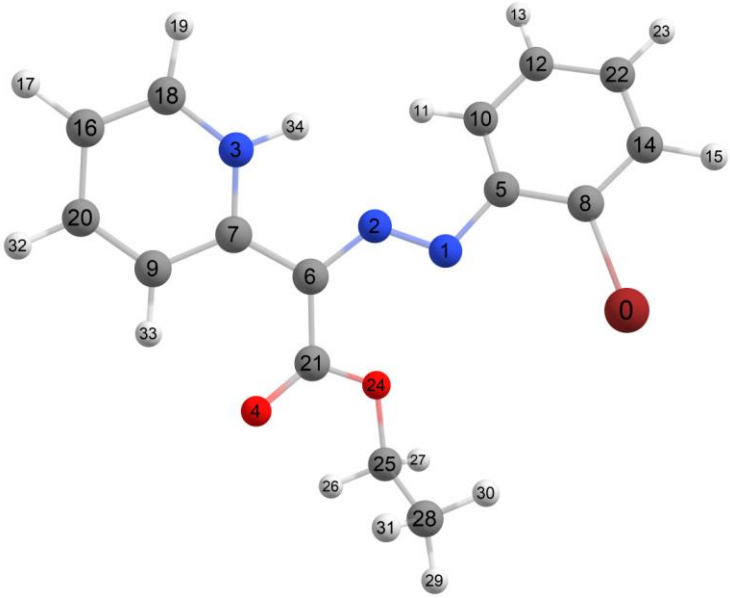
	13	7.79	1.00	
	15	8.07	1.00	
	17	7.18	1.00	
	19	8.16	1.00	
	23	7.58	1.00	
	26	5.13	1.00	
	27	3.97	1.00	
	29	1.13	1.00	
	30	1.58	1.00	
	31	1.62	1.00	
	32	8.31	1.00	
	33	9.18	1.00	
	34	12.44	1.00	
E	11	8.37	1.00	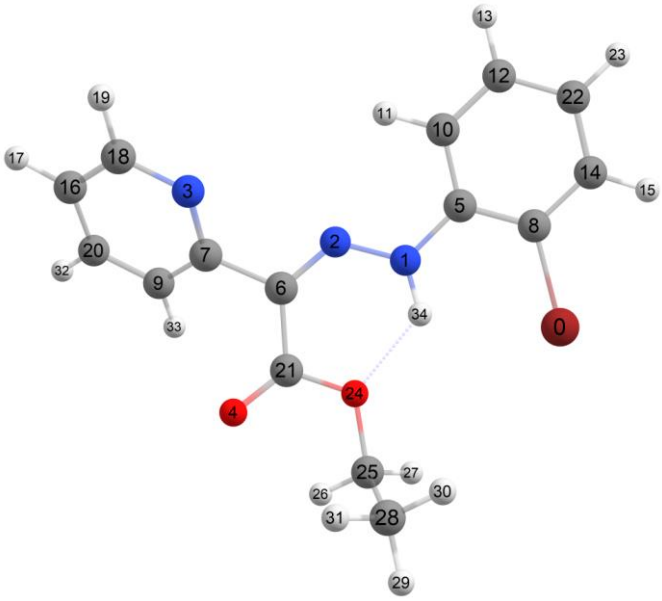
	13	7.87	1.00	
	15	7.98	1.00	
	17	7.72	1.00	
	19	9.11	1.00	
	23	7.42	1.00	
	26	5.31	1.00	
	27	4.40	1.00	
	29	1.27	1.00	
	30	1.54	1.00	
	31	1.63	1.00	
	32	8.24	1.00	
	33	8.00	1.00	
	34	11.97	1.00	

*Z**	2	15.23	1.00	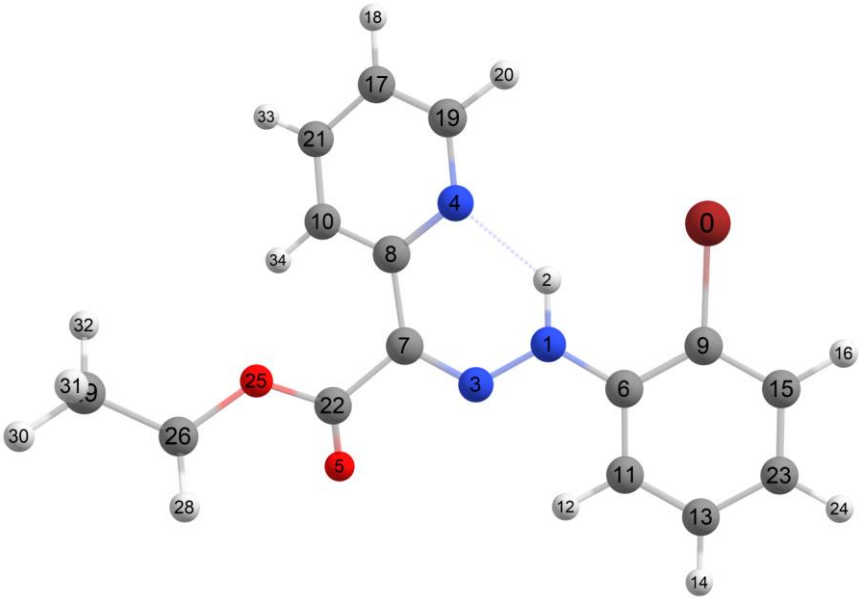
	12	8.48	1.00	
	14	7.87	1.00	
	16	7.98	1.00	
	18	7.80	1.00	
	20	9.24	1.00	
	24	7.40	1.00	
	27	4.48	1.00	
	28	4.32	1.00	
	30	1.39	1.00	
	31	1.41	1.00	
	32	1.53	1.00	
	33	8.39	1.00	
	34	8.20	1.00	
*Z**-a	2	20.64	1.00	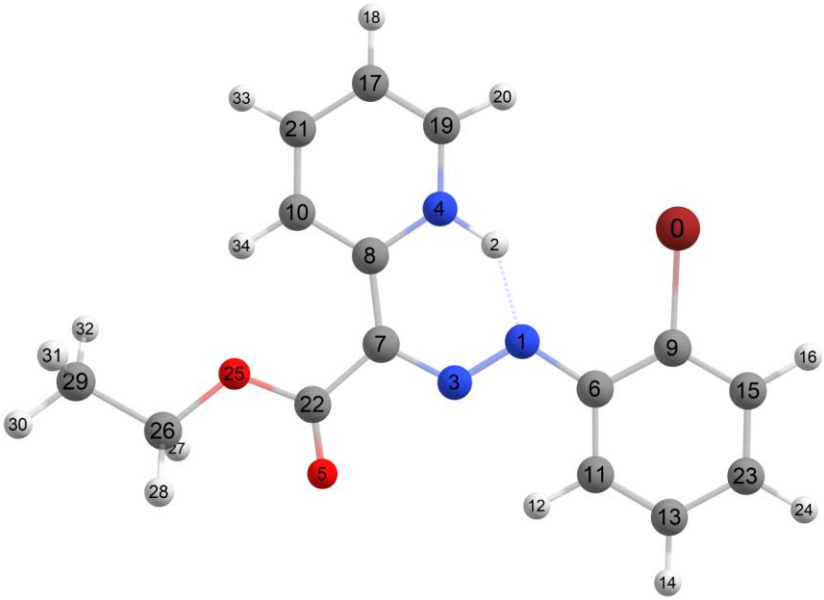
	12	8.71	1.00	
	14	7.85	1.00	
	16	8.06	1.00	
	18	7.56	1.00	
	20	8.63	1.00	
	24	7.55	1.00	
	27	4.49	1.00	
	28	4.36	1.00	
	30	1.49	1.00	
	31	1.63	1.00	
	32	1.72	1.00	
	33	8.51	1.00	
	34	9.05	1.00	
*E**-b	2	12.81	1.00	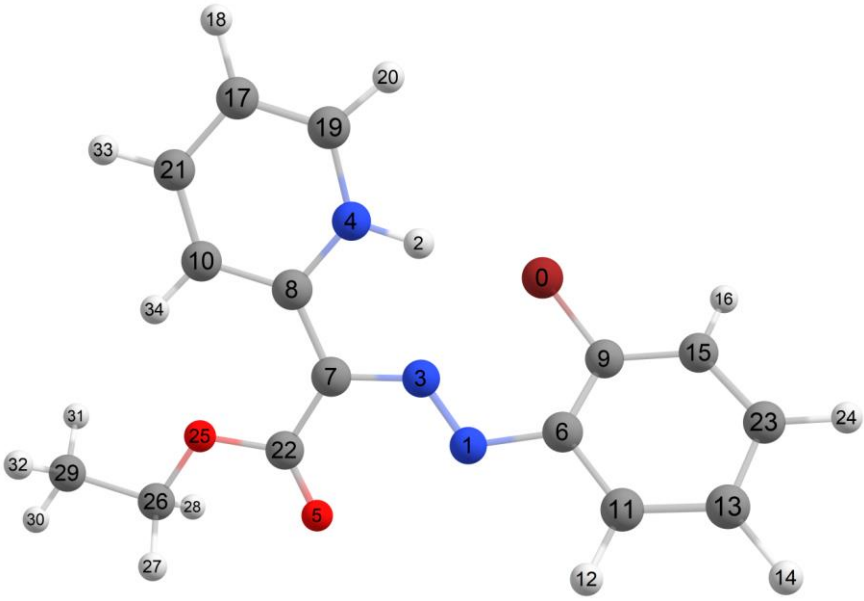
	12	7.90	1.00	
	14	7.85	1.00	
	16	8.02	1.00	
	18	7.18	1.00	
	20	8.14	1.00	
	24	7.56	1.00	
	27	4.27	1.00	
	28	4.26	1.00	
	30	1.47	1.00	
	31	1.64	1.00	
	32	1.64	1.00	
	33	8.35	1.00	
	34	9.09	1.00	

*E**-c	11	7.73	1.00	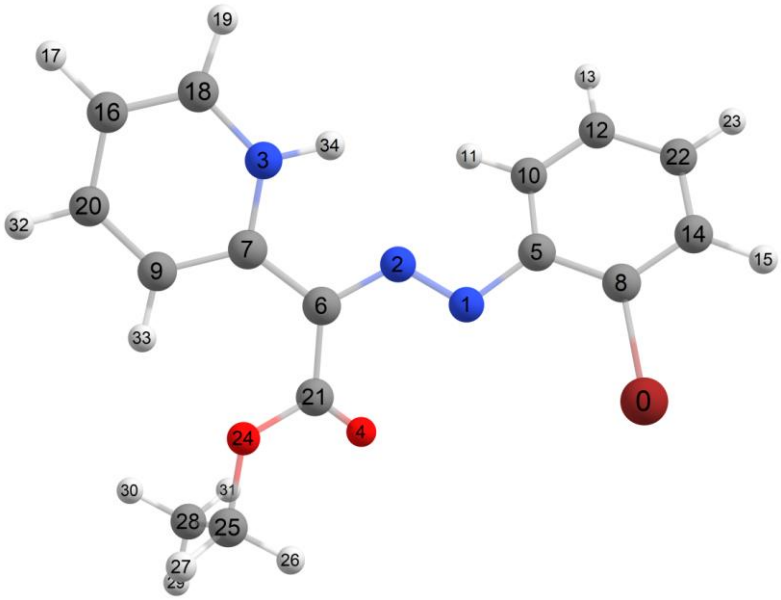
	13	7.77	1.00	
	15	8.04	1.00	
	17	7.06	1.00	
	19	8.07	1.00	
	23	7.57	1.00	
	26	5.15	1.00	
	27	3.96	1.00	
	29	1.22	1.00	
	30	1.44	1.00	
	31	1.69	1.00	
	32	8.19	1.00	
	33	8.50	1.00	
	34	12.09	1.00	
*E**	11	8.39	1.00	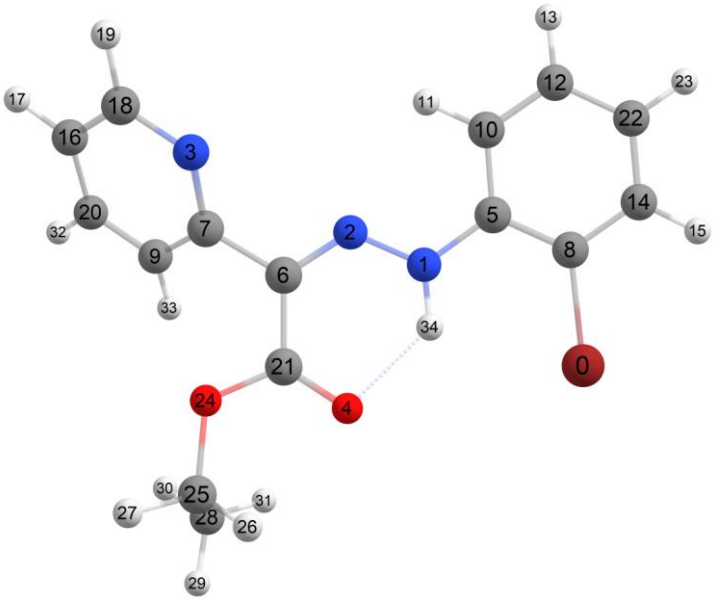
	13	7.84	1.00	
	15	7.99	1.00	
	17	7.73	1.00	
	19	9.12	1.00	
	23	7.44	1.00	
	26	5.05	1.00	
	27	3.97	1.00	
	29	1.27	1.00	
	30	1.50	1.00	
	31	1.81	1.00	
	32	8.25	1.00	
	33	8.02	1.00	
	34	13.50	1.00	

Table S7. The isomer shifts of ^{1}H NMR relative to TMS together with atom numbering scheme, calculated with CAM-B3LYP/PCSSEG-2/C-PCM($CHCl_3$), for **2-I**.

Z	Atom shift[ppm] rel.intensity 2 15.82 1.00 12 8.51 1.00 14 7.90 1.00 16 8.09 1.00 18 7.80 1.00 20 9.28 1.00 24 7.40 1.00 27 4.39 1.00 28 4.31 1.00 30 1.48 1.00 31 1.72 1.00 32 1.65 1.00 33 8.41 1.00 34 8.71 1.00	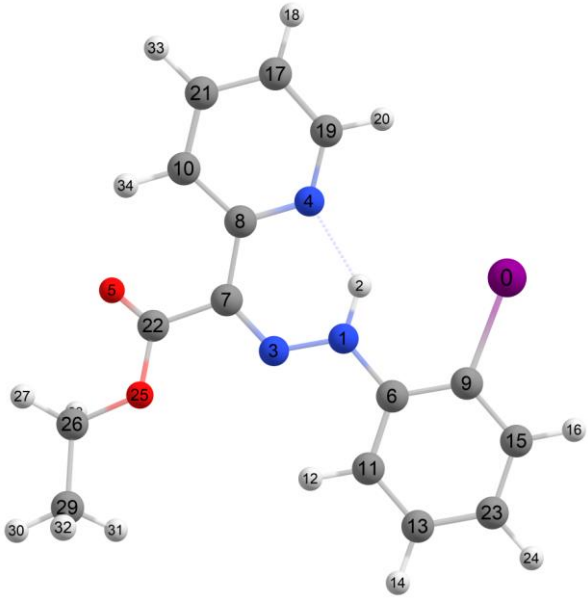
Z-a	2 19.93 1.00 12 8.63 1.00 14 7.87 1.00 16 8.17 1.00 18 7.61 1.00 20 8.71 1.00 24 7.52 1.00 27 4.31 1.00 28 4.29 1.00 30 1.46 1.00 31 1.66 1.00 32 1.67 1.00 33 8.58 1.00 34 9.85 1.00	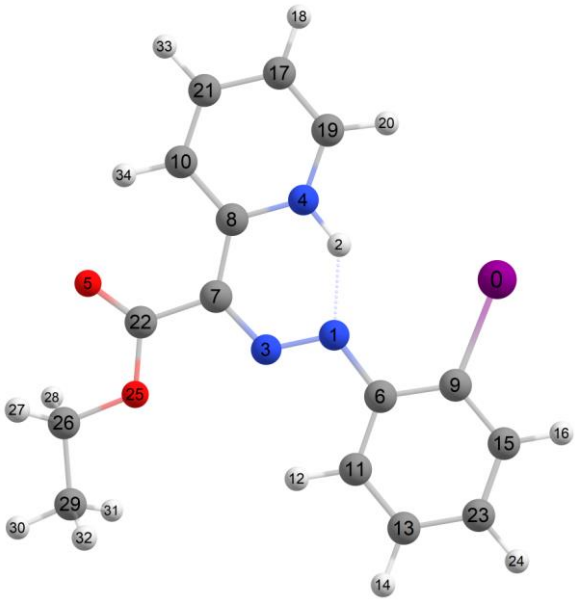

E-b	2	12.47	1.00	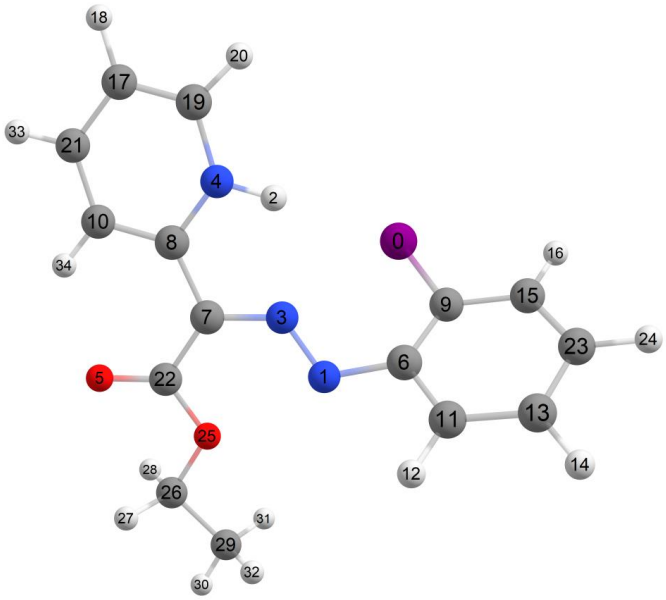
	12	7.78	1.00	
	14	7.86	1.00	
	16	8.10	1.00	
	18	7.21	1.00	
	20	8.11	1.00	
	24	7.54	1.00	
	27	4.27	1.00	
	28	4.24	1.00	
	30	1.32	1.00	
	31	1.46	1.00	
	32	1.57	1.00	
	33	8.36	1.00	
	34	9.55	1.00	
E-c	11	7.78	1.00	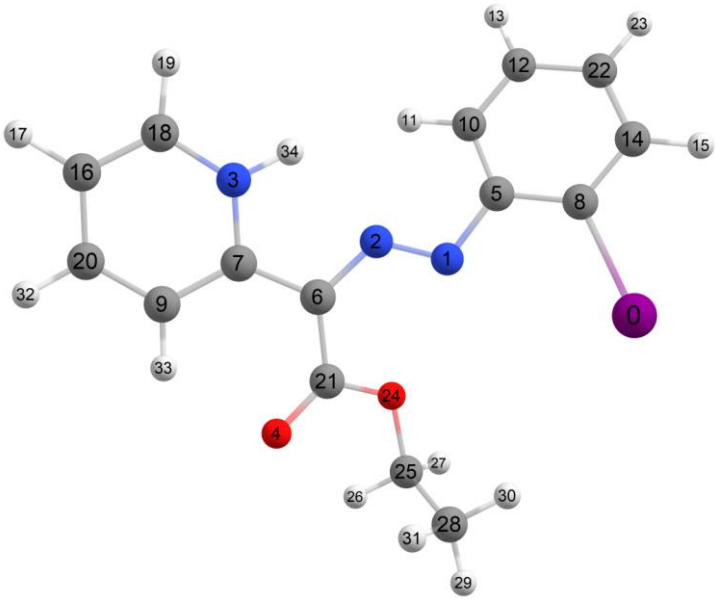
	13	7.82	1.00	
	15	8.18	1.00	
	17	7.19	1.00	
	19	8.17	1.00	
	23	7.55	1.00	
	26	5.13	1.00	
	27	4.00	1.00	
	29	1.12	1.00	
	30	1.70	1.00	
	31	1.63	1.00	
	32	8.32	1.00	
	33	9.25	1.00	
	34	12.47	1.00	
E	11	8.39	1.00	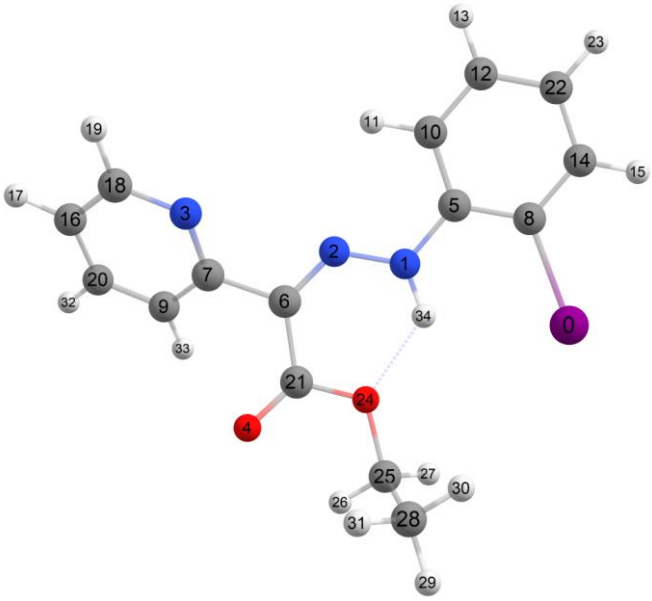
	13	7.89	1.00	
	15	8.05	1.00	
	17	7.72	1.00	
	19	9.11	1.00	
	23	7.39	1.00	
	26	5.32	1.00	
	27	4.45	1.00	
	29	1.27	1.00	
	30	1.61	1.00	
	31	1.64	1.00	
	32	8.24	1.00	
	33	7.99	1.00	
	34	11.86	1.00	

*Z**	2	15.15	1.00	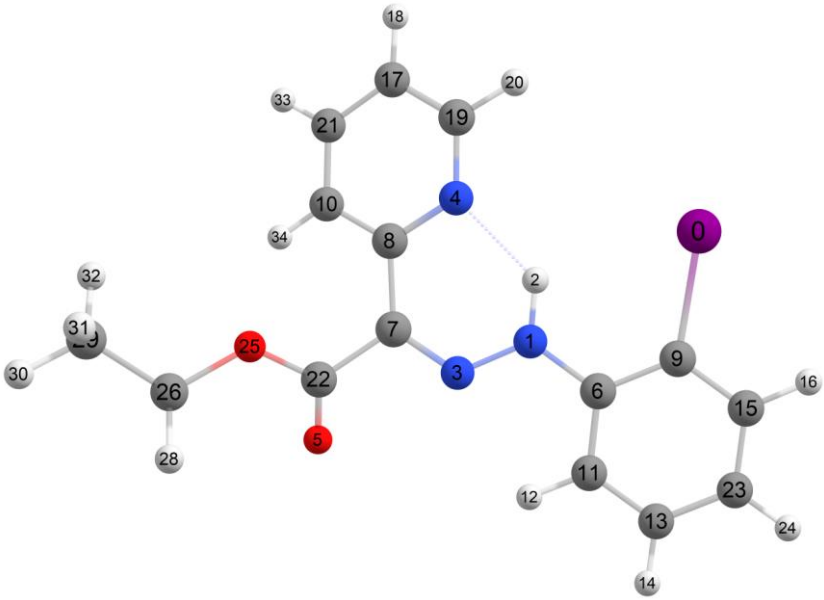
	12	8.50	1.00	
	14	7.88	1.00	
	16	8.07	1.00	
	18	7.80	1.00	
	20	9.29	1.00	
	24	7.37	1.00	
	27	4.48	1.00	
	28	4.31	1.00	
	30	1.38	1.00	
	31	1.41	1.00	
	32	1.52	1.00	
	33	8.39	1.00	
	34	8.20	1.00	
*Z**-a	2	20.17	1.00	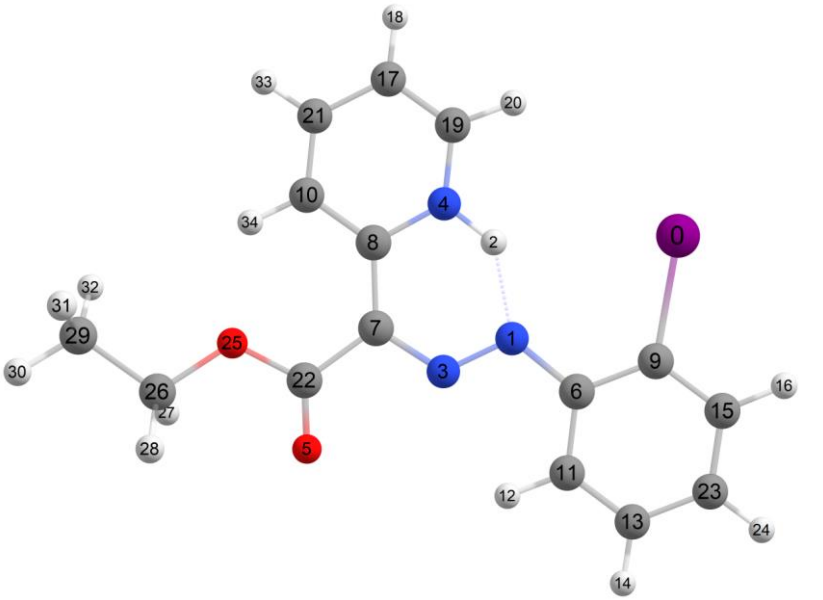
	12	8.71	1.00	
	14	7.87	1.00	
	16	8.15	1.00	
	18	7.55	1.00	
	20	8.73	1.00	
	24	7.51	1.00	
	27	4.50	1.00	
	28	4.35	1.00	
	30	1.48	1.00	
	31	1.62	1.00	
	32	1.71	1.00	
	33	8.50	1.00	
	34	9.04	1.00	
*E**-b	2	12.35	1.00	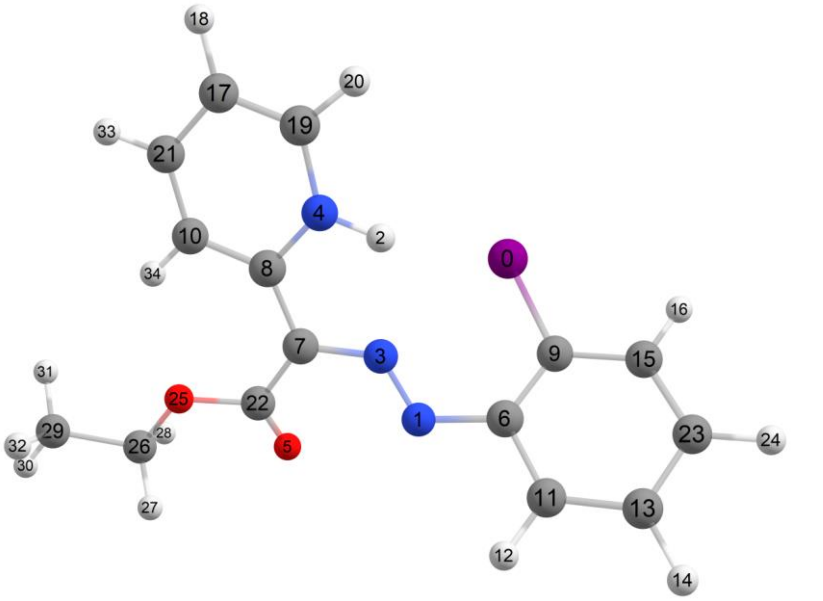
	12	7.76	1.00	
	14	7.84	1.00	
	16	8.09	1.00	
	18	7.10	1.00	
	20	8.06	1.00	
	24	7.52	1.00	
	27	4.25	1.00	
	28	4.32	1.00	
	30	1.44	1.00	
	31	1.63	1.00	
	32	1.55	1.00	
	33	8.26	1.00	
	34	8.76	1.00	

*E**-c	11	7.68	1.00	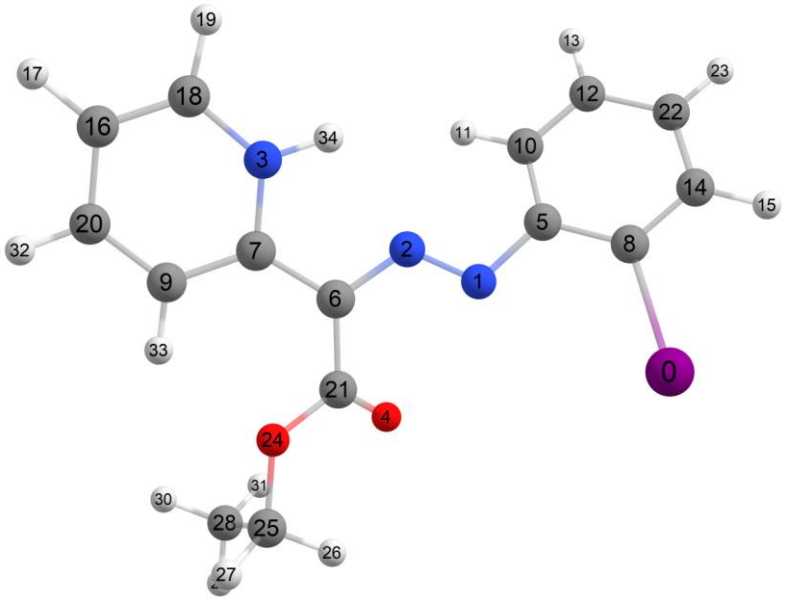
	13	7.79	1.00	
	15	8.14	1.00	
	17	7.06	1.00	
	19	8.07	1.00	
	23	7.54	1.00	
	26	5.16	1.00	
	27	3.96	1.00	
	29	1.22	1.00	
	30	1.43	1.00	
	31	1.69	1.00	
	32	8.20	1.00	
	33	8.53	1.00	
	34	12.08	1.00	
*E**	11	8.40	1.00	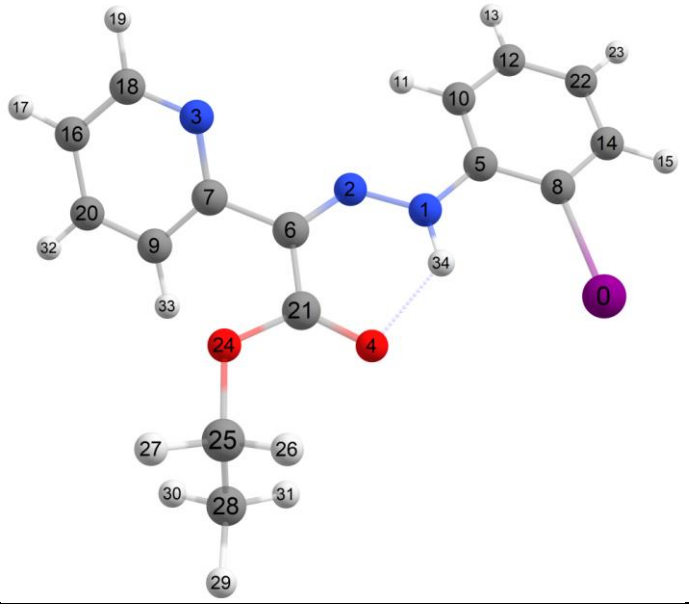
	13	7.86	1.00	
	15	8.07	1.00	
	17	7.73	1.00	
	19	9.12	1.00	
	23	7.40	1.00	
	26	5.06	1.00	
	27	3.97	1.00	
	29	1.27	1.00	
	30	1.50	1.00	
	31	1.82	1.00	
	32	8.25	1.00	
	33	8.02	1.00	
	34	13.38	1.00	

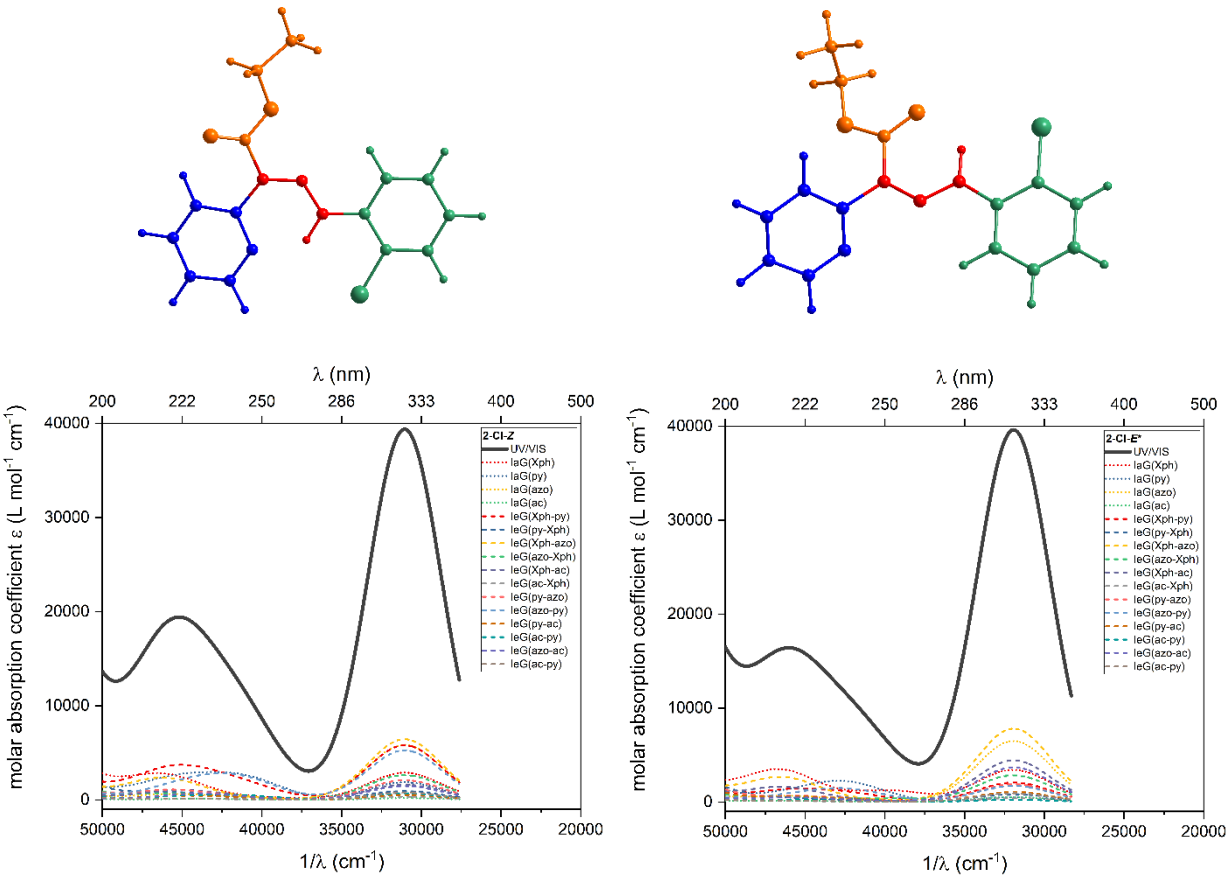

Figure S55. The graphically marked fragments of **2-Cl-*Z*** (left) and **2-Cl-*E**** (right) used for ICFT analysis of TD-DFT spectra.

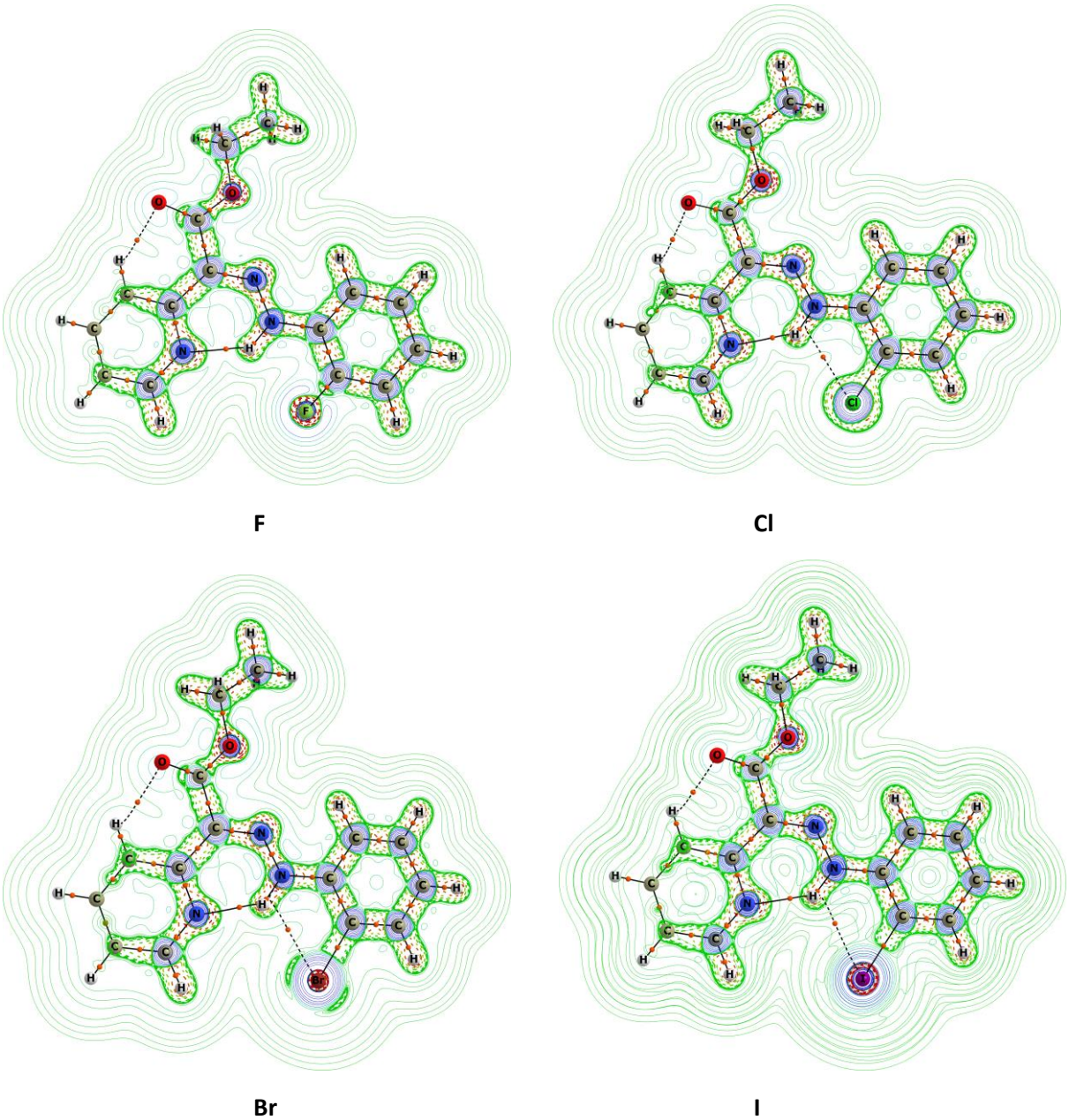

Figure S56. Depiction of the Laplacian of calculated electron density $\nabla^2\rho(\mathbf{r})$ for the optimized geometries (implicit solvation model C-PCM) of studied hydrazone switches in the *Z*-configuration. The (3, -1) bond critical points (brown dots) and bond paths (black solid and dashed lines) are depicted.

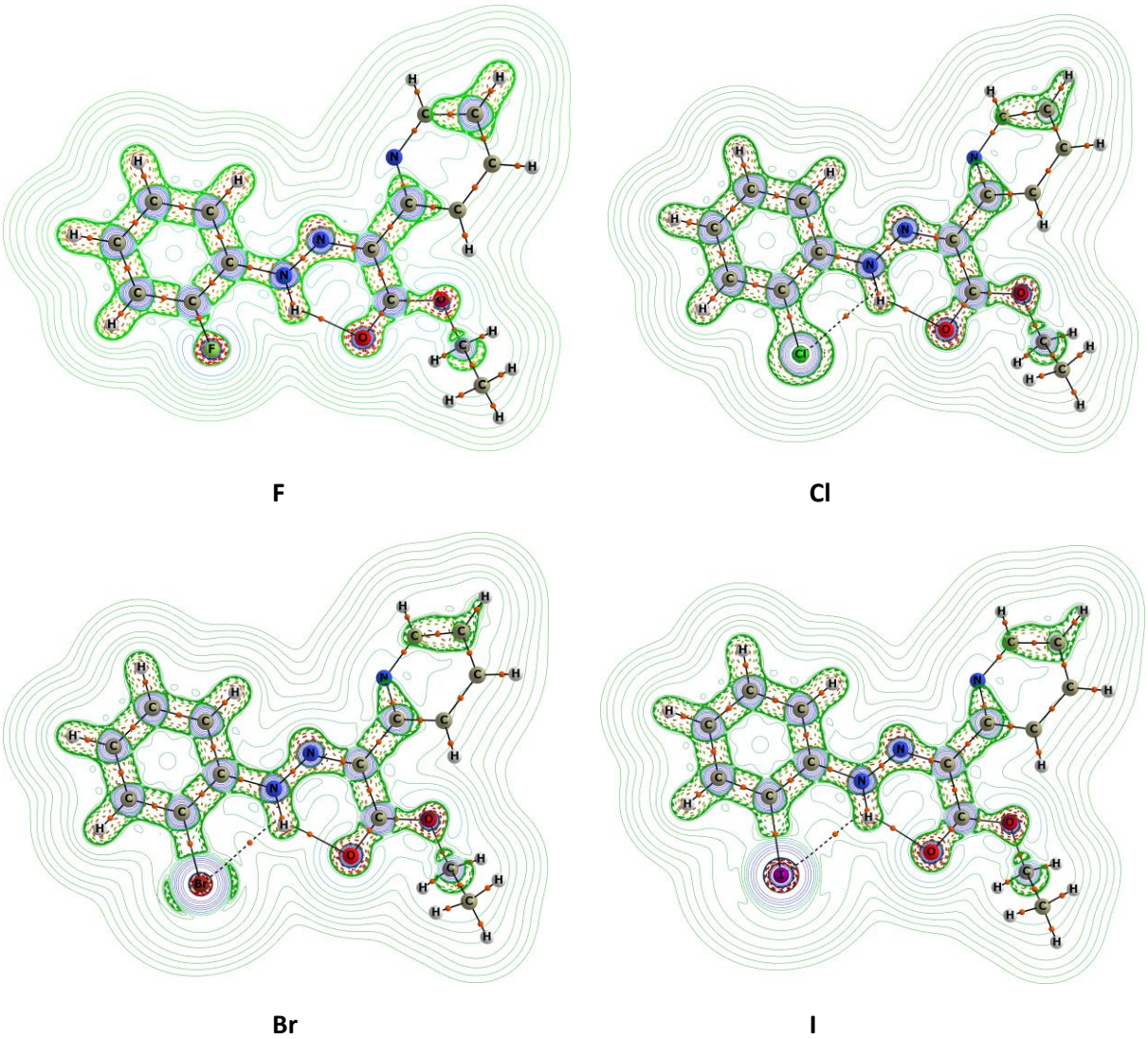

Figure S57. Depiction of the Laplacian of calculated electron density $\nabla^2\rho(\mathbf{r})$ for the optimized geometries (implicit solvation model C-PCM) of studied hydrazone switches in the *E*-configuration. The (3, -1) bond critical points (brown dots) and bond paths (black solid and dashed lines) are depicted.

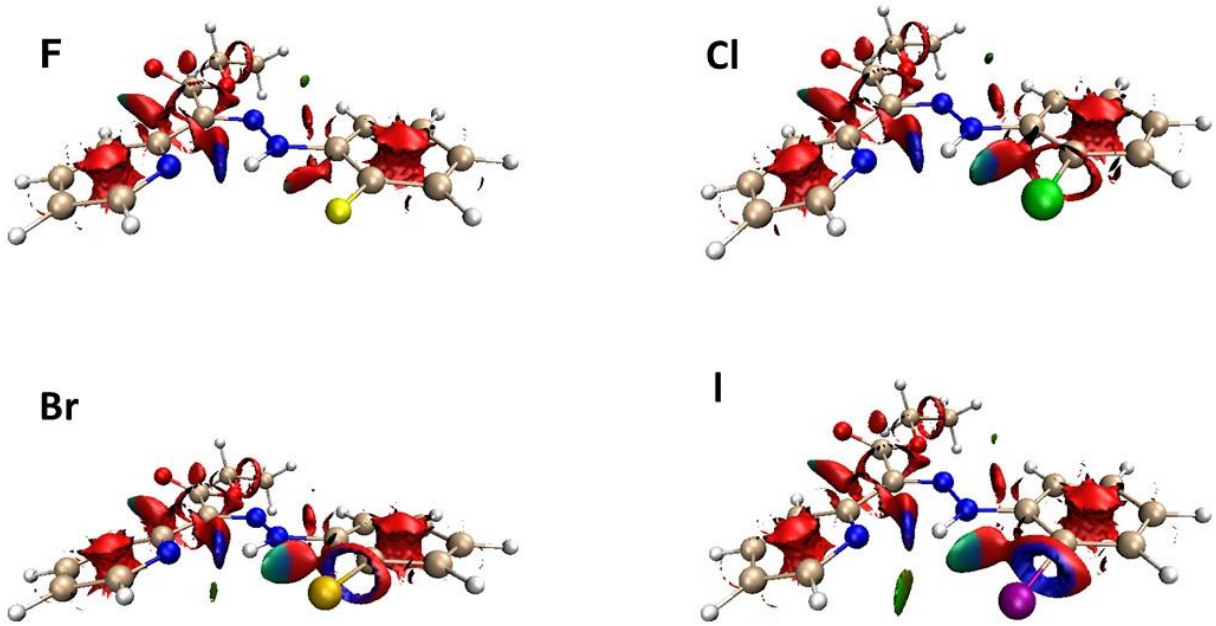

Figure S58. Gradient isosurfaces (s = 0.42 au) for the optimized geometries (implicit solvation model C-PCM) of studied hydrazone switches in the *Z*-configuration. The surfaces are colored on a blue-green-red scale according to values of sign(λ_2)r, ranging from -0.04 to 0.04 au. Blue indicates strong attractive interactions, and red indicates strong nonbonded overlap.

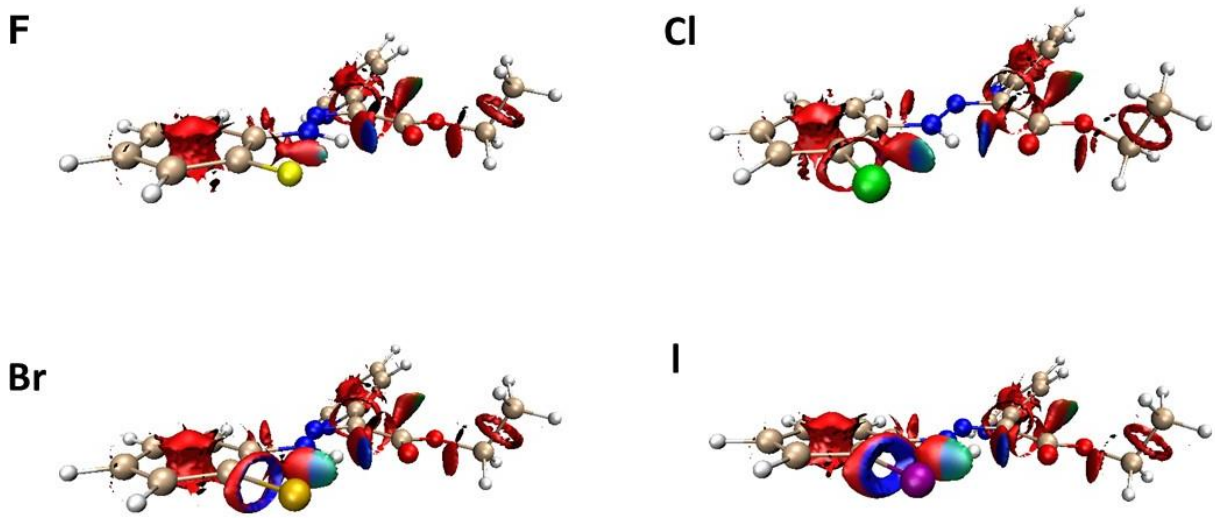

Figure S59. Gradient isosurfaces (s = 0.42 au) for the optimized geometries (implicit solvation model C-PCM) of studied hydrazone switches in the *E*-configuration. The surfaces are colored on a blue-green-red scale according to values of sign(λ_2)r, ranging from -0.04 to 0.04 au. Blue indicates strong attractive interactions, and red indicates strong nonbonded overlap.

Table S8. Topological and energetic properties of $\rho(\mathbf{r})$ calculated at the selected (3, -1) critical points optimized geometries (implicit solvation model C-PCM) of studied hydrazone switches in the *Z*-configuration. All values are provided in atomic units (a. u.) unless stated otherwise.

	$\nabla^2\rho(\mathbf{r})$	$h_e(\boldsymbol{r})$	$G(\mathbf{r})$	$V(\mathbf{r})$	$\lvert V(\mathbf{r})\rvert/G(\mathbf{r})$	ε	E_{int}/kcal.mol^{-1}
2-F N–H···N	0.12198	-0.000819	0.0313	-0.03213	1.03	0.005	10.1
N–H···F	–	–	–	–	–	–	–
2-Cl N–H···N	0.12356	-0.000891	0.031779	-0.032669	1.03	0.00603	10.3
N–H···Cl	0.06519	0.00199	0.01431	-0.01231	0.86	1.1195	3.9
2-Br N–H···N	0.123537	-0.000899	0.03177	-0.032662	1.03	0.00671	10.2
N–H···Br	0.05507	0.001252	0.012515	-0.01126	0.90	0.6856	3.5
2-I N–H···N	0.12335	-0.000852	0.03169	-0.03254	1.03	0.008143	10.2
N–H···I	0.04736	0.000937	0.0109025	-0.009966	0.91	0.529034	3.1

Table S9. Topological and energetic properties of $\rho(\mathbf{r})$ calculated at the selected (3, -1) critical points optimized geometries (implicit solvation model C-PCM) of studied hydrazone switches in the *E*-configuration. All values are provided in atomic units (a. u.) unless stated otherwise.

	$\nabla^2\rho(\mathbf{r})$	$h_e(\boldsymbol{r})$	$G(\mathbf{r})$	$V(\mathbf{r})$	$\lvert V(\mathbf{r})\rvert/G(\mathbf{r})$	ε	E_{int}/kcal.mol^{-1}
2-F N–H···O	0.12360	+0.00078	0.03012	-0.02934	0.97	0.0166	9.2
N–H···F	–	–	–	–	–	–	–
2-Cl N–H···O	0.12538	+0.00076	0.03058	-0.02982	0.98	0.01979	9.4
N–H···Cl	0.06427	+0.00185	0.01422	-0.01237	0.87	0.8039	3.9
2-Br N–H···O	0.12498	+0.00079	0.03046	-0.02967	0.97	0.02222	9.3
N–H···Br	0.05464	+0.00112	0.01254	-0.01143	0.91	0.5115	3.6
2-I N–H···O	0.12448	+0.00086	0.03026	-0.02940	0.97	0.02512	9.2
N–H···I	0.04691	+0.00081	0.01092	-0.01012	0.93	0.39755	3.2

Table S10. The values of sign $(\lambda_2)\rho$ calculated at (3, -1) critical points of the N–H···X for optimized geometries (implicit solvation model C-PCM) of studied hydrazone switches.

	Cl	**Br**	**I**
Z-configuration	+0.026878	+0.023961	–0.022858
E- configuration	+0.026700	–0.024296	–0.02323